November 2000 • NREL/SR-500-27066

Subcontractor Report

Variable-Speed Generation Subsystem Using the Doubly Fed Generator

Period of Performance
February 9, 1994—April 30, 1999

C.H. Weigand, H.K. Lauw, and D.A. Marckx
Electronic Power Conditioning Incorporated
Salem, Oregon

National Renewable Energy Laboratory

1617 Cole Boulevard
Golden, Colorado 80401-3393

NREL is a U.S. Department of Energy Laboratory
Operated by Midwest Research Institute • Battelle • Bechtel

Contract No. DE-AC36-99-GO10337

November 2000 • NREL/SR-500-27066

Variable-Speed Generation Subsystem Using the Doubly Fed Generator

Period of Performance
February 9, 1994—April 30, 1999

C.H. Weigand, H.K. Lauw, and D.A. Marckx
Electronic Power Conditioning Incorporated
Salem, Oregon

NREL Technical Monitor: Paul Migliore

Prepared under Subcontract No. ZAA-4-12272-02

National Renewable Energy Laboratory

1617 Cole Boulevard
Golden, Colorado 80401-3393

NREL is a U.S. Department of Energy Laboratory
Operated by Midwest Research Institute • Battelle • Bechtel

Contract No. DE-AC36-99-GO10337

Available electronically at http://www.doe.gov/bridge

Available for a processing fee to U.S. Department of Energy
and its contractors, in paper, from:

U.S. Department of Energy
Office of Scientific and Technical Information
P.O. Box 62
Oak Ridge, TN 37831-0062
phone: 865.576.8401
fax: 865.576.5728
email: reports@adonis.osti.gov

Available for sale to the public, in paper, from:

U.S. Department of Commerce
National Technical Information Service
5285 Port Royal Road
Springfield, VA 22161
phone: 800.553.6847
fax: 703.605.6900
email: orders@ntis.fedworld.gov
online ordering: http://www.ntis.gov/ordering.htm

Printed on paper containing at least 50% wastepaper, including 20% postconsumer waste

Foreword

Variable-speed wind turbine technology has come a long way in the last five years. When the Electronic Power Conditioning (EPC) project was initiated, under the Department of Energy Next Generation Innovative Subsystems Program, little was known about variable-speed operation. Of course, variable-speed turbines had been field tested before and Enercon and Kenetech were installing turbines in large numbers. But scant technical data were available on which to base judgements of the advantages and disadvantages of the technology. Speculation focused on several critical issues: Would the gains from operation at peak power coefficient be offset by power converter losses? Would voltage transients cause damage to generator windings or cause overheating? Would the cost of power electronics be prohibitive? In response to a competitive solicitation, EPC proposed an innovative concept having two noteworthy, although not absolutely new, features. The use of a wound rotor was suggested whereby the conditioning of only the rotor current would reduce the cost of power electronics by as much as 75% compared to full power conditioning of an induction generator. EPC also proposed using its own soft-switching (series resonant) technology to reduce voltage transients and obtain good power quality. The information contained herein describes the process of designing, fabricating, and laboratory testing several EPC converters, and then field testing them on two contemporary, utility-scale wind turbines. The project was as interesting for its unexpected turns and technical results as it was for its pursuit of the original objectives.

In its statement-of-work, the National Renewable Energy Laboratory (NREL) required EPC to collaborate with an industry partner (systems integrator) who had broad knowledge of turbine operations and was qualified to test EPC's variable-speed technology on an existing turbine. EPC chose to work with Advanced Wind Turbines, Inc, (AWT), formerly R. Lynette and Associates, of Seattle, Washington. For various business reasons, AWT later declined to support the anticipated field tests. This decision by AWT precipitated a fortuitous consequence, in that EPC then contacted Zond Energy Systems (now part of Enron Wind Corporation), which was evaluating variable-speed operation for its commercial turbines. At the same time, NREL's National Wind Technology Center (NWTC) was developing simulation models and conducting field tests of various control strategies for variable-speed, variable-pitch operation. This confluence of events—the cooperation among NREL, EPC, and Zond—was a catalyst in the development of Zond's 750 Series wind turbines, for which Trace Engineering now manufactures power converters.

In another turn of events, EPC eventually did field test improved versions of its power converter on an AWT-26 wind turbine at the NWTC. This afforded NWTC researchers the opportunity to develop advanced control strategies for variable-speed fixed-pitch (stall regulated) operation. Field tests of these controls showed controlled variable-speed operation and acceptable power regulation without the cost and complexity of a variable-pitch system.

The availability of a variable-speed turbine for field tests was beneficial in other ways. Some ancillary experiments conducted at the NWTC produced interesting and useful results. For example, because great pains were taken to measure the EPC/AWT-26 drivetrain component efficiencies (gearbox, generator, and power converter) in the laboratory, it was possible to deduce *rotor* power coefficients from *generator* power measurements. From power curves obtained at several discrete rotor speeds, the impact of Reynolds Number on power coefficient was then observed. In another experiment, operation at several discreet rotor speeds enabled researchers to demonstrate the powerful relationship between tip speed and acoustic noise.

The report that follows provides information on all aspects of the project, including events that were unanticipated at the outset. A great deal of information is available in the references, comprised of NREL reports, journal articles, and conference papers on specific project results.

I would like to acknowledge the outstanding performance of EPC's project manager, Claus Weigand. Throughout the project, Claus managed technical details and subcontract reporting requirements admirably. He has been cooperative, responsive, and respectful of NREL's role as the contracting party. I would like to express my personal thanks to Claus for his professional and congenial demeanor.

_____
Paul Migliore, Senior Project Manager
National Renewable Energy Laboratory

Notice

Preface

The following employees of Electronic Power Conditioning, Inc., have written or contributed to this project report:

Dr. Hian K. Lauw	Principal Investigator
Claus H. Weigand	Technical Services Manager
Dallas A. Marckx	Vice-President, Business Development
Ashok Ramchandran, Ph.D.	Senior Project Engineer

Over the course of the project, EPC has made extensive use of subcontractors, as well as test and R&D personnel at the National Wind Technology Center in Golden, Colo. The efforts of the following individuals deserve special recognition:

Advanced Wind Turbines, Inc.:	- Shawn Lawlor
	- Ian Robertson
	- Tim McCoy
	- Dayton Griffin
	- Robert Poore
Zond Systems, Inc.:	- Amir Mikhail
	- Steve Atkins
	- Craig Christenson
	- Kevin Cousineau
	- Tom Nemila
	- John Admire
National Wind Technology Center:	- Paul Migliore
	- Brian Gregory
	- Kirk Pierce
	- Ed Muljadi
	- Greg Heine
	- Scott Larwood

TABLE OF CONTENTS – Volume 1

TABLE OF CONTENTS – Volume 1 (cont'd)

List of Figures

Name Page

List of Tables

Name Page

Executive Summary

Introduction

Over the past decade, fixed-speed, utility-scale wind turbines have technically advanced to a point where they can economically compete against nuclear and fossil-fuel-based power plants in geographical areas with a sufficient wind resource.

Preliminary investigations and some early implementations showed that variable-speed operation of wind turbines can improve turbine performance—further reducing the Cost of Energy (COE) of wind turbines—in the following areas: Increased Annual Energy Production (AEP) because the turbines will more often operate at maximum aerodynamic efficiency, reduced dynamic stresses on the drive-train components, which results in less costly drive-trains, reduced audible noise output, and better compatibility with the utility grid with which the turbine interfaces. Some early implementations, however, exhibited technical problems, such as premature generator failure, incompatibility with the utility grid with which the turbine interfaces, decreased operating reliability due to control equipment failure, and problems due to improper control strategies used.

The objective of this project was to compare various electrical topologies allowing variable-speed turbine operation, identify the most suitable for a 275 kW (or larger) utility-scale wind turbine, and then design, build, lab test, and field test this variable-speed generation subsystem based on the previously identified optimum approach, which then would be capable of showing all of the above benefits without incurring the known problems.

Approach

In this subcontract, NREL provided EPC with funds to predict the performance of an advanced utility-scale wind turbine operating at variable speed, trade-off viable electrical system topologies allowing variable-speed operation of a 275 kW (or larger) advanced wind turbine, identify the one topology that results in the greatest reduction in COE, specify the components required for this particular variable-speed generation system (VSGS), purchase the generator, design and manufacture the power conditioner and system controller, lab-test and characterize these components in isolation and operating as overall system, and finally, field-test this system on two existing turbines.

Results

Preliminary tests of the controls for a doubly fed variable-speed generation system (VSGS) rated at 750 kW were performed on a wind turbine. A 275-kW VSGS was thoroughly tested in the laboratory and on a wind turbine. Using field-oriented control excellent dynamic behavior of the drive train was demonstrated, acoustic tests revealed an 11 dB reduction in turbine noise in low-wind, low-RPM operation compared to fixed-speed operation. The overall efficiency of the electrical system suffered from inadequate efficiency of the power converter at low power. Consequently, a different converter topology has been proposed that will satisfy both efficiency and power quality requirements for future use.

1.0 INTRODUCTION

1.1 Background

In 1993, the National Renewable Energy Laboratory (NREL) awarded Electronic Power Conditioning (EPC), Inc., a subcontract under its Innovative Subsystems Program to investigate the technical and economic benefits of operating utility-scale, fixed-speed wind turbines at variable speed using an advanced resonant power electronic converter. The contract also called for EPC to design, build, laboratory-test, and field-test the one variable-speed generation system (VSGS) that would most likely yield the greatest economic benefit, expressed in reduction of cost of energy (COE).

Today, fixed-speed wind turbines are capable of producing electric power at a COE of just below $0.05/kilowatt-hour (kWh) if operating at a site with an average wind speed of at least 13 miles per hour (mph). To become more competitive with power produced using fossil fuels such as natural gas (COE of approximately $0.025/kWh), the COE of electric power produced by wind turbines must be reduced. One way to reach this goal (in combination with such steps as increased turbine size) is the transition from fixed-speed to variable-speed operation. The following factors contribute to the overall reduction of COE for variable-speed wind turbines:

- The annual energy production (AEP) of a turbine increases because the turbine rotor revolutions per minute (RPM) can be controlled in such a way that the aerodynamic rotor efficiency is close to maximum at all times for as long as its power output does not exceed the rated value.

- The cost of the turbine drivetrain components (low-speed shaft and gearbox) will be reduced, because drivetrain torque transients, which are a significant rating factor for fixed-speed drivetrains, can be eliminated by means of dynamic generator control. The variable-speed system may also be used as a dynamic brake, potentially reducing the rating of the brakes.

- State-of-the-art, variable-speed generation systems (VSGS) allow control of the power factor at which the turbine feeds power into the utility grid. A wind-farm supervisory control and data acquisition system (SCADA) can control the power factor at the substation at all times, without the need for additional power factor compensation equipment. Utilities are aware of the economic value of reactive power and voltage stabilization that some producers of wind power are able to provide.

- Some electrical hardware in fixed-speed wind turbine controllers (such as soft-starters and power-factor correction equipment) can be eliminated.

Acoustic noise reduction is yet another benefit of variable-speed operation, although its economic value is difficult to quantify. Acoustic noise criteria, however, are playing an increasingly important role in the process of siting new wind farms.

A few utility-scale, variable-speed wind turbines are commercially available today. A number of engineering prototypes have been built and extensively tested, though mostly in Europe. One or more of the following technical and economical difficulties were encountered with these units:

- Too much of the additional aerodynamic energy gained from the turbine rotor was lost in the power electronic converter located between the generator and the utility grid.

- The fully rated power electronic converter added too much cost.

- The power electronic converter(s) used required reactive power from the utility grid, and caused serious power quality problems on the grid. Costly electrical filtering hardware had to be added.

- Dynamic control of the low-speed shaft torque was not possible with some of the electrical system topologies used. Therefore, the drivetrain components could not be downsized.

- More advanced power converters imposed excessive electrical stresses on the generator windings, resulting in premature generator winding failure. More expensive and less efficient generators had to be used.

1.2 Objectives

The primary objectives of this project were to:

1. Conduct trade-off studies of viable VSGS topologies together with advanced resonant power electronic converters, with the goal identifying the one topology that maximizes the benefits of variable-speed generation for wind turbines while avoiding its known disadvantages as much as possible

2. Specify, design, and manufacture the optimized VSGS, including power electronic converter, generator, system controller, and required switchgear for the selected test turbines

3. Characterize the above components through laboratory testing individually and as complete systems

4. Install the VSGSs on the selected test turbines and characterize their performance

5. Compare the performance of the original and the modified turbines and predict the reduction of COE if these turbines were optimized for variable-speed operation.

1.3 Period of Performance, Schedule, and Deliverables

The project was divided into eight major tasks, from the preparation of a project work plan to the review of the final project report. The schedule for these tasks and their major subtasks can be found in appendix A.1.

The deliverables and milestones for the project are listed in Table 1.1.

Table 1.1. Project Deliverables and Meetings

Deliverable	Meeting	Date
	Technical Review Meeting	2-16-94
Project Work Plan	Kickoff Meeting	5-26-94
Design Review Package (AWT-26)	Design Review Meeting (AWT-26)	4-19-95
Design Review Package (Z-40M)	Design Review Meeting (Z-40M)	10-11-95
Laboratory Test Plan	not applicable	7-31-94
Field Test Plan (Z-40M)	Test Readiness Review Meeting (Z-40M)	6-4-96
Field Test Plan (AWT-26)	Test Readiness Review Meeting (AWT-26)	3-23-98
Draft Final Project Report	Final Project Review Meeting	3-27-00

The original scope of the subcontract was changed twice, which expanded the period of performance, budget, and the lower-tier subcontractors. Field tests on a three-bladed, upwind, pitch-controlled turbine (Z-40M) were added. In addition, the AWT-26 turbine, located at NREL's National Wind Technology Center (NWTC), became the test-bed instead of the AWT-26 in Tehachapi, California, which was owned by Advanced Wind Turbines, Inc. (AWT).

We submitted the draft final report in January 2000. We documented the details of the project's progress in monthly reports submitted to the NREL technical monitor and subcontract administrator.

1.4 Organization of this Report

This report does not describe technical details of the power electronic converter or the VSGS controller used in the implementation of the VSGS, unless these details directly pertain to the performance enhancements of the variable-speed turbines tested. Instead, emphasis is being placed on the following:

- The rationale leading to a particular VSGS topology
- The VSGS optimization process
- The prediction of the variable-speed turbine performance improvements
- The effect of the VSGS on turbine dynamics and mechanical loads
- The laboratory and field-test results.

The second section of this report, "Summary of VSGS Preliminary Design," describes the trade-off studies that we conducted. These studies led us to one VSGS topology that promised the most benefits while having the least disadvantages. We applied this topology to the predicted variable-speed performance characteristics of both test-turbines (Z-40M and AWT-26) and derived specifications for the generator, power electronic converter, switchgear, and VSGS controller.

The third section of this report, "VSGS Component Development," describes the design, assembly, and individual testing of the power electronic converter, the doubly fed generator (DFG), and the VSGS controller.

The fourth section of this report, "VSGS Laboratory Testing," describes the laboratory test setup, test matrix, and the test results for the integrated VSGS. Test results from a VSGS test performed at the facilities of a generator manufacturer are included.

The fifth section of this report, "VSGS Field Testing," describes the test setup, test matrices, and test results from all field tests performed under the scope of this project.

The sixth section, "Conclusions," discusses achievements of this project and proposes commercial solutions for an advanced VSGS for wind applications.

The final section, "Recommendations," outlines steps that should be undertaken based on the results of this project.

Not all design information that led to the final implementation of the VSGS is included in this report. Only the most relevant information is included. Additional design data are available at the subcontractor's facility. Some of the design information is regarded as commercially sensitive and, therefore, available for review by NREL personnel only.

2.0 Summary of VSGS Preliminary Design

2.1 Trade-off Studies

We conducted generalized trade-off studies concerning the beneficial impacts of a variety of electrical VSGS topologies, as well as different VSGS control strategies (or combinations thereof) on AEP, critical mechanical stresses (static and dynamic), and system cost of the most common utility-scale turbine types. The ultimate figure of merit is the resulting reduction of COE.

2.1.1 VSGS Control Strategies

We considered the following VSGS control strategies:

- Variable-speed operation only at low wind speeds
- Variable-speed operation throughout the entire wind-speed range
- Torque-limited, thrust-limited, bending-moment limited, and power-limited strategies.

One VSGS control strategy that sets itself apart from others is the low-wind-speed variable-speed approach. Figure 2.1 shows the VSGS configuration that allows variable-speed operation at low windspeeds. The strategy aims at capturing additional energy by maintaining peak-C_p of the turbine rotor from zero output power up to where peak-C_p operation coincides with the fixed-speed rotor RPM. At that point, the power electronic converter is bypassed and the turbine operates as a fixed-speed turbine at all power levels above that point up to rated power. All turbine characteristics, mechanical loads, and dynamics are identical with their fixed-speed counterparts above that point. The additional energy captured by the turbine rotor at low windspeeds is partially offset by the electrical losses in the power electronic converter. The only generator type feasible for this VSGS topology is the induction generator, because the generator has to operate part-time when directly grid-connected. The additional cost of the power electronic converter (including bypass contactor) is partially offset by the elimination of the soft-starter and the power-factor correction equipment. The approach also benefits from reduced acoustical noise at lower windspeeds due to reduced rotor RPM. However, depending on the IEC class wind site for which the turbine is designed, the trade-off between this approach and the use of longer blades combined with fixed-speed operation has to be investigated. Either action moves the turbine power curve to the left, resulting in additional energy output. Because we were not planning to implement this approach during the field tests, we did not quantitatively trade-off one approach against the other, nor will we have test data available showing that one approach reduces COE more than the other.

For some VSGS topologies, the useful RPM range of the retrofitted turbine has a strong impact on the specifications and, thus, the cost of the VSGS components. The following considerations, which depend only on the turbine rotor performance and the turbine rating, were applied to define the minimum useful and maximum allowable RPM set points:

- Minimum useful rotor RPM:

  For any given turbine rotor there is a minimum rotor RPM below which the minimum electrical VSGS power losses exceed the aerodynamic rotor power output. Depending on the VSGS topology used, these minimum losses are about 2.5% to 3% of the rated VSGS power output. If the turbine rotor were to be operated below this RPM, electric power would be drawn from instead of supplied to the grid.

  Conditions have to be defined and programmed into the VSGS controller; based on the conditions, the turbine can be disconnected from the grid if it remains at this RPM and either draws power from the grid for a duration longer than a certain time limit or draws more power than a maximum allowable instantaneous value. In either case, the controller will not reconnect the turbine to the grid until either the windspeed remains above a predetermined minimum value for a certain length of time (for turbines that require a stopped rotor after shutdown) or the idling rotor RPM exceeds a preset minimum idle RPM. This

kind of approach avoids a condition called "pendeling," in which the turbine is connected to and disconnected from the grid repetitively over an extended period.

- Maximum allowable rotor RPM:

  Depending on the turbine rotor design, one or two considerations apply. For the case of a pitch-controlled rotor, the steady-state rotor power output at this RPM (given peak-C_p operation) must not exceed rated rotor power. In this case, it is expected that the pitch-controller is capable of limiting potential dynamic power excursions beyond rated output power to magnitudes that do not noticeably impact component life expectancies (generally less than about 115% of rated power), even under worst-case conditions.

For the case of a stall-controlled rotor, a second, more stringent, condition applies. For stall-controlled rotors, rotor RPM must be controlled such that maximum dynamic turbine output power under worst-case conditions does not substantially exceed rated output power even as the VSGS controller forces the rotor into stall. Practically, this more stringent requirement calls for an RPM-control algorithm that deviates from the peak-C_p curve of the turbine rotor well below rated power output [1], resulting in a lower AEP gain than theoretically possible.

2.1.2 VSGS Impact on the Turbine

To determine the effects of variable-speed turbine operation on torque, thrust, and bending-moment, we considered the following commonly used turbine designs:

- Two-bladed, downwind, free-yaw, stall-controlled, teetered-hub
- Three-bladed, upwind-yaw, pitch-controlled, rigid hub.

For the case of stall-controlled, teetered-hub, downwind rotors and torque-based VSGS control-algorithms using an early-stall approach, steady-state rotor thrust reaches a local maximum at the highest RPM-point [2]. This maximum is about equal to the thrust at cut-out wind speed. However, this maximum may have an impact on fatigue life because the turbine will operate for more hours at this higher thrust (compared to fixed-speed operation), as this thrust occurs at a lower wind speed. Blade bending-moments qualitatively show the same behavior as rotor thrust. Therefore, the same considerations relative to blade fatigue apply as seen for thrust. Dynamic effects deserve special attention for this rotor type. Preliminary results of simulations [3] have shown that at low RPM and low wind speeds, the teeter mode is more highly excited in turbulent winds compared to the fixed-speed mode. This is because of the reduced centrifugal forces on the rotor blades holding the blades in a steady plane of rotation while operating in light winds at low RPM. Also, the rotor's first and second symmetric flapwise modes have been shown to respond strongly at various rotor RPM, even though some of these RPM points may be outside the useful RPM range. Depending on the results of an RPM scan performed on the test turbine, it may be necessary to exclude certain RPM set points from the useful RPM range ("Critical RPMs"). On the other hand, the same simulation showed that the variable-speed rotor exhibited fewer extreme torque loads, which indicates the potential for cost savings in the gearbox and low-speed shaft design. Verification of these simulation results through field tests will be necessary.

For pitch-controlled, rigid-hub, upwind rotors and torque-based VSGS control-algorithms, rotor thrust, bending-moment, and power all reach their respective rated values at maximum RPM and rated power [4]. If the turbine operates inside the maximum RPM/rated-power envelope, none of the other critical parameters will exceed its respective rated value. Depending on how well the turbine torque is dynamically controlled, the fatigue-life of all drivetrain components is prolonged compared to fixed-speed operation. Dynamic effects have been investigated in a similar way for the downwind, teetered-hub rotor. However, in practice, no critical RPMs were observed during operation of the turbine tested in this project.

2.1.3 VSGS Electrical Topologies

Figures 2.2 through 2.4 show the electrical VSGS topologies allowing variable-speed operation over the full range of wind-speeds, which we considered viable for turbine power ratings of 275 kW or more. System cost and performance calculations for all topologies can be found in section 2.2.

Figure 2.2 shows the VSGS topology that uses the existing induction generator with a power electronic converter inserted between the generator and the utility grid. When vector-control for the induction generator is implemented, this system is capable of tightly controlling the turbine torque up to rated torque. Although the induction generator is very efficient and cost-effective, the overall VSGS suffers greatly in terms of efficiency and cost because the converter has to be rated for the rated power of the turbine (plus transient overloads).

Figure 2.3 shows the VSGS topology that uses a synchronous generator with a power electronic converter inserted between the generator and the utility grid. This topology has been used for some of the first high-power (> 1 megawatt [MW]) variable-speed wind turbine prototypes. Because of the use of a synchronous generator, it is possible to use either a thyristor-based, load-commutated inverter or a rectifier-inverter for this topology. A recent implementation of this topology uses a direct-drive generator that eliminates both the cost and the efficiency loss of the gearbox at the cost of a more expensive generator (Enercon GmbH, Germany, E40 and E66 turbines). Although the efficiency of the synchronous-generator/load-commutated inverter topology is somewhat higher than the efficiency of the induction-generator-based topology, it has the drawback of less accurate dynamic control. For VSGS using the load-commutated inverter, problems with power quality and grid power factor require hardware filters and power-factor-correction equipment. Another variation of this topology is a VSGS that uses a permanent-magnet generator, which is more efficient than any other generator. Even though widely used for small wind turbines, this generator type is much too expensive for utility-scale wind turbines.

Figure 2.4 shows the VSGS topology that uses a doubly fed induction generator in connection with a fractionally rated power electronic converter. The doubly fed induction generator is a wound-rotor induction generator. The three-phase rotor windings are connected through slip rings to a four-quadrant, power electronic converter capable of exciting the rotor with currents between DC and 60 Hz. The rotor frequency is chosen such that—together with the mechanical rotation of the rotor—a rotational magnetic field results that rotates at the same speed as the field of the stator which is directly connected to the utility grid (see Figure 2.4). While allowing tight dynamic control over the full torque range, this topology offers both the highest efficiency combined with the lowest system cost of all topologies for VSGS ratings of 300 kW or more. It is for this reason that we proposed this topology for utility-scale, variable-speed wind turbine applications.

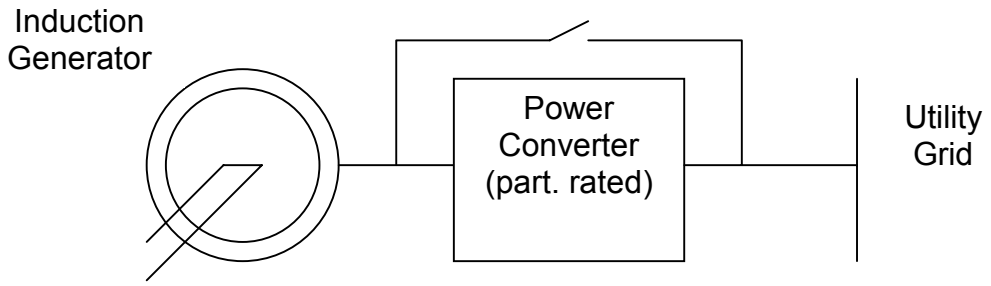

Figure 2.1 VSGS using an induction generator with a partially rated converter and a bypass switch

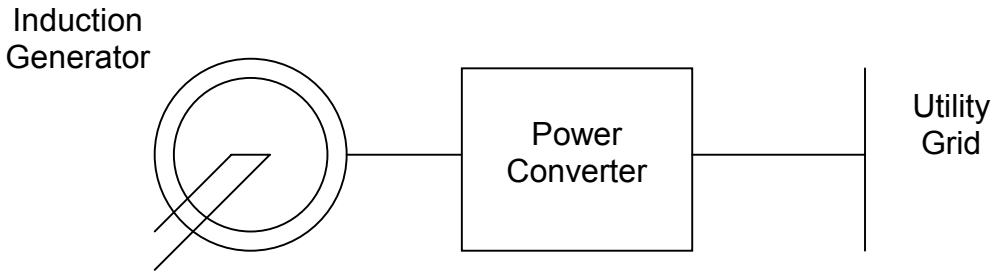

Figure 2.2 VSGS using an induction generator with a fully rated converter

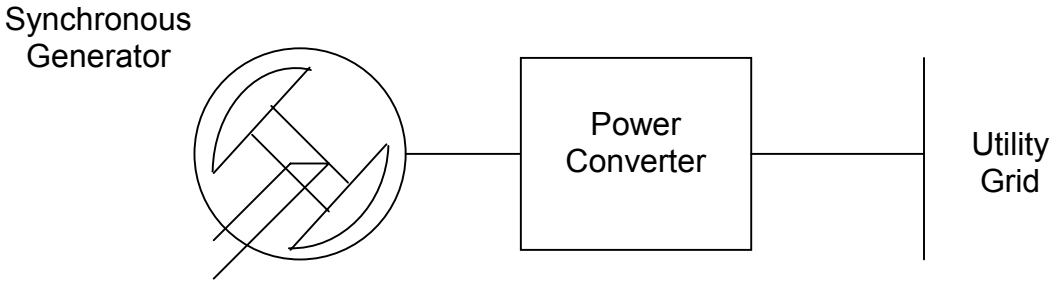

Figure 2.3 VSGS using a synchronous generator with fully rated converter

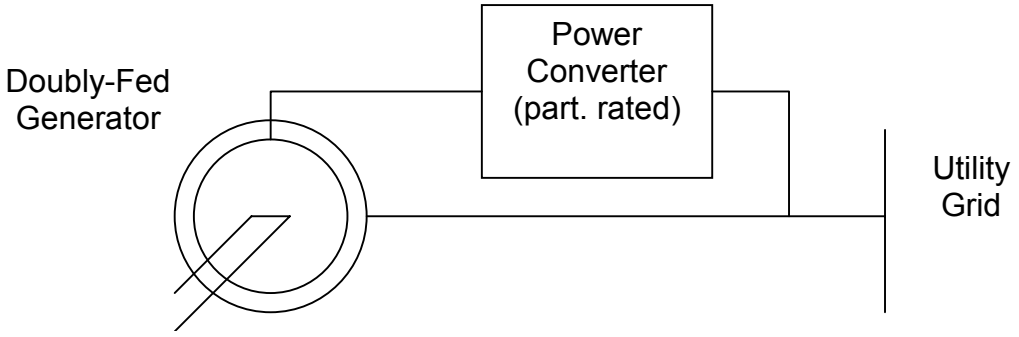

Figure 2.4 Doubly fed generator with partially rated converter

2.1.4 Power Quality Considerations

Early VSGS designs suffered—among other technical shortcomings—from very high Total Demand Distortion (TDD) and low power factor at the Point of Common Coupling (PCC) with the utility grid. This shortcoming quickly became a serious issue when power quality problems on weak utility grids in coastal regions of Europe were traced back to newly installed variable-speed wind turbines. Because of increasing power quality problems in the United States, the Institute of Electrical and Electronics Engineers (IEEE) Standard 519-1992 was established. It requires that any type of power-generation equipment inject no more than 5% of harmonic current relative to the rated system current at the Point of Common Coupling with the utility grid (also referred to as TDD). The relative figure of merit, however, is not Total Harmonic Distortion (THD), which is based on the rated current of the equipment that has been connected to the PCC, but rather based on the current rating of the utility transformer itself. Only in the unlikely case that a VSGS using the full power-conditioning approach was connected to a utility transformer of equal rating, would TDD be equal to THD.

For a VSGS using the doubly fed approach, the situation allows for a considerably higher converter THD on the utility grid because only a small fraction of the total VSGS output power is contributed by the converter. The following two examples show the maximum allowable THD limits for converters in connection with doubly fed generation systems that still meet IEEE 519-1992 requirements.

Example 1:

Utility transformer:	350 kilovolt-amperes (kVA), 480 VAC secondary, 420 amps rated
Doubly-fed generator:	300-kW, 6-pole, operating at full power and 1600 RPM, with 225-kW stator power and 75-kW rotor (and converter) power (all losses neglected)

The stator current is 270 amps and the converter grid current is 90 amps. Five percent TDD at the PCC based on 420 amps rated transformer current results in 21 amps of permissible harmonic current. Because the harmonic output of the generator stator can be considered negligible, the converter is allowed to inject 21 amps of harmonic current into the grid. Based on its grid current rating of 90 amps, that results in 23% of permissible converter THD.

Example 2:

Utility transformer:	1000 kVA, 480 VAC secondary, 1200 amps rated
Doubly-fed generator:	750 kW, 6-pole, operating at full power and 1600 RPM, with 563 kW stator power and 187 kW rotor (and converter) power (all losses neglected)

The stator current is 675 amps and the converter grid current is 225 amps. Five percent TDD at the PCC based on 1200 amps rated transformer current results in 60 amps of permissible harmonic current. Because the harmonic output of the generator stator can be considered negligible, the converter is allowed to inject 60 amps of harmonic current into the grid. Based on its grid current rating of 225 amps, that results in 27% of permissible converter THD.

The two examples show clearly that, for the doubly fed approach, the harmonic performance of the power-electronic converter does not have to be exceptionally good to meet IEEE 519-1992 requirements. Another issue, however, is power factor. Early VSGS designs utilizing controlled rectifier-bridges on the grid side were drawing large amounts of reactive power from the utility grid. Power factor compensation required by the local utility proved costly and—due to frequently encountered grid resonance using capacitors—technically difficult. Therefore, a VSGS is needed that inherently allows power factor control at the PCC. The doubly fed VSGS allows power factor control through either the rotor current magnitude or through control of the out-of-phase component of the grid-side converter current.

2.2 Performance and Cost Analyses

In cooperation with our lower-tier subcontractors, we conducted variable-speed turbine performance and cost analyses on the two most representative utility-scale turbine types. The results of these analyses are summarized separately for each turbine type below. Details of the analyses can be found in [2] and [4].

- AEP gains caused by variable-speed operation decrease as the site-specific average wind speed increases. Therefore, variable-speed operation shows higher AEP increases at sites with low average wind speeds.

- AEP gains resulting from variable-speed operation decrease as the useful RPM range decreases. There is a trade-off between VSGS cost, AEP gain, and peak-loads (especially in the case of stall-controlled turbines). This will require further study, especially with respect to the effects that various VSGS control algorithms have on turbine structural loads.

- For large turbines (> 500 kW), the majority of the COE reduction may result from the cost reduction in drivetrain (and other mechanical) components due to tightly controlled peak loads, rather than from increases in AEP. Unfortunately, we were not able to obtain exact figures for cost reductions for the major mechanical components (such as the gearbox). This was mostly because we could not obtain more than estimates and results of computer simulations indicating variable-speed loads. Nor could we obtain cost figures for an optimized gearbox based on these figures.

2.2.1 Z-40M Analysis

The analysis of AEP gains resulting from variable-speed operation of this turbine showed a gain of 6.0% over fixed-speed operation for an NREL site (13 miles per hour annual average wind speed at 10 meters above ground, wind-shear exponent of 0.14). These projected gains are based on conservative estimates for the electrical component efficiencies. The estimated variable-speed power curve for this turbine can be found in [4].

The following table shows the cost comparison for a 550-kW turbine. It compares the cost of the electrical system for the standard fixed-speed version, the full power conversion, variable-speed version (induction generator with fully rated inverter), and the variable-speed version based on the doubly fed induction generator. A substantial production volume (at least 100 units/year) is accounted for in all cost figures. The cost basis for the converters is $100/kVA of rating. The converter for the full power conversion system has a rating allowance for overloads of 115%. The power converter rating for the doubly fed VSGS is 40% of the VSGS rating. One thousand dollars has been added for each converter for proper environmental packaging.

Table 2.1 Z-40M VSGS Cost Comparison

Component Cost	Topology		
	Fixed-Speed Baseline	Full Power Conversion	Doubly Fed
Generator Cost	$21,000	$21,000	$24,100
Switchgear/Power Converter Cost	$7,500	$64,250	$23,000
Total Cost	$28,500	$85,250	$47,100
Cost Relative to Baseline	1.0	2.99	1.65

The projected cost increase of this turbine in production quantities resulting from the implementation of the doubly fed VSGS is $18,600.

2.2.2 AWT-26 Analysis

The analysis of the AEP gains for the AWT-26 turbine (24.4-m tower) at a standard NREL wind site (13 mph average wind-speed) showed a gain of 6.5%. Applying the same cost calculation as above, the cost increases for the full power conversion and doubly fed generation system relative to the fixed-speed baseline are:

Table 2.2 AWT-26 VSGS Cost Comparison

Component Cost	Topology		
	Fixed-Speed Baseline	Full Power Conversion	Doubly-Fed
Generator Cost	$7,000	$7,000	$9,000
Switchgear/Power Converter Cost	$4,500	$32,625	$12,000
Total Cost	$11,500	$39,625	$21,000
Cost Relative to Baseline	1.0	3.45	1.83

The projected cost increase of this turbine in production quantities resulting from the implementation of the doubly fed VSGS is $9500. This projection does not allow for cost reductions of any mechanical components (e.g., the gearbox or tower) resulting from reduced structural loads, or for the integration of the computerized turbine controls with the VSGS controls.

2.3 Operations and Maintenance Analysis

We attempted to predict the impact that the addition of the VSGS would have on both the mechanical and electrical subsystems of the turbine. However, only extensive field-testing will give an accurate picture of the operations and maintenance (O&M) requirements and their impact on O&M cost.

In general, addition of the VSGS will have a positive impact on the O&M cost of turbine mechanical subsystems. This is because the turbine will operate under reduced mechanical loads compared to fixed-speed operation, resulting in a potential increase of maintenance intervals for a number of components and reduced wear on such items as brake pads. Under normal operating conditions, it is possible to shut down

the turbine by means of the generator only, eliminating the wear on the aerodynamic and high-speed shaft brake components. Initially, the condition of the teeter-dampers will deserve more attention because of the suspected increase in teeter-movement during low-RPM operation. Only extended operation can confirm whether this is a maintenance concern.

Inspection of the generator brushes is the only special maintenance requirement for the doubly fed generator. The inspection should be performed at six-month intervals and focus on the condition and remaining length of the brushes. Brush replacement is required if a brush is worn below a minimum length or damaged in any way. This work can be performed by a service technician having minimal additional training and using standard tools. There is some concern about the possible damage to the brushes and rotor slip rings that can be caused by dust and sand contained in the cooling air. For the case of a totally enclosed, fan-cooled (TEFC) generator design, no cooling air from outside can come into contact with the brushes or slip-rings. This type of generator design is being used for the field test. Operating experience should be gained with the less expensive, open drip-proof (ODP) generator design that has been fitted with cooling-air filters. All other service requirements for the generator (periodic bearing lubrication, eventually total overhaul) are identical with the service requirements for fixed-speed induction generators. The life expectancy of the generator windings remains the same as for fixed-speed turbines, but only because we use soft-switching converter topologies that do not apply excessive voltage transients to the rotor windings. Although it is possible to use a standard four-quadrant, pulse-width modulated (PWM) inverter instead, the life expectancy of the generator rotor windings would be substantially reduced. The generators would have to be rewound much more often than in our case. This could have a substantial impact on O&M costs.

The power electronic converter that operates the turbine at variable speeds is as reliable, but also as susceptible to damage from external transients (such as incoming transients on the utility grid, or direct lightning hits on the turbine or nearby power transmission lines), as the solid-state soft-starters that are commonly used in fixed-speed wind turbines. Fast-acting protective devices (solid-state rectifier fuses, metal-oxide varistors, and lightning arrestors) are being used at the input and output of the converter to protect the power circuit from such disturbances to the extent possible. If the converter sustains damage from such an event, the sustained damage should be perceived as somewhat greater than for a fixed-speed turbine. In such a case, an additional allowance ($80 per year per turbine) in the estimated O&M costs should be made to cover more expensive repairs. The converter itself does not contain parts that require any periodic maintenance. Intakes and outlets of cooling air may have to be checked periodically for any accumulation of dust or other foreign matter. Some training for service technicians on how to trouble-shoot the VSGS will be required.

Considering both the reduction in maintenance cost for the mechanical systems and the increase in maintenance for the VSGS, the overall O&M cost for the turbine is expected to remain unchanged. VSGS operating experience gained during the field test has provided a more accurate picture of the system's reliability. Field-test results will be covered in Chapter 6.

2.4 Special Considerations for the Baseline Turbines

Once the useful RPM range for a turbine rotor has been established, the turbine designer has to determine the optimal power/RPM curve for the turbine rotor. RPM will increase linearly with wind speed for peak-C_p operation in Region II (turbine output power below rated output power). In Region III (turbine output power at rated output power), for a stall-regulated rotor, RPM has to be reduced with increasing wind speed to maintain constant output power. For a least-cost design, the transmission-ratio has to be chosen such that the doubly fed generator operates at synchronous RPM halfway between the minimum useful and maximum allowable RPM. Synchronous RPM for the generator can be derived from the following equation:

$$RPM_{synch} = 120 * \text{line-frequency [Hz]} / \text{Number of poles}$$

i.e., synchronous RPM of a six-pole generator operating on a 60-Hz utility grid is 1200 RPM. There is a trade-off between the size, weight, and cost of the generator, which increases with the number of poles, and the size, weight, and cost of the gearbox, which increases with the transmission ratio. Regarding the brushes,

operating experience on the MOD-5B prototype in Hawaii indicates that operation below 1800 RPM results in acceptable brush wear. We chose a synchronous RPM of 1200 RPM for both generator designs. We also developed a spreadsheet-based design program that requires the VSGS designer to enter a series of rotor mechanical output power points together with their respective RPM set points. Based on this information and a given transmission ratio, utility grid voltage, grid frequency, and the number of generator poles, the program will calculate generator RPM and all electrical characteristics of the doubly fed generator and the power electronic converter (assuming unity power factor operation on the generator stator) for each operating point. If the generator losses are already known (friction, rotor- and stator-resistances, and iron losses), and an efficiency curve of the power converter is available, the program will also calculate component and overall efficiencies. Finally, the program calculates generator and converter ratings based on the extreme operating points of the turbine rotor.

2.4.1 Special Considerations for the Z-40M

Details regarding the impact of variable-speed operation on this baseline turbine can be found in [4].

The useful RPM range was found to be 21–38 RPM. Using a gearbox ratio of 1:40.6 resulted in a generator RPM-range of 850-1550 RPM. From the estimated power curve of the turbine rotor, the following specifications resulted for the doubly-fed generator for operation on a 480-VAC, 60-Hz utility grid:

Number of poles:	6
Synchronous RPM:	1200 RPM
Stator voltage:	480 VAC
Stator current:	660 Amps
Rotor voltage:	480 VAC
Rotor current:	280 Amps
Rotor:stator winding ratio:	2.6:1
Service factor:	1.15

Zond Systems, Inc., purchased a wound-rotor generator with these specifications from Marathon Electric Company.

The resulting specifications for the variable-frequency, four-quadrant power converter were:

Power rating:	250 kVA
Voltage rating:	480 VAC
Current rating:	300 Amps
Overload rating:	133% for 1 minute

A simple overall protection scheme for the turbine was implemented. This scheme allowed both the VSGS and the turbine controller to shut each other down after detecting a fault.

In terms of adequacy of the mechanical design, the strength of the yaw deck and the components of the yaw drives had the lowest projected safety factors. However, for the purpose of a limited-duration test, the design of these components was considered adequate. As predicted, thrust and bending-moments reach their peak values at rated power output at cutout wind speed. Neither parameter exhibits local maximums.

The analysis of the structural dynamics shows several operating points that could potentially excite mechanical resonance (i.e., at approx. 29 RPM). However, only an RPM scan performed during initial turbine testing will reveal whether there are any critical RPMs at which prolonged operation could cause resonance problems.

2.4.2 Special Considerations for the AWT-26

Details regarding the impact of variable-speed operation on this baseline turbine can be found in [2].

The useful RPM range was found to be 30–62 RPM. Using a gearbox ratio of 1:26.1 yielded a generator RPM range of 780–1620 RPM. From the estimated power curve of the turbine rotor, the following specifications resulted for the doubly fed generator for operation on a 480-VAC, 60-Hz utility grid:

Number of poles:	6
Synchronous RPM:	1200 RPM
Stator voltage:	480 VAC
Stator current:	285 amps
Rotor voltage:	480 VAC
Rotor current:	120 amps
Rotor:stator winding ratio:	2.6:1
Service factor:	1.0

We purchased a wound-rotor generator with these specifications from Reuland Electric Company.

The resulting specifications for the variable-frequency, four-quadrant power converter were:

Power rating:	110 kVA
Voltage rating:	480 VAC
Current rating:	130 amps
Overload rating:	150% for 1 minute

A simple overall protection scheme for the turbine was implemented. This scheme allowed both the VSGS and the turbine controller to shut each other down after detecting a fault.

In terms of adequacy of the mechanical design, we focused on the capabilities of the aerodynamic and high-speed shaft braking components. The theoretically desirable peak rotational speed of 78 RPM had to be severely restricted due to the limited braking capacity. Unless a major redesign were performed, neither braking system was considered capable of stopping the turbine above 67 RPM. (The 5-RPM margin is necessary to account for delays in executing a hard-stop command.) This restriction will result in a measurable reduction of AEP gain. As predicted, thrust and bending-moments reach their peak values at rated power output at cutout wind speed. Both parameters exhibit a local maximum at peak rotational speed at approximately 29-mph wind speed. With 62 RPM as peak rotational speed, the safety margins of all other mechanical components remain virtually unaffected.

Independent from the investigations into the effects of variable-speed operation on this turbine, Advanced Wind Turbines, Inc., found that the existing design of the nacelle mainframe required reinforcement. Therefore, a recommendation was made to implement a mainframe stiffener while the nacelle was being retrofitted for variable-speed operation.

The analysis of the structural dynamics shows several RPM points that could excite mechanical resonance (i.e., at approximately 30 and 57 RPM). However, only an RPM scan performed during initial turbine testing will reveal whether there are any critical RPMs at which prolonged operation could cause resonance problems. The potential for teeter instability at low RPM in light but turbulent winds deserves particular attention.

2.5 VSGS Control Strategies and Real-Time Turbine Simulations

2.5.1 Z-40M VSGS Controls

The variable-speed turbine control strategy evolved over two iterations. Initially, we proposed an RPM-based control approach for the doubly-fed generator that was dynamically softened. The expected result was damping of the low-speed shaft-torque oscillations. The average operating RPM followed a target RPM curve that is based on the optimal power-RPM characteristic of the turbine rotor for peak-C_p operation. Limitation of the output power was the task of the pitch-controller. Figure 2.5 shows the block diagram of this controller.

Results of simulations [5] showed that some interference between the different controls could be expected. In addition, power excursions caused by attempts to rapidly slow the turbine rotor (inertia effects) were seen, and the ability of the pitch-controller to limit dynamic power excursions was limited because of its inherently slow response. Undesirable excursions in power were observed while transitioning back and forth between Regions II (maximum C_p operation) and III (constant RPM operation).

As a result, a much more simplified approach (in theory) was chosen: directly control the high-speed shaft-torque of the doubly-fed generator using field-oriented control, and control the peak RPM with pitch. The average operating torque follows a target torque curve that is based on the optimal torque-RPM characteristic of the turbine rotor for peak-C_p operation. Maximum power limitation is inherent due to maximum RPM limitation of the pitch-controller combined with maximum torque operation of the generator. There are several advantages to this approach:

- The two control loops are well decoupled,
- The slow-acting pitch-controller controls RPM, which by itself can only vary slowly because of the large rotor inertia involved, and
- Transitions between Regions II and III are smooth.

Although the high-speed shaft torque will be tightly controlled, we expect some undesired torque dynamics on the low-speed shaft resulting from the finite stiffness of the gearbox.

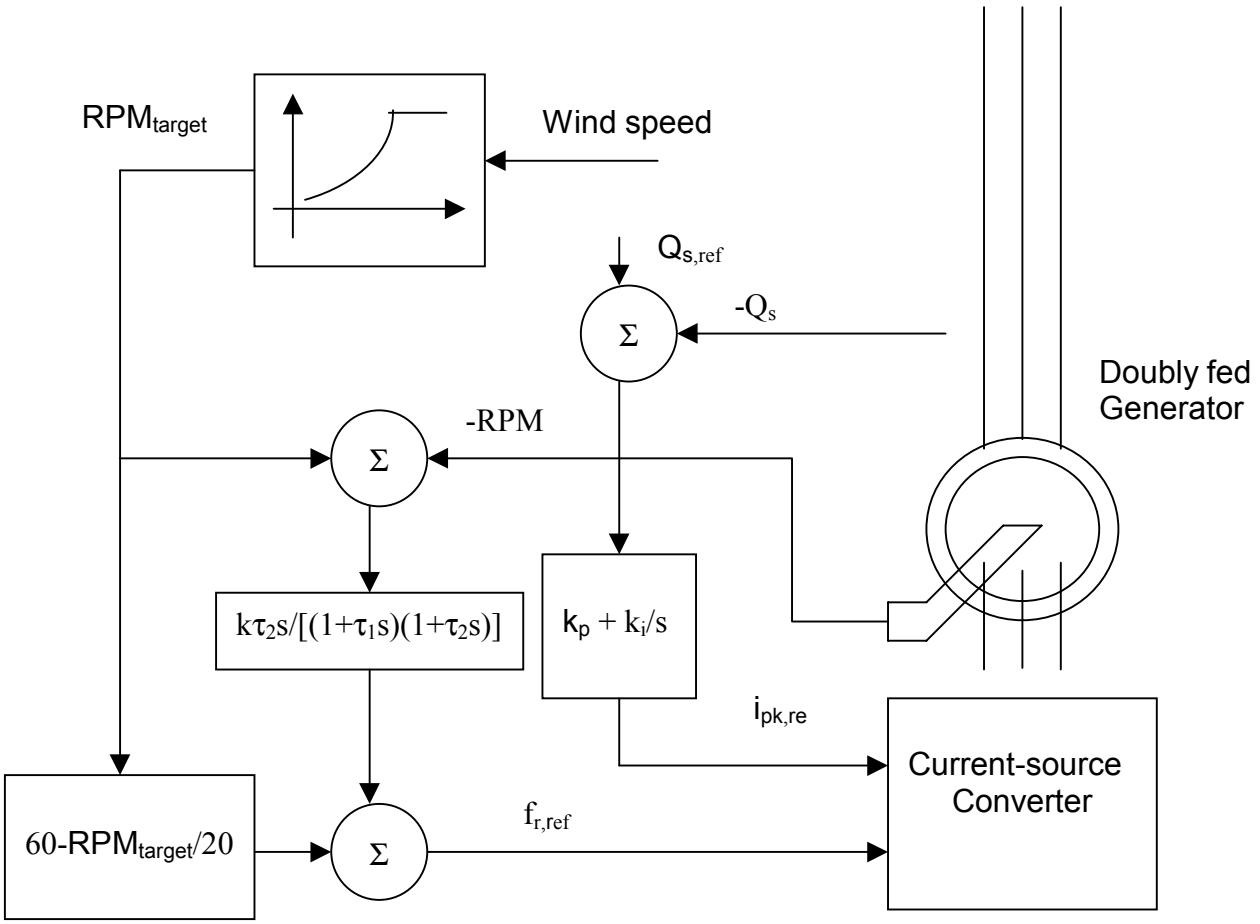

Figure 2.5 Block diagram of RPM-based control scheme

2.5.2 AWT-26 VSGS Controls

The main difference between the Z-40M VSGS controls and the AWT-26 VSGS controls is that the only means of control for the AWT-26 is either generator RPM or generator torque. Control of maximum C_p-operation and peak-power limitation have to be accomplished with one single means of control.

2.5.2.1 RPM-based Control Scheme

Initially, we proposed an RPM-based control algorithm. This approach tracks a target RPM curve up to the maximum allowable rotor RPM in Region II, then maintains maximum allowable RPM until the output power reaches its rated value. It then reduces RPM (Region III), forcing the rotor into stall by reducing RPM such that rated output power is maintained. Simulations showed that the transition from maximum RPM to rated-power operation may result in substantial power excursions if the VSGS controller attempts to decelerate the turbine rotor too fast. Conversely, during wind gusts there will be power excursions if the VSGS controller does not decelerate the turbine rotor fast enough. The only way to avoid this problem is to reduce the maximum allowable RPM until the magnitude of the power excursions becomes acceptable. However, this may not happen until the maximum RPM setting has been reduced to the fixed-speed RPM of the turbine rotor. At that point, a large portion of the potential variable-speed AEP gain has been foregone.

2.5.2.2 Soft-Stall Control

Another, more promising, approach is based on generator torque control. The generator torque follows a target-torque curve as outlined in the second Z-40M VSGS control approach; however, it will not follow this curve all the way up to rated output power. At some earlier point, the target-torque curve will deviate from the optimum target-torque curve and command an increasingly higher torque (higher than the optimum target-torque curve), resulting in a gradual stall-entry of the turbine rotor. Figure 2.6 shows the general concept of this approach. The increase in target-torque has to be rapid enough so that the turbine rotor is not able to exceed a desired maximum RPM_C and maximum power P_C (see target power-curve O-A-B-C). The maximum Cp-curve is given by O-A-D [1]. Some experimentation will be required to find the optimum parameter settings for the algorithm (i.e., RPM_A, P_A). However, there will always be a trade-off between maximizing AEP gain and minimizing output power transients.

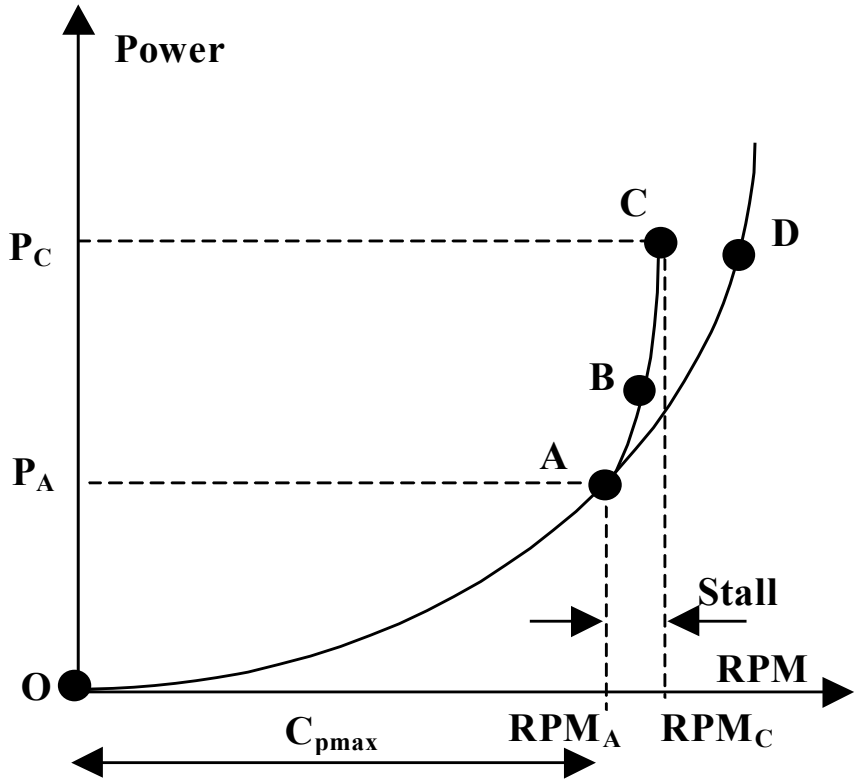

Figure 2.6 Target power-RPM curve for soft-stall control method

Simulations have shown that it is possible to limit RPM and power with little overshoot to their desired maximum values. Additional simulations showed that this approach reduces dynamic flap bending-moments on the blades (and torque oscillations on the drivetrain) at low and medium wind speeds compared to fixed-speed operation, whereas tower loads were slightly increased at low and medium wind speeds. Differences between both modes of operation at high wind speeds were insignificant [1].

2.5.2.3 Maximum Energy Capture Control

We simulated yet another control approach that is similar to the approach described in Section 2.5.2.1; however, this approach uses generator torque control as its innermost control loop, thus avoiding the drawbacks of the earlier attempt. A block diagram of this approach, which was developed and simulated extensively by engineers at NREL [6], is shown in Figure 2.7.

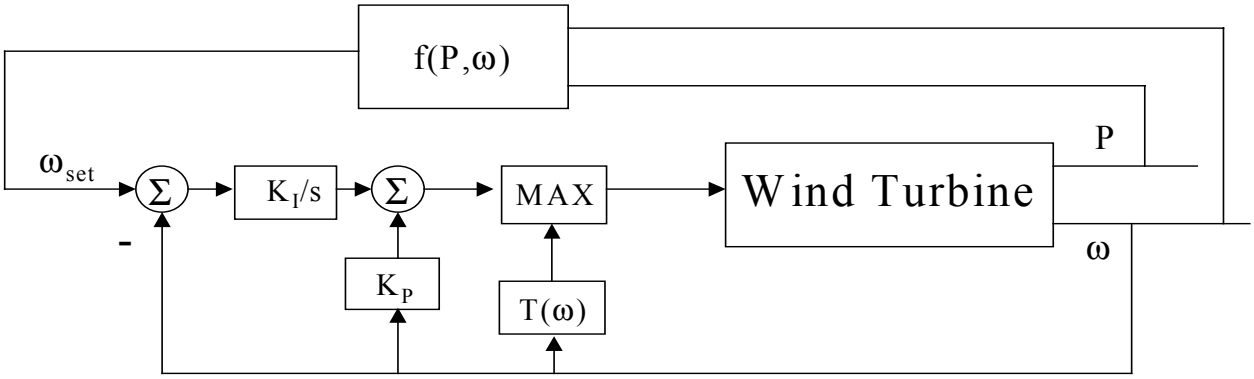

Figure 2.7 Maximum energy capture control approach

This approach involves maintaining maximum C_p operation until the turbine reaches maximum operating RPM, then transitioning into a constant RPM mode until rated output power has been reached, and finally transitioning into a constant power mode of operation by reducing operating RPM. Compared to the soft-stall approach, this method should yield most of the additional output power that the soft-stall approach loses by early deviation from constant C_p operation. Figure 2.8 shows the theoretical RPM vs. output power characteristic of this method.

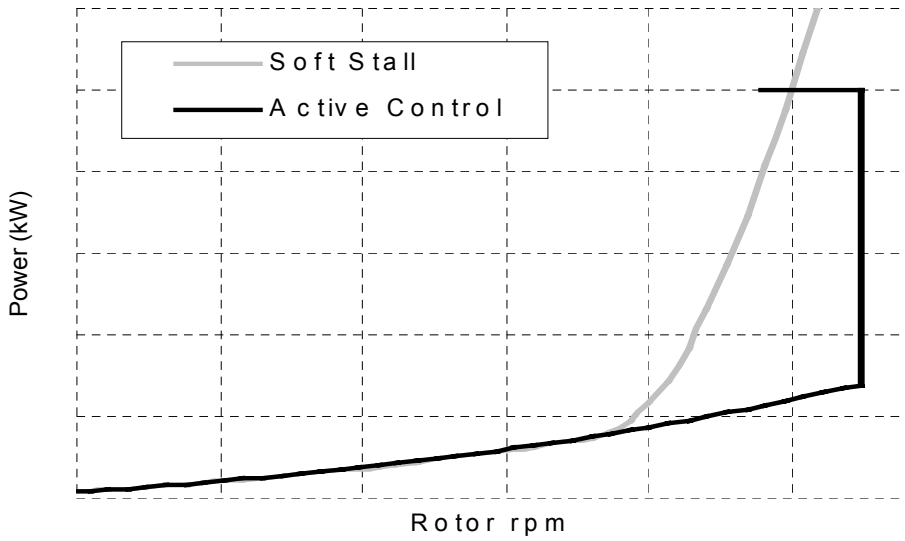

Figure 2.8 Comparison of power-RPM characteristic of soft-stall vs. max. energy capture approaches

3.0 VSGS Component Development

3.1 Converter Design, Assembly, and Testing

3.1.1 USRC Specifications and Design

We designed, built, and tested two unipolar series-resonant converters (USRCs) for the two turbines on which we tested the VSGS. A unipolar, series-resonant converter is a bidirectional power electronic converter that is based on a patented soft-switching power circuit topology. The main power switches are inverter-grade thyristors. It is therefore possible to build this type of converter for high power levels (300-500 kVA at 480 VAC). The converter is characterized by a high power-conversion efficiency and exceptional power quality, on both the grid and the load sides. It exceeds IEEE 519-1992 power quality standards. The converter is capable of operating at unity power factor on the grid side. The mode of operation on the load side can be selected for each particular application (current source, voltage source, or voltage/frequency). For this particular application (control of the doubly fed generator), the converter must be operated in current-source mode.

The specifications for the two USRCs are (see also sections 2.4.1 and 2.4.2):

Table 3.1 USRC Specifications

Specification	Z-40M VSGS	AWT-26 VSGS
Power (kVA)	250	109
Voltage (VAC)	480	480
Output Current (amps)	300	130
Overload (% of rated, instantaneous/1 minute)	133	150
Output Frequency Range (Hz)	0 to 60	0 to 60

Using a proprietary spreadsheet-based design program that we developed outside this project, we derived the specifications for all electrical components of the two converters. We selected the components based on these specifications. After we selected the semiconductors, we projected their heat losses under operation at rated currents, an ambient temperature not to exceed 40ºC, and forced cooling, and derived specifications for their respective heat sinks based on the projected heat losses. The passive components of the power circuit (inductors, capacitors, and resistors) were selected thereafter. Circuit diagrams for the USRC power circuit can be found in Appendix A.2.

A complex control circuit is required to operate the USRC power circuit. The controller hardware and the extensive software for the digital controls were developed outside this project. The converter controller is contained on a single printed circuit board (PCB), which includes the high-voltage and current transducer inputs, the analog circuits, the digital circuits, and the optical transmitters sending firing signals to the semiconductor drivers, as well as the digital interface to the VSGS controller. With the exception of timing parameter settings, the USRC controllers are identical for both converters.

3.2 Doubly Fed Generator Design, Assembly, and Testing

3.2.1 Doubly Fed Generator Specifications and Design

The electrical specifications for the doubly fed generators were derived in sections 2.4.1 and 2.4.2. Because of the retrofit situation, the mechanical specifications for both generators were dictated by the existing fixed-speed generators and by space constraints in the turbine nacelles.

Cooling of doubly fed generators requires careful consideration. Because the doubly fed generator requires slip rings and brushes, operation of this type of machine in an environment with considerable dust and sand contamination may cause maintenance and reliability problems. For the retrofit of the AWT-26 turbine, we resolved the issue by using a totally enclosed and fan-cooled generator (TEFC). Air circulates internally in the generator and transfers heat to the generator frame, which has cooling fins on the outside. A motor-driven blower blows cooling air through the cooling fins from the back towards the front. The flow of cooling air around the generator is aligned with the wind direction because the turbine is a downwind turbine. The only possible contamination inside the generator is brush dust. However, for the doubly fed generator of the Z-40M, this approach was not feasible. Except for a cast-iron spider holding the rear shaft bearing, the rear end of this generator is open. A motor-driven blower mounted on the rear end draws air through the generator windings and the air gap and blows it out the back. (The blower is oriented downwind once the generator is installed on the turbine.) The cooling-air intake at the front of the generator should be equipped with an intake air filter.

Table 3.2 Summary of Doubly Fed Generator Specifications

Specification	Z-40M DFG	AWT-26 DFG
Number of Poles	6	6
Service Factor	1.15	1.0
Shaft	custom	3⅜"
Frame	544	449T
Flange	custom	end-bell
Stator Voltage (VAC)	480	480
Stator Current (amps)	660	285
Rotor Voltage (VAC)	480	480
Rotor Current (amps)	280	120
Stator:Rotor Winding Ratio	2.76:1	2.6:1
Efficiency (%)	> 96	> 95
Insulation Class	H	H
Ambient Temperature (°C)	50	50
Shaft-Speed Encoder (PPR)	A:1200; B:1	A:240; B:1

Both generators are equipped with analog temperature sensors, thermostats for the cooling fan, and over-temperature switches to shut down the turbine if the generator temperature exceeds its maximum allowable value. Furthermore, they are equipped with optical RPM encoders mounted on the rear of the generator shaft. The encoder output signals (one signal being a symmetric pulse, the other a pulse-per-revolution [PPR] index pulse) are required for field-oriented control of the doubly fed generator and are transmitted to the VSGS controller via fiber optic links.

The required generator frame size for the retrofit of the AWT-26 turbine proved to be a major obstacle. A much less costly generator could have been chosen if there would have been latitude in the generator frame size. For new turbine designs, it is important to include generator manufacturers from the beginning through the drivetrain design process in order to arrive at a cost-optimized solution. The only generator manufacturer who was able to fit the wound-rotor generator design for the AWT-26 turbine in a size 449T frame was Reuland Electric Company of Industry, California.

The only size restriction for the Z-40M generator was dictated by the pitch actuator that is located directly below the generator on the gearbox. Zond Systems purchased this wound-rotor generator from Marathon Electric Company of Wausau, Wisconsin.

3.2.2 Doubly Fed Generator Test Results

The generator manufacturers tested the generators as induction generators with shorted rotor windings to determine the fixed-speed generator efficiency curves. They also performed no-load electrical tests to determine the winding resistance and machine impedance. The results of the tests performed on the doubly fed generator configuration are provided in section 4.3.2.

3.2.2.1 Z-40M Doubly Fed Generator

The doubly fed generator for the Z-40M was tested as a fixed-speed induction motor with shorted rotor windings at Marathon Electric Company on November 15, 1995.

The following parameters for the Thevenin equivalent single-phase circuit diagram were determined:

Stator resistance:		0.0064	Ohms
Rotor resistance (reflected back to stator):		0.005	Ohms
Magnetizing impedance:		1.140	Ohms
No-load test:	Stator voltage:	480.0	Volts
	Stator current:	232.9	Amps
Open rotor test:	Stator voltage:	200	Volts
	Stator current:	96.2	Amps
	Rotor voltage:	552	Volts
Load-independent losses:	Friction and windage:	1908	Watts
	Iron loss:	4780	Watts
	Blower:	2780	Watts

The fixed-speed motor efficiencies as function of % of rated load for the Marathon generator can be found in Volume 2, Chapter 1 of this report.

3.2.2.2 AWT-26 Doubly Fed Generator

The doubly fed generator for the AWT-26 was tested as a fixed-speed induction generator with shorted rotor windings at Reuland Electric Company in March 1997.

We determined the following parameters for the Thevenin equivalent single-phase circuit diagram:

Stator resistance (per phase):		0.0085	Ohms
Rotor resistance (per phase):		0.125	Ohms
Stator leakage impedance:		0.102	Ohms
Magnetizing impedance:		2.325	Ohms
Load-independent losses:	Friction and Windage:	1050	Watts
	Iron Losses:	2600	Watts

The fixed-speed efficiencies as function of % of rated load for the Reuland generator can be found in Volume 2, Chapter 1 of this report.

3.3 VSGS Controller Design, Assembly, and Testing

3.3.1 VSGS Controller Specifications, Architecture, and Design

The major tasks of the VSGS controller are:

(1) Real-time control of the doubly fed generator (by means of the power electronic converter):
- Execution of the field-oriented control algorithm for the doubly fed generator
- Execution of the aerodynamic efficiency maximization algorithm.

(2) Real-time VSGS protection:
- Continuous monitoring of all system fault inputs
- Execution of VSGS safe shut down.

(3) Operator interface:
- Display of major system variables
- Input capability of control parameters
- Start/stop/emergency stop.

(4) Turbine controller interface:
- Mutual safe turbine shutdown
- VSGS enable input
- DFG on-line output.

Executing these tasks, particularly task (1), requires a microprocessor-based controller capable of handling a multitude of digital input/output (I/O) channels while performing the required calculations fast enough to provide the power electronic converter with instantaneous output current references (in digital form) which, converted into analog signals, resemble nearly distortion-free sinusoidal waveforms.

Figure 3.1 shows a block diagram of the VSGS controller architecture that we have chosen. At the core of the controller is a digital signal processor (DSP, 32-bit floating point) that executes the high-speed calculations of task (1). Tasks (2), (3), and (4) are handled by a separate micro-controller. The controller hardware has been subdivided into three printed circuit boards (PCBs):

The microprocessor PCB, consisting of

- The DSP (Texas Instruments TMS320C)
- The micro-controller (Intel 80C196)
- A field-programmable gate array (FPGA, Xilinx XC4003H)
- Erasable programmable read-only memory (EPROMs) containing the code for each of the processors
- Nonvolatile random access memory (RAM)
- Parallel I/O ports to the USRC, the operator interface, and the analog and digital I/O PCB
- A serial port.

The display PCB, which features a 4 x 20-character display and a touch pad for operator input.

The I/O-PCB, which features 16 digital and 20 analog input channels, 16 digital and 4 analog output channels, as well as 2 optical input and 2 optical output channels.

The actual connections between the VSGS controller and the USRC controller, the display, the switchgear, and the analog sensing PCBs are shown in the circuit diagrams in Appendix A.2.

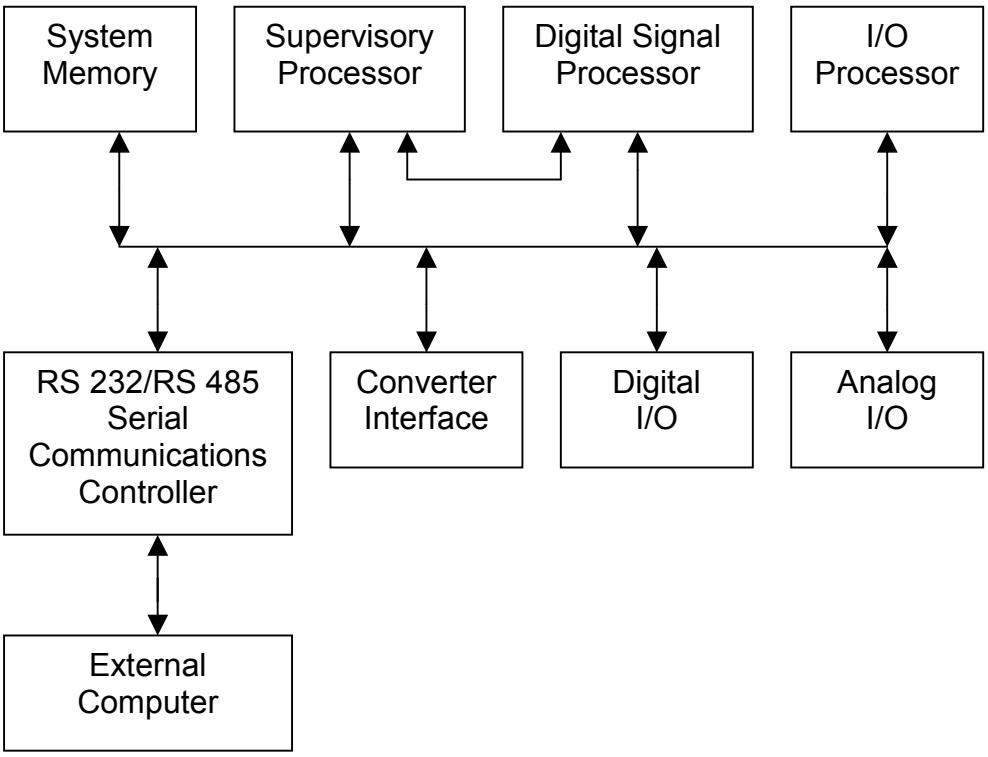

Figure 3.1 VSGS controller architecture

Currently, implementing the VSGS controller requires three additional PCBs that sense the following analog and digital parameters inside the DFG switchgear:

Analog: - Instantaneous stator reactive power (Q_s)
- Instantaneous stator active power (P_s)
- Instantaneous stator voltages (V_a, V_b, and V_c)
- Instantaneous total reactive power ($Q_{t)}$)
- Instantaneous total active power (P_t)

Digital: - Synchronization enable signal

The stator voltages, as well as the stator active and stator reactive power inputs, are required for the field-oriented control of the DFG, whereas total active and reactive power currently is used only for display purposes. These values may be transmitted to a SCADA system for wind-farm-control purposes.

The synchronization enable signal is required during start-up of the VSGS. To ensure a smooth synchronization process without adverse torque transients, the stator voltage phasors are being matched to the grid-voltage phasors before the stator is being connected to the grid. The VSGS controller accomplishes this task by adjusting the frequency and amplitude of the rotor currents. As soon as the stator and grid-voltage phasors are closely aligned, the synchronization enable signal enables closure of the stator circuit breaker.

Circuit diagrams for all three PCBs can be found in Appendix A.2.

3.3.2 VSGS/Turbine Controller Interface

We implemented a VSGS/turbine controller interface that provides minimal enable/fault communication between the VSGS and the turbine controller. The interface consists of one line from the turbine controller to the VSGS enabling the VSGS (i.e., requesting a VSGS start-up) upon contact closure, or requesting the VSGS to shut down upon contact opening. The second line communicates the occurrence of a VSGS fault to the turbine controller by means of a contact opening and results in a turbine shutdown. The third line indicates to the turbine controller by means of a contact closure that the doubly fed generator has been synchronized to the utility grid. We implemented the interface in such a way that an accidental interruption of any one of these lines is interpreted by the respective receiver as a command to stop the turbine. A circuit diagram for this interface can be found in Appendix A.2. For cases in which an exchange of operating data between the two controllers is desired, a serial interface can be added later on.

3.3.3 VSGS Controller Software Description

3.3.3.1 VSGS Controller Software Partitioning

The VSGS controller software is divided into the following segments:

(1) Keyboard/display interface
(2) VSGS protection
(3) USRC interface
(4) Data acquisition
(5) Generator control.

Each of these segments is described in detail below. Figures 3.2 through 3.11 show the flow charts of the VSGS software.

3.3.3.2 Keyboard/Display Interface

The keyboard and display software enables the operator to enter VSGS parameters and commands such as RUN/STOP from the keyboard. It also displays, with a periodic 0.03-second update, important operational data such as power, RPM, currents, and voltages on the front panel. This piece of software interfaces the keyboard and display with a micro-controller on the main control PCB.

3.3.3.3 VSGS Protection

The VSGS protection software monitors certain digital signals periodically (0.03-second update) to make sure that there is no emergency or other fault in the VSGS. In case of a fault, it takes appropriate action to shut down the VSGS (e.g., open contactors, stop the converter, stop the turbine). A converter fault is considered the most serious of all faults and is therefore detected instantaneously. The protection software can also monitor power-supply voltages to make sure that the converter controller can operate properly. Currently, the main diagnostics implemented are Emergency Fault, Converter Fault, Turbine Fault, and Internal Micro-controller Fault.

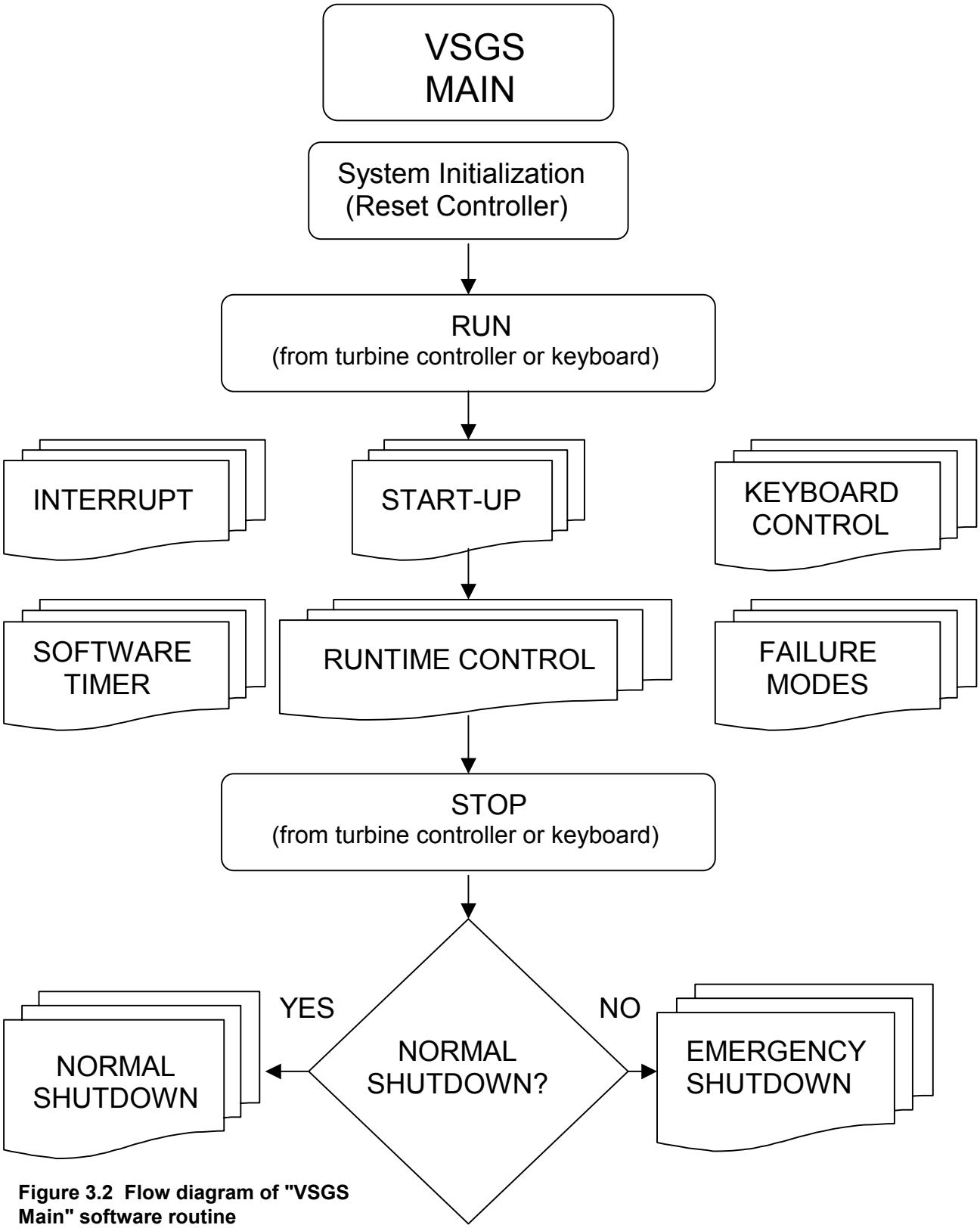

Figure 3.2 Flow diagram of "VSGS Main" software routine

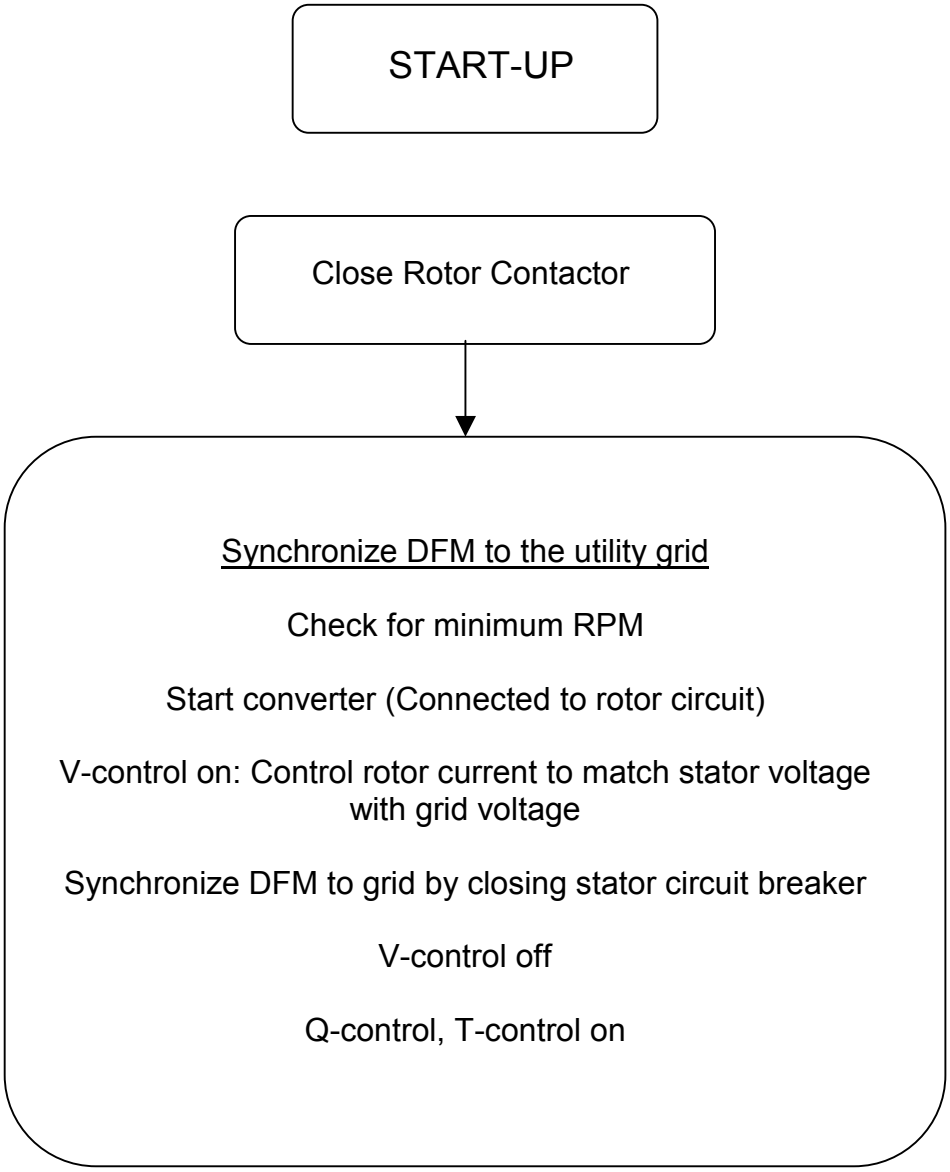

Figure 3.3 Flow diagram of "Start-up" software routine

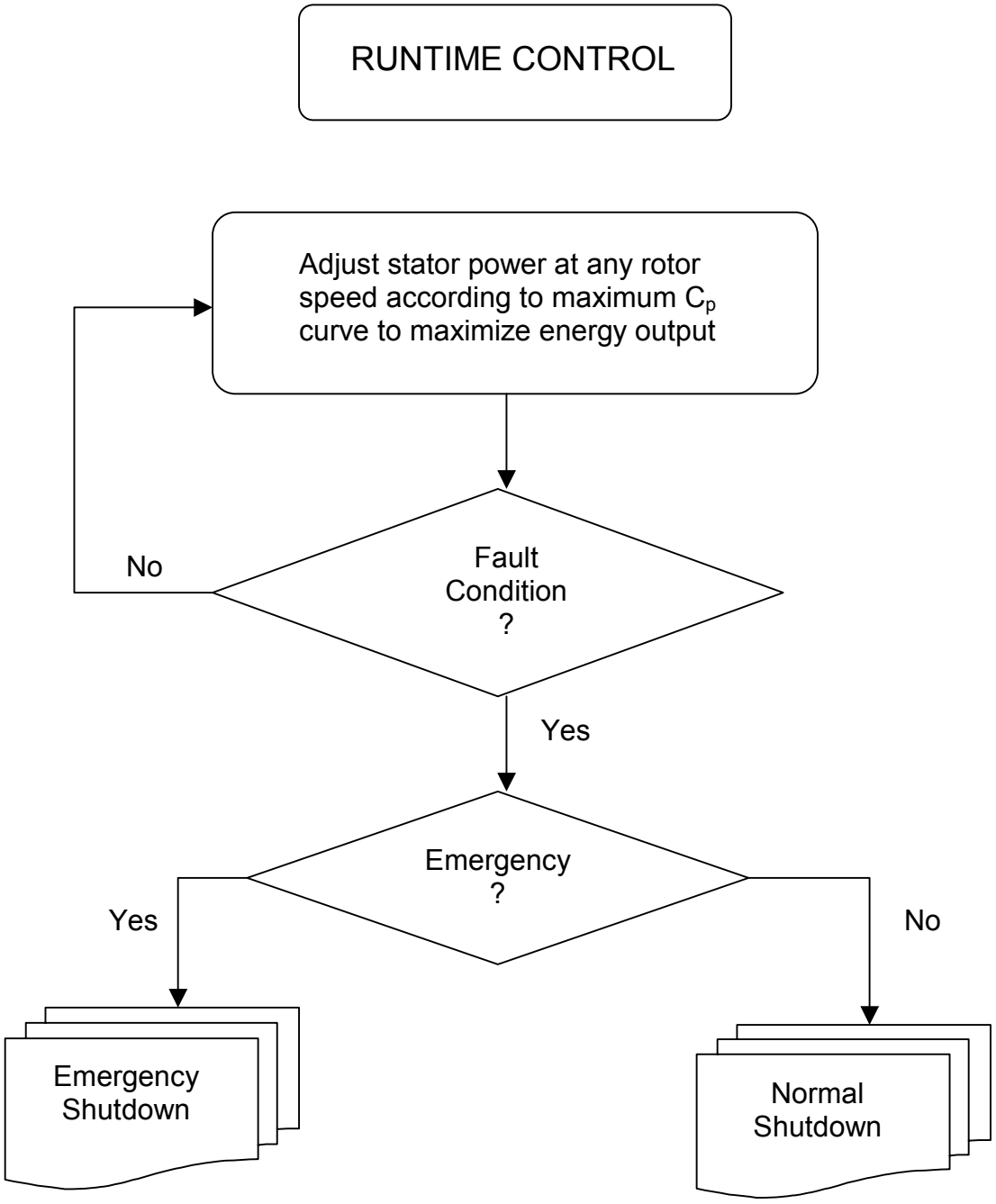

Figure 3.4 Flow diagram of "Runtime Control" software routine

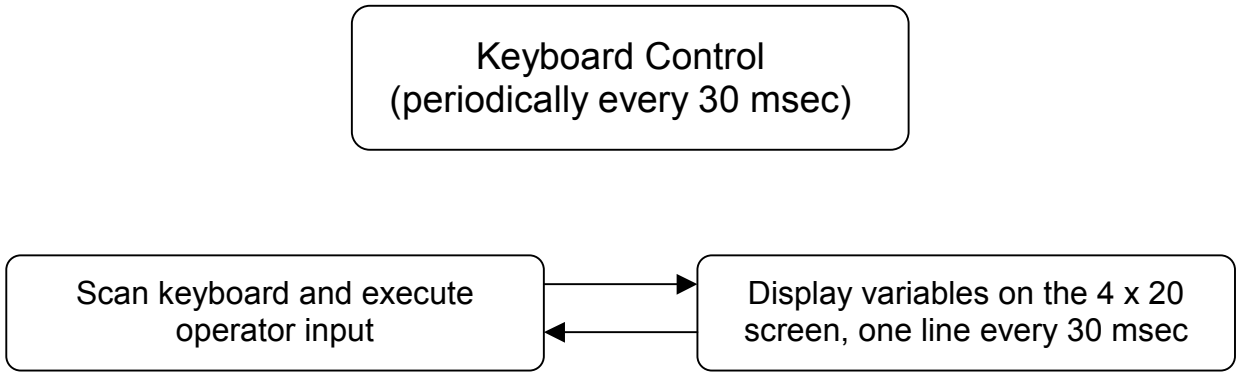

Figure 3.5 Flow diagram of "Keyboard Control" software routine

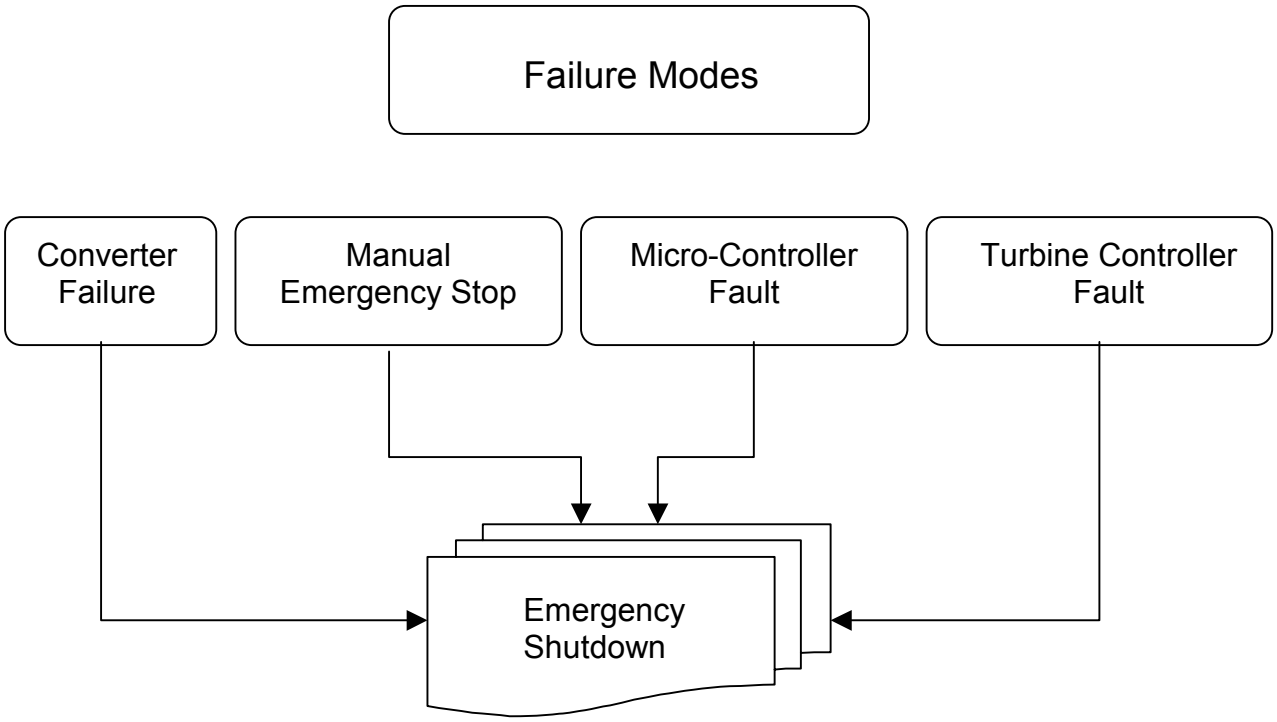

Figure 3.6 Flow diagram of "Failure Modes" software routine

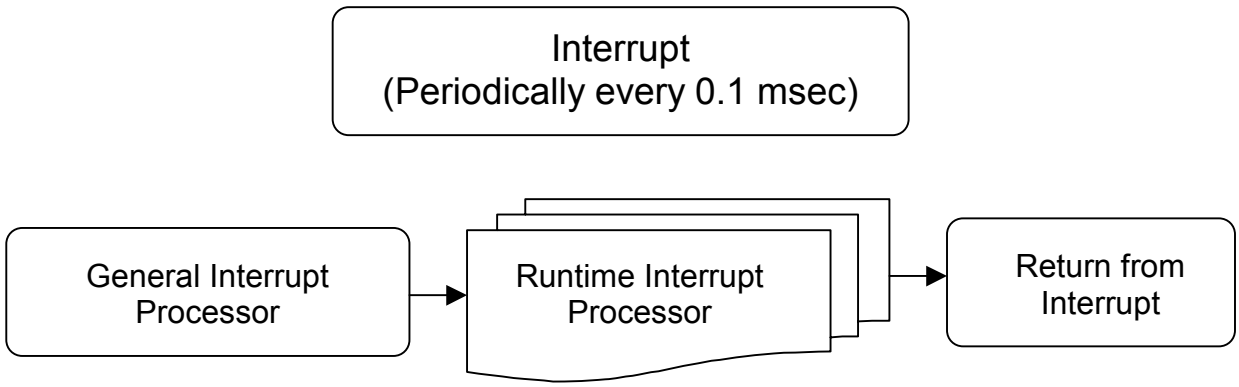

Figure 3.7 Flow diagram of "Interrupt" software routine

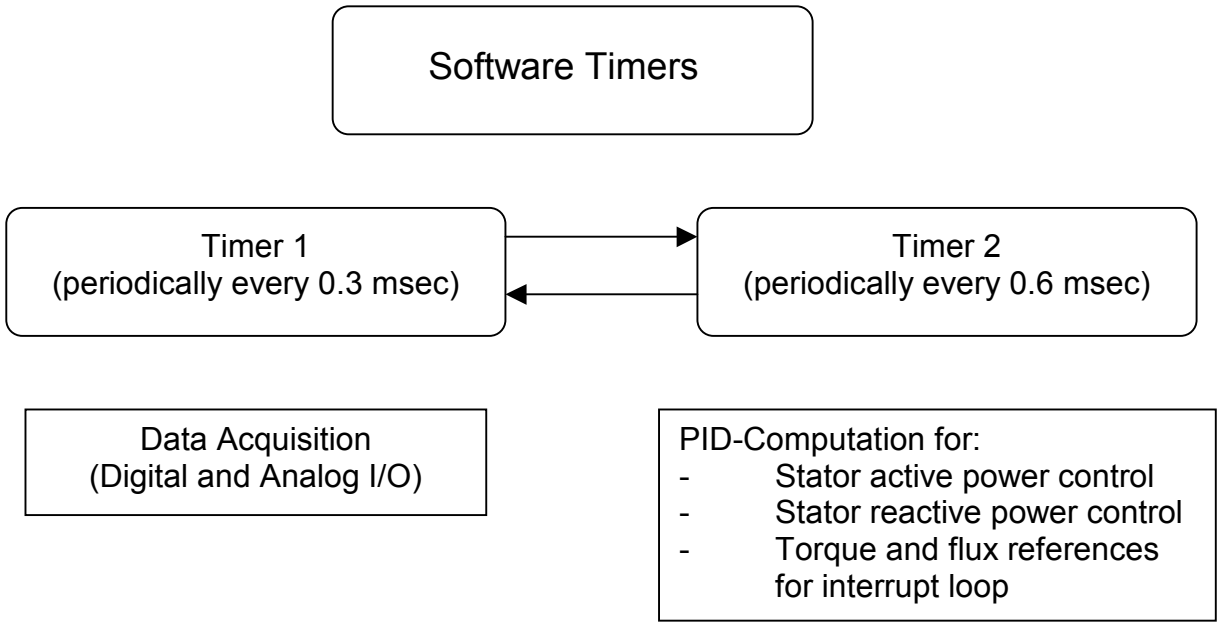

Figure 3.8 Flow diagram of "Software Timers" software routine

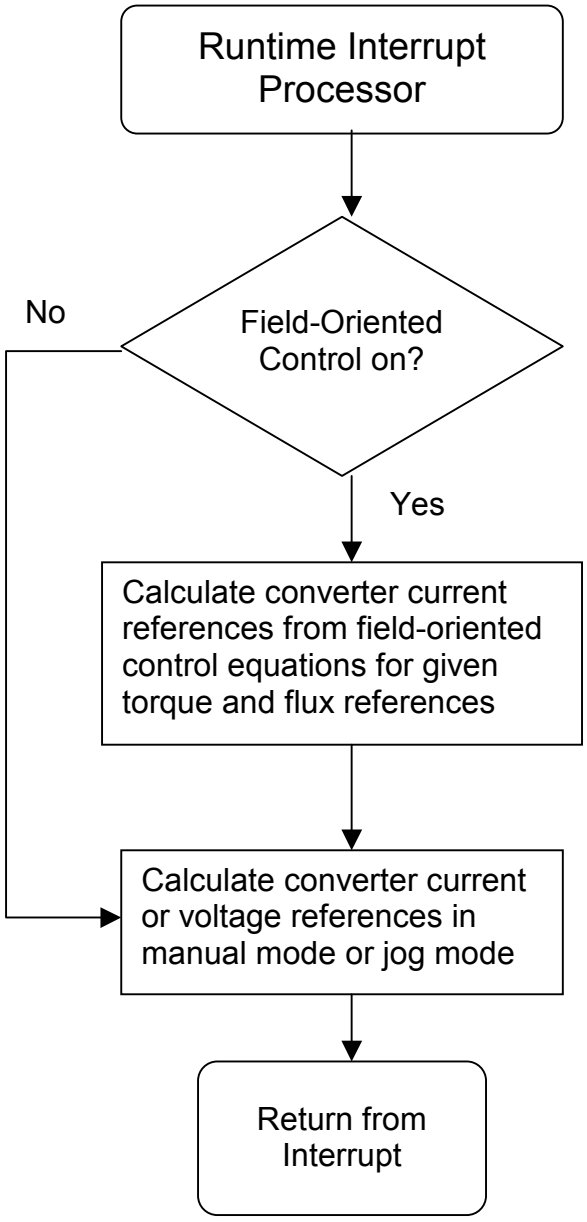

Figure 3.9 Flow diagram of "Runtime Interrupt Processor" software routine

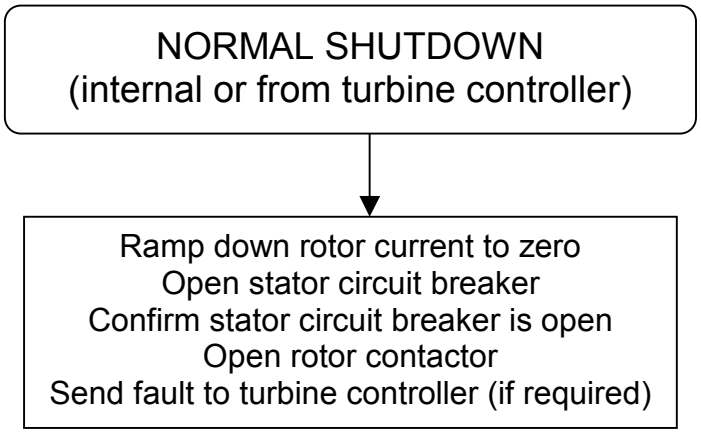

Figure 3.10 Flow diagram of "Normal Shutdown" software routine

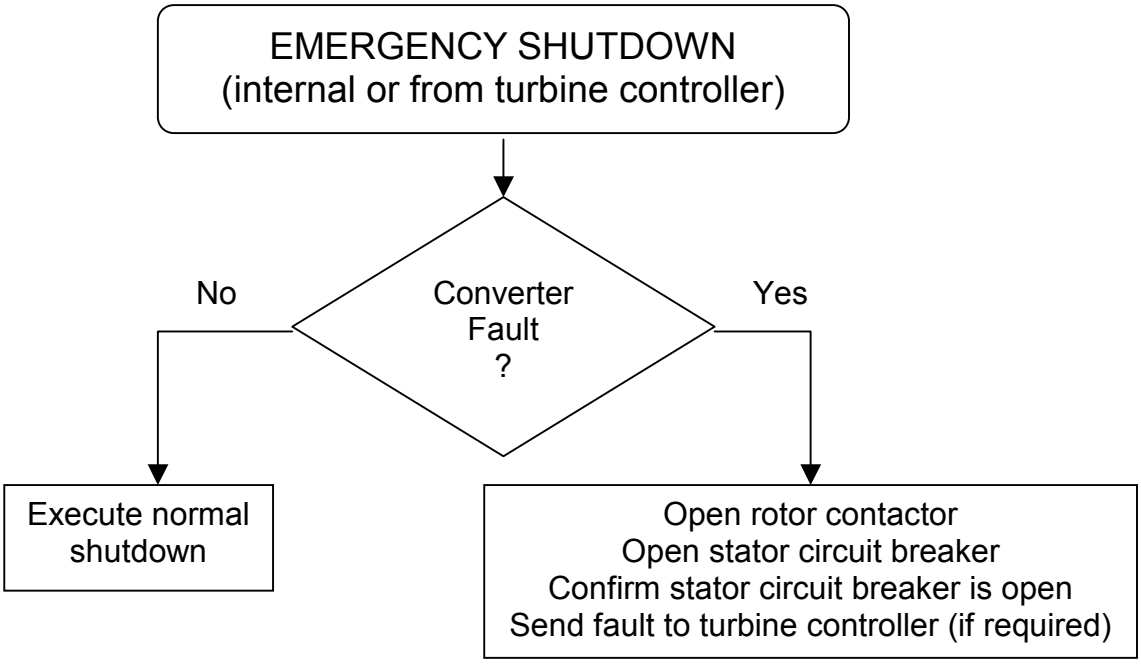

Figure 3.11 Flow diagram of "Emergency Shutdown" software routine

3.3.3.4 USRC Interface

The Converter Interface software allows the VSGS controller PCB to communicate with the converter controller PCB. Information on current or voltage references, operational modes, and converter parameters is exchanged digitally through a parallel interface between the two PCBs. Current or voltage references are updated every 100 μs, whereas other information is exchanged at a 30 msec rate.

3.3.3.5 Data Acquisition

The Data Acquisition software obtains analog and digital data from the I/O-PCB every 300 μs. The analog signals include those that are required for VSGS control such as stator voltages and those that are used to display operational data such as total power. The digital signals acquired are those that are associated with VSGS protection, or those that are required for VSGS start-up such as the synchronization enable signal. Digital signals are also sent out at appropriate times through the I/O-PCB to operate relays for contactors or circuit breakers, or to signal a VSGS fault to the turbine controller.

3.3.3.6 Doubly Fed Generator Control

The Generator Control software forms the core of the VSGS software. It includes software segments for VSGS start-up, normal operation, and VSGS shutdown. Over the course of the project, we developed, lab-tested and field-tested two fundamentally different strategies to control the doubly fed generator:

- The first strategy, based on synchronous machine theory, including a torque-stabilization algorithm that results in an RPM-based control behavior
- The second strategy, based on field-oriented control theory, results in a torque-based control behavior.

Each of these software segments is described in detail below.

3.3.3.6.1 VSGS Start-up

For the Z-40M, the converter is enabled whenever the idle generator RPM exceeds a predetermined minimum RPM. The converter adjusts frequency and amplitude of the generator rotor currents to match the generator stator voltages with the grid voltages. Once synchronization is complete, field-oriented control is enabled, providing torque control for the generator. This process takes less than 5 seconds to complete. Generator torque is adjusted according to a look-up table that correlates operating RPM to desired generator torque in order to maintain maximum turbine rotor efficiency. Upon reaching rated power output, the generator torque is held constant and RPM is maintained by blade- pitch control, resulting in constant power output.

For the AWT-26, the VSGS waits for an ENABLE command from the turbine controller, after which the generator is motored to the minimum operating RPM (operating as an induction motor with shorted stator windings). Upon reaching the minimum operating RPM, the converter is shut down momentarily and the stator short is removed. The converter is then enabled again, and the generator is synchronized to the grid in doubly fed mode. After successful synchronization, field-oriented control is enabled. The startup process takes about 30 seconds to complete. Generator torque is adjusted according to a look-up table that correlates operating RPM to desired generator torque in order to maintain maximum turbine rotor efficiency. Unlike the case of the Z-40M control strategy, above a certain generator torque, the requested generator torque is being increased progressively faster than required for peak turbine rotor efficiency. This causes the turbine rotor to gradually stall ("soft stall"). The soft stall is implemented in such a way that maximum turbine rotor RPM cannot exceed a desired value under any normal operating condition.

3.3.3.6.2 RPM-Based Control Algorithm

This control algorithm is based on synchronous-machine theory. In such a case, the doubly fed generator is known to operate stably, as long as two conditions are satisfied: (1) the rotor currents are controlled externally by a three-phase current source, and (2) the stator reactive power is constantly maintained at a high enough level by controlling the rotor current amplitude, so that the generator load-angle is less than 90 degrees under all dynamic conditions. RPM, meanwhile, is controlled by the frequency of the rotor currents.

However, in this mode of operation, the doubly fed generator behaves dynamically like a synchronous generator. This behavior is undesirable for operation on a wind turbine because it results in huge torque excursions in the drivetrain. A torque-stabilization algorithm has been implemented that dynamically adjusts RPM by small amounts so that torque oscillations are well damped. Figure 2.5 shows the block diagram of this control strategy. A target-RPM curve correlates the desired RPM to the actual turbine output power, resulting in maximum-C_p operation of the turbine rotor.

The following difficulties were observed using this approach:

- For the pitch-controlled turbine rotor, peak power output would have to be controlled by blade pitch using closed-loop output power control. This type of control results in more erratic operation because output power can change very rapidly, whereas the speed of pitch adjustment is rather slow. Turbine operation is much smoother if the generator controls torque and the pitch controller controls RPM; in this case, we can make use of the fact that RPM cannot change rapidly because of the turbine rotor inertia.

- For the case of a stall-controlled turbine, rotor transitions between maximum C_p-control and maximum output power control may result in large power excursions, unless maximum operating RPM is restricted to the same value as normal fixed-speed operation. In that case, however, a substantial part of the expected energy gains due to variable-speed operation will be lost.

- The control approach is suitable, however, to obtain turbine rotor power curves at different RPMs, in order to determine the optimum variable-speed power curve. This approach also lends itself better to investigating turbine structural dynamics, by allowing a careful scan of the entire RPM range and pinpointing RPM set points that result in an adverse structural response of the turbine ("critical RPM").

3.3.3.6.3 Torque-Based Control Strategy ("Field-Oriented Control")

The field-oriented control software is divided into two parts:

- A fast, 100-μs interrupt loop that forms converter current references from torque and flux references
- A slower, 600-μs loop that calculates the torque and flux references for the stator active and reactive power controllers.

The field-oriented control algorithm used to control the doubly fed generator is based on d-q electrical machine theory, and will not be discussed here. In essence, it shows that the electromagnetic torque of a wound-rotor induction generator, with its stator connected to the grid, can be directly controlled by the torque (or q-axis) component of the impressed rotor currents, expressed in a stator flux-oriented d-q reference [12].

The fast control loop estimates stator flux from measured instantaneous voltages, and breaks the demanded rotor current into two components, one in phase (flux component) and the other in quadrature (torque component) with the stator flux. The 2-axis rotor currents are then transformed by Park's transformation to form 3-phase line currents.

The torque control loop is an outer feedback loop and features two PI-controllers to control stator active power and stator reactive power independently. The outputs of these two controllers serve as the references for the torque and flux components of the rotor currents.

The stator active power reference for the PI-controller is derived from a turbine-rotor-specific, RPM-based look-up table. The turbine manufacturer determines the optimum torque vs. RPM relationship, which depends mainly on the rotor C_p-curve. However, it also depends on whether the blades used are stall-regulated or pitch-controlled. The reactive power reference is normally set to zero for unity power-factor operation.

Apart from regular, automatic turbine operation, the VSGS control software is capable of operating the converter in stand-alone mode, or manual system operation. It also provides jogging capability of the blades to facilitate maintenance work on the turbine.

Figure 3.12 shows the block diagram of the field-oriented control scheme, along with the relevant equations.

3.3.3.6.4 VSGS Shutdown

The VSGS can be shut down in one of the following ways:

(1) A STOP command entered by the operator from the keyboard
(2) An ENABLE/STOP command sent from the turbine controller
(3) A manual EMERGENCY STOP command from the operator
(4) Any internal fault detected by the VSGS controller.

The stopping sequences of (1) and (2) employ regenerative breaking. When the VSGS controller receives the command to stop the turbine it increases the generator torque to above rated torque, thus braking the turbine. As soon as the rotor RPM falls below the minimum operating RPM, the VSGS controller disconnects the generator stator from the utility grid, shuts down the converter, and opens the rotor contactor. In the meantime, the turbine controller deploys the tip brakes (or pitches the blades) and applies the high-speed shaft brake, thus reducing the turbine rotor to zero from minimum operating RPM.

For the case of a USRC-generated fault, the VSGS controller opens the rotor contactor immediately, followed by the opening of the stator circuit breaker. In parallel, a VSGS fault signal to the turbine controller will cause deployment of the tip brakes (or pitching of the blades) and application of the high-speed shaft brake.

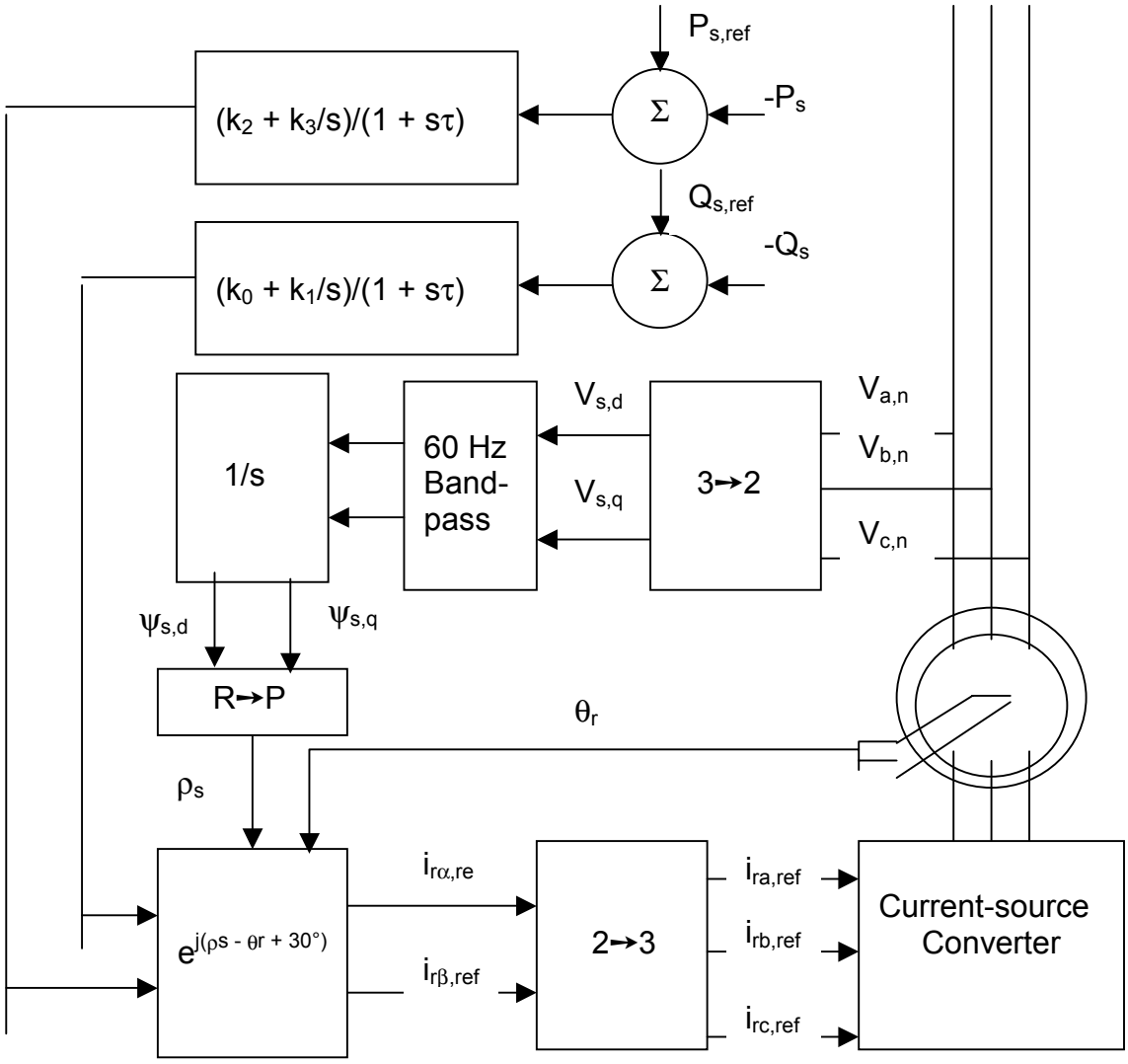

Figure 3.12 Block diagram of field-oriented control for the DFG

2→3: $(2/3)^{1/2}\begin{bmatrix} 1 & 0 \\ -0.5 & 3^{1/2}/2 \\ -0.5 & -3^{1/2}/2 \end{bmatrix}$ R→P: $\rho_s = \tan^{-1}(\psi_{s,d}/\psi_{s,q})$ 3→2: $(2/3)^{1/2}\begin{bmatrix} 1 & -0.5 & -0.5 \\ 0 & 3^{1/2}/2 & -3^{1/2}/2 \end{bmatrix}$

$e^{j\theta}$: $\begin{bmatrix} \cos\theta & -\sin\theta \\ \sin\theta & \cos\theta \end{bmatrix}$ Band-pass filter transfer function: $\dfrac{s(\tau_1 + \tau_2)}{(1 + s\tau_1)(1 + s\tau_2)}$

4.0 VSGS Laboratory Testing

4.1 Purpose of Laboratory Testing

Because of the dynamic nature of wind, it is almost impossible to obtain accurate converter, generator, and gearbox efficiency data from an operating wind turbine. On the other hand, the only possible way to characterize the aerodynamic performance of the turbine rotor is to measure wind speed and turbine electrical output power, and then determine the aerodynamic power at the low-speed shaft by applying the previously determined drivetrain component efficiencies. Therefore, to quantify results accurately at the conclusion of the field test of the effects of variable-speed operation on the aerodynamic performance of the turbine rotor, we included a laboratory efficiency test of the drivetrain components. We suspected that at low turbine-output power levels, substantial differences in gearbox efficiency would exist between fixed-speed and variable-speed operation. If confirmed by the gearbox efficiency tests, this would significantly impact the AEP because of the substantial number of hours that wind turbines spend operating at low wind speeds.

4.2 Z-40M VSGS Laboratory Testing

4.2.1 Marathon Electric Company 1-MW VSGS Test Set-up

Because a high-power test facility is unavailable at both EPC and Zond, we conducted the Z-40M VSGS efficiency test (excluding the gearbox) at the test facility of the generator manufacturer, Marathon Electric Company, in Wausau, Wisconsin. Figure 4.1 shows a block diagram of the test set-up. To obtain variable-speed drive capability, Marathon Electric rented a 1.5-MW engine-generator set on which the fixed-RPM governor was disabled. During testing, we manually adjusted the engine-throttle setting (torque input) to obtain the desired mechanical-input power settings. Because of the operation of an SCR-controlled arc furnace on the same grid, power quality at the test facility was so poor that an additional 1-MW synchronous motor-generator set had to be inserted between the VSGS and the utility grid. Attempts to operate the VSGS directly on the utility grid resulted in the immediate failure of the metal-oxide varistors protecting the USRC. Although this test set-up was somewhat cumbersome to operate, we were able to collect VSGS efficiency data at operating points between 850 and 1550 RPM and power levels up to 400 kW. Output current limitations of the USRC prevented us from operating at higher power levels. Figure 4.2 shows the actual test set-up. (The diesel engine-generator was located in a trailer outside the building; the 1-MW synchronous motor-generator set was located in an adjacent control room.)

4.2.2 Marathon Electric Company Data Acquisition System

The standard data acquisition system (DAS) of the test facility was set up for calibrated measurements of DFG torque and RPM from the torque-transducer, stator voltages, currents, and active and reactive power (see Figure 4.1, point ②), as well as total voltages, currents, and active and reactive power (see Figure 4.1, point ③). Marathon Electric recalibrates the entire test set-up whenever any one component of the set-up is being replaced or exchanged, or at least once a year. Reading accuracy of the digital readouts is ±1 of the least-significant digit.

To derive DFG and converter efficiency, we measured the rotor voltages, currents, and active power (see Figure 4.1, point ①) with a Voltech PM3000A power analyzer. The measurement of the rotor electrical quantities had to be made with a more sophisticated instrument because these quantities vary in frequency between DC and 20 Hz and are floating relative to earth ground. The accuracy of these measurements is largely determined by the accuracy of the current transducers used (± 0.6%).

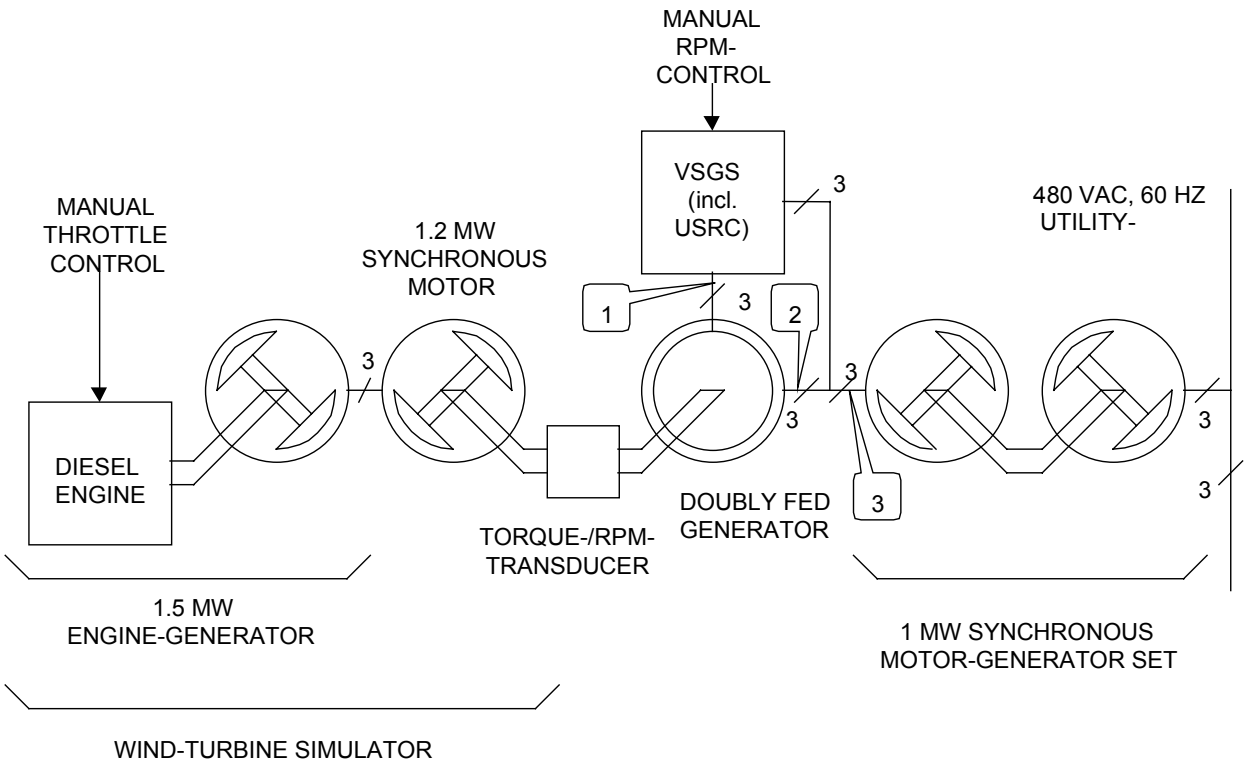

Figure 4.1 VSGS Test Set-up at Marathon Electric

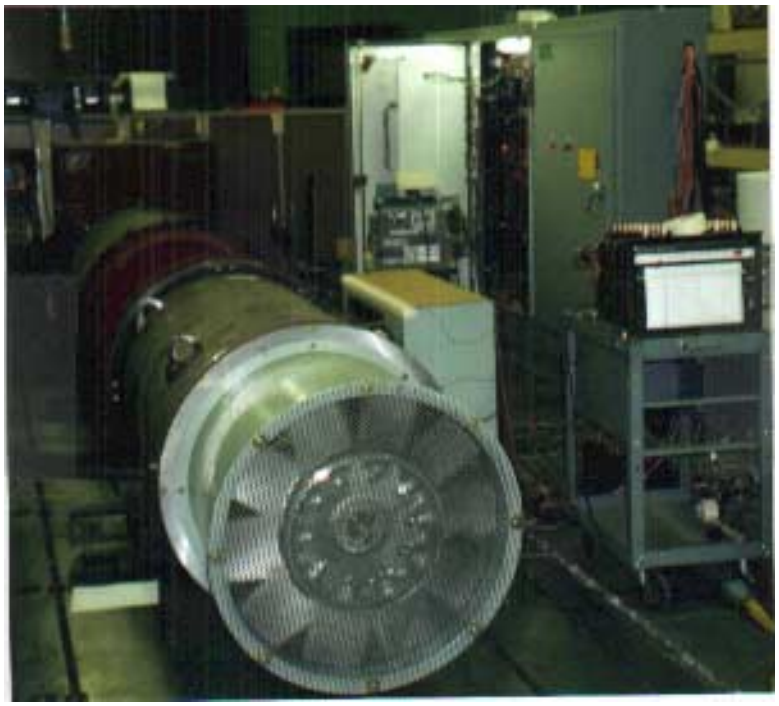

Figure 4.2 VSGS Test at Marathon Electric Co.

4.2.3 750-kW VSGS Test Matrix

We set up a matrix of efficiency test points for the VSGS around the peak-efficiency RPM vs. power-curve of the turbine rotor. Even though the component efficiencies are of greatest interest while operating exactly on this curve, we included several measurement points in its vicinity, because the VSGS controller will not be able to maintain operation exactly on this curve; rather, it will operate mostly in close vicinity of the curve. Therefore, it is important to know how rapidly the component efficiencies change as actual turbine rotor operation deviates from the optimum rotor efficiency curve. In general, we expect the most rapid component efficiency changes around the peak rotor efficiency curve below about 20% of rated system power. Above that, only gradual efficiency changes are expected.

4.2.4 USRC Efficiency

We calculated the USRC efficiencies η_{USRC} applying the active power measurements at measurement points ①, ②, and ③ of each operating point of the test matrix to the following equations:

$$\eta_{USRC} = -P_{rotor} / (P_{Stator} - P_{Grid}) \text{ if } RPM_{DFG} < 1200 \text{ RPM, and}$$

$$\eta_{USRC} = (P_{Grid} - P_{Stator})/ P_{rotor} \text{ if } RPM_{DFG} > 1200 \text{ RPM,}$$

where P_{rotor} is the active power measured at point ① (positive for power flowing towards the USRC),
P_{Stator} is the active power measured at point ② (positive for power flowing towards the grid), and
P_{Grid} is the active power measured at point ③(positive for power flowing towards the grid).

Volume 2, Chapter 2, shows the calculated USRC efficiencies for each operating point.

4.2.5 Doubly Fed Generator Efficiency

We calculated the doubly fed generator efficiencies η_{DFG} applying the active power measurements at measurement points ①, ②, and ③, as well as the mechanical input power of each operating point of the test matrix to the following equations:

$$\eta_{DFG} = P_{Stator}/ (P_{mech} - P_{rotor}) \text{ if } RPM_{DFG} < 1200 \text{ RPM, and}$$

$$\eta_{DFG} = (P_{Stator} + P_{Rotor})/ P_{mech} \text{ if } RPM_{DFG} > 1200 \text{ RPM,}$$

where P_{rotor} is the active power measured at point ① (positive for power flowing towards the USRC),
P_{Stator} is the active power measured at point ② (positive for power flowing towards the grid),
P_{Grid} is the active power measured at point ③ (positive for power flowing towards the grid), and
P_{mech} [kW] = Torque [lbs.–ft.] * RPM[1/min]/7040.3

Volume 2, Chapter 2, shows the calculated doubly fed generator efficiencies for each operating point.

4.2.6 Electrical System Efficiency Curves

We calculated the electrical system (VSGS) efficiencies η_{VSGS} applying the active power measurements at measurement point ③, as well as the mechanical input power of each operating point of the test matrix to the following equation:

$$\eta_{VSGS} = P_{Grid} / P_{mech},$$

where P_{Grid} is the active power measured at point ③ (positive for power flowing towards the grid), and
P_{mech} [kW] = Torque [lbs.–ft.] * RPM[1/min]/7,040.3

Volume 2, Chapter 2, shows the calculated electrical system efficiencies for each operating point. Figure 4.3 shows the electrical system efficiency as a function of system output power while operating at peak rotor efficiency.

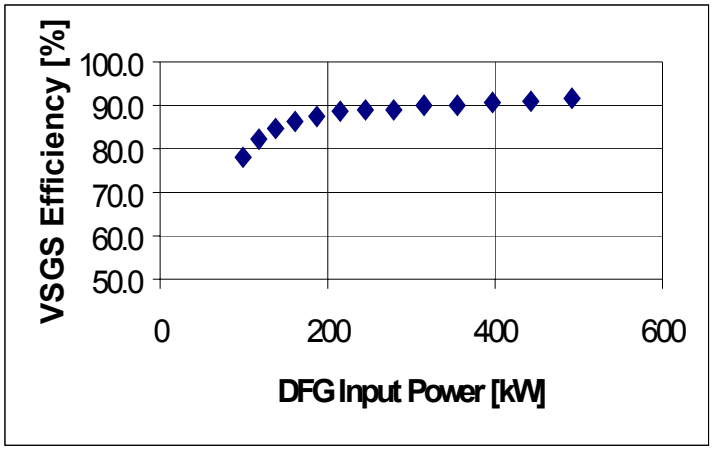

Figure 4.3 750-kW VSGS Efficiency Curve

4.3 AWT-26 VSGS Laboratory Testing

4.3.1 EPC 500-hp VSGS Test Set-up

To test the 275-kW VSGS intended for operation on the AWT-26, we designed and installed a variable-speed generation test facility capable of simulating wind turbine operation at up to 2400 RPM (on the high-speed gearbox shaft) and up to 500-hp mechanical input power. The mechanical output of the wind turbine is simulated by a variable-speed drive operating an induction motor. The variable-speed drive operates on the principle of field-oriented control and features instantaneous control of either the motor torque or the motor RPM. This feature can be used in conjunction with a PC-based wind turbine simulation algorithm to simulate the dynamic effects of the wind turbine in real time, thus enabling us to optimize the dynamic response of the VSGS. Figure 4.4 shows a block diagram of the test set-up. Figure 4.5 shows the test set-up itself. The VSGS test set-up is connected to a 750-kVA, 480-VAC utility transformer with an approximate short-circuit impedance of 2.3%.

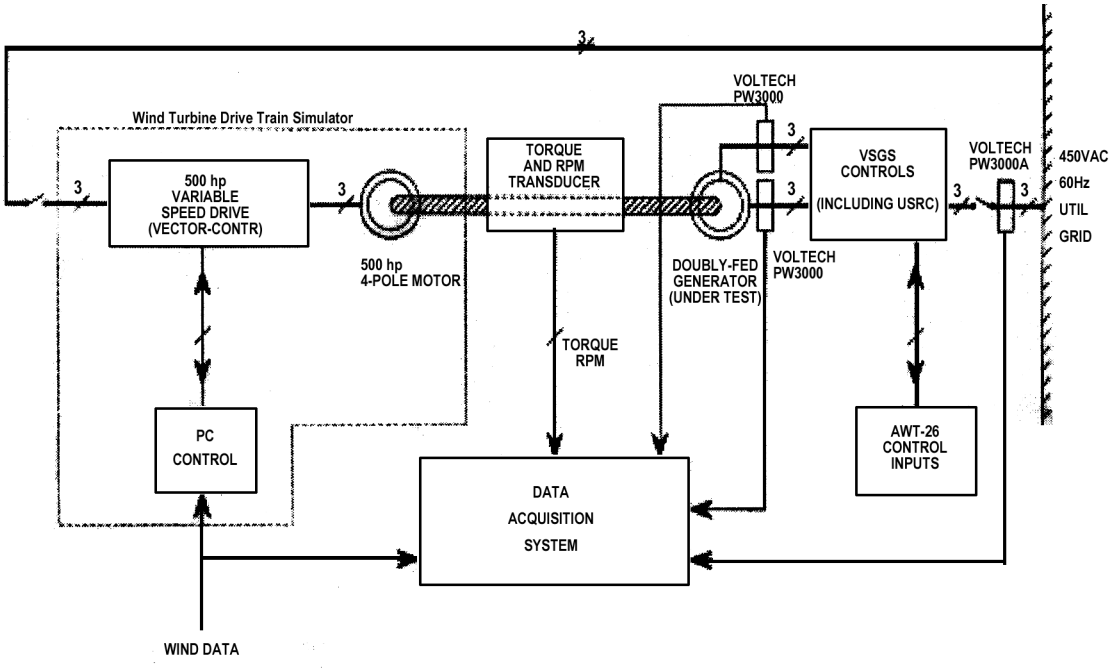

Figure 4.4 Block diagram 500-hp VSGS wind turbine simulator test set-up

Figure 4.5 EPC's 500-hp VSGS test set-up

4.3.2 EPC Data Acquisition System

We equipped the test set-up with a torque transducer (Himmelstein MCRT 2807T) in order to determine the shaft torque and RPM of the generator under-test. The analog output of the torque transducer is connected to a PC-based data acquisition system based on the LABVIEW software that allows us to obtain either high-speed instantaneous or long-term average torque and RPM data. Also connected to this data-acquisition system through a GPIB interface are three Voltech power analyzers (PM3000 series), which supply voltage, current, and active and reactive power data from the DFG rotor, DFG stator, and the point of common coupling with the utility grid. Based on this information, we were able to determine the VSGS component efficiencies as well as the overall VSGS efficiency for every point of operation on the test matrix.

4.3.3 275-kW VSGS Test Matrix

As we compiled the VSGS test matrix for this smaller system, we were guided by the same considerations as when we were compiling the test matrix for the 750-kW VSGS. A sufficient number of test points in the vicinity of the peak-efficiency curve of the turbine rotor is required to see changes in system efficiency as the VSGS departs from the peak-efficiency curve of the turbine rotor. Again, the VSGS efficiency is expected to change only gradually at high (> 20% of rated power) VSGS power levels, whereas it is expected to change more rapidly at low (< 20% of rated power) VSGS power levels.

4.3.4 USRC Efficiency

We calculated the USRC efficiency η_{USRC} from the following equations:

$$\eta_{USRC} = -P_{rotor} / (P_{Stator} - P_{Grid}) \quad \text{if } RPM_{DFG} < 1200 \text{ RPM, and}$$

$$\eta_{USRC} = (P_{Grid} - P_{Stator}) / P_{rotor} \quad \text{if } RPM_{DFG} > 1200 \text{ RPM,}$$

where P_{rotor} is the measured rotor active power of the doubly fed generator
P_{Stator} is the measured stator active power of the doubly fed generator, and
P_{Grid} is the measured grid active output power of the VSGS.

Volume 2, Chapter 3, shows the calculated USRC efficiency for each operating point.

4.3.5 Doubly Fed Generator Efficiency

We calculated the doubly fed generator efficiency η_{DFG} from the following equations:

$$\eta_{DFG} = P_{Stator} / (P_{mech} - P_{rotor}) \text{ if } RPM_{DFG} < 1200 \text{ RPM, and}$$

$$\eta_{DFG} = (P_{Stator} + P_{Rotor}) / P_{mech} \text{ if } RPM_{DFG} > 1200 \text{ RPM,}$$

where P_{rotor} is the measured rotor active power of the doubly fed generator,
P_{Stator} is the measured stator active power of the doubly fed generator,
P_{Grid} is the measured grid active output power of the VSGS, and
P_{mech} [kW] = Torque [lbs.-ft.] * RPM [1/min]/7040.3 is the generator-shaft mechanical power.

Volume 2, Chapter 3, shows the calculated doubly fed generator efficiency for each operating point.

4.3.6 Electrical System Efficiency Curves

We calculated the electrical system (VSGS) efficiency η_{VSGS} from the following equation:

$$\eta_{VSGS} = P_{Grid} / P_{mech},$$

where P_{Grid} is the measured grid active power, and
P_{mech} [kW] = Torque[lbs.–ft.] * RPM[1/min]/7040.3 is the generator-shaft mechanical power.

Volume 2, Chapter 3, shows the calculated electrical system efficiency for each operating point. Figure 4.6 shows the electrical system efficiency as a function of the VSGS input power while operating on the peak-Cp curve.

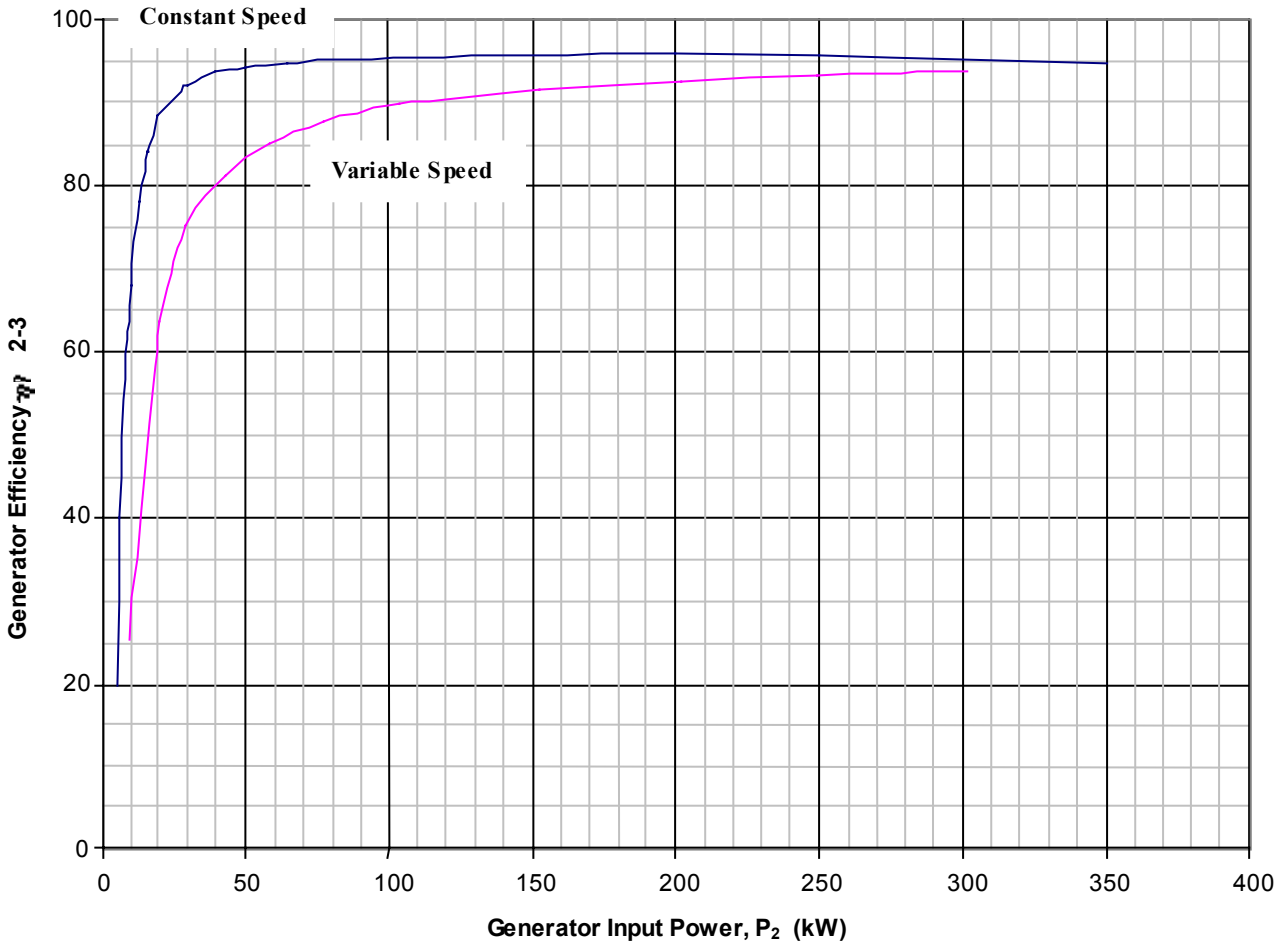

Figure 4.6 Constant- and variable-speed electrical system efficiencies

4.3.7 Gearbox Efficiency Test and Results

In May 1997, AWT engineers performed gearbox efficiency tests at The Gearworks of Seattle, Washington, both on the original AWT-26 fixed-speed gearbox (Mark V, gearbox ratio 1:28.47) and on the optimized AWT-26 VS gearbox (Mark III, gearbox ratio 1:26.07) using a 150-hp dynamometer. The test was to determine gearbox losses on both gearboxes under no-load and loaded conditions and under a variety of operating conditions. Based on the measured losses, we calculated families of gearbox efficiency curves. The detailed gearbox test plan, including test matrices, can be found in [7].

The following is a summary of the test results:

- For both gearboxes, the majority of all losses are splashing losses of the lubricant. These losses are strongly temperature-dependent. Because of the variable viscosity of the lubricant, splashing losses at ambient temperature are more than 2.5 times higher than at rated temperature (91°C).
- Splashing losses are also strongly RPM-dependent. For any given operating temperature, no-load losses at maximum RPM are almost three times higher than the no-load losses at minimum RPM.
- Reverse power flow tests show a consistent, but small effect.
- Repeatability of data points was generally good; worst-case deviation was approximately 1% at no-load.

Figure 4.7 shows the no-load losses as a function of RPM, both at ambient and at rated temperatures. Figure 4.8 shows the family of efficiency curves at rated temperature, and Figure 4.9 shows the gearbox efficiency curve for the optimal AWT-26 power-RPM characteristic (compared to the efficiency of the original gearbox).

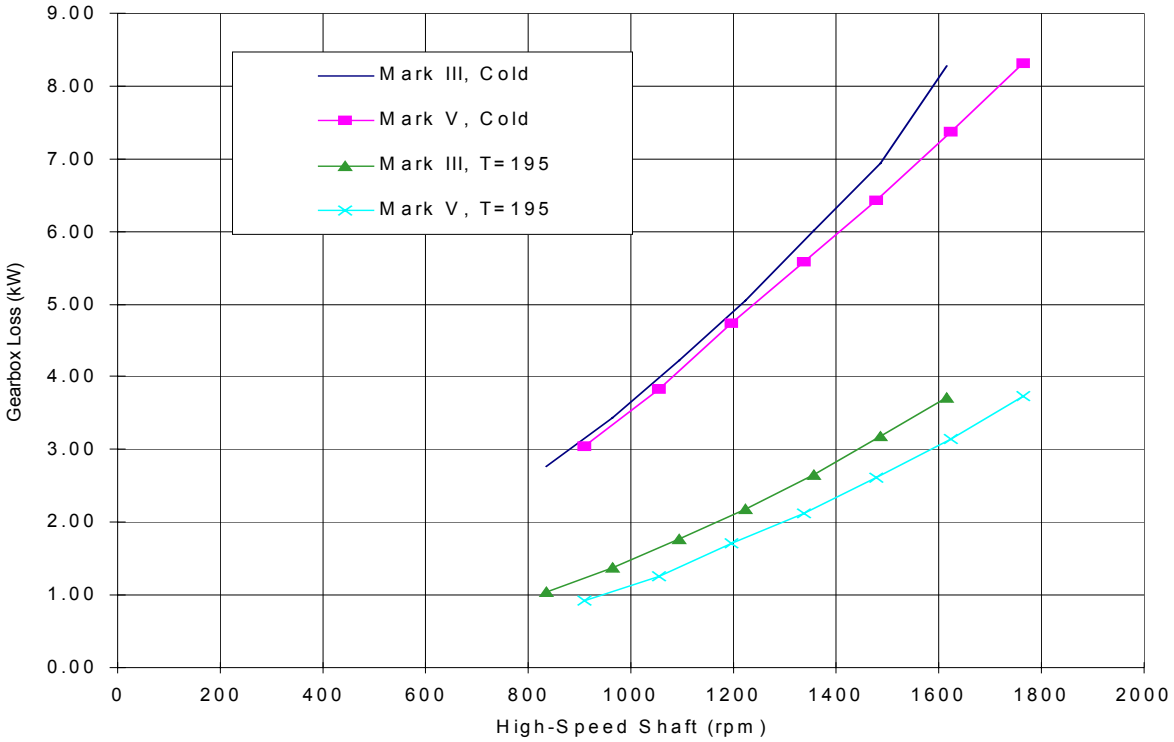

Figure 4.7 Gearbox no-load losses as function of RPM

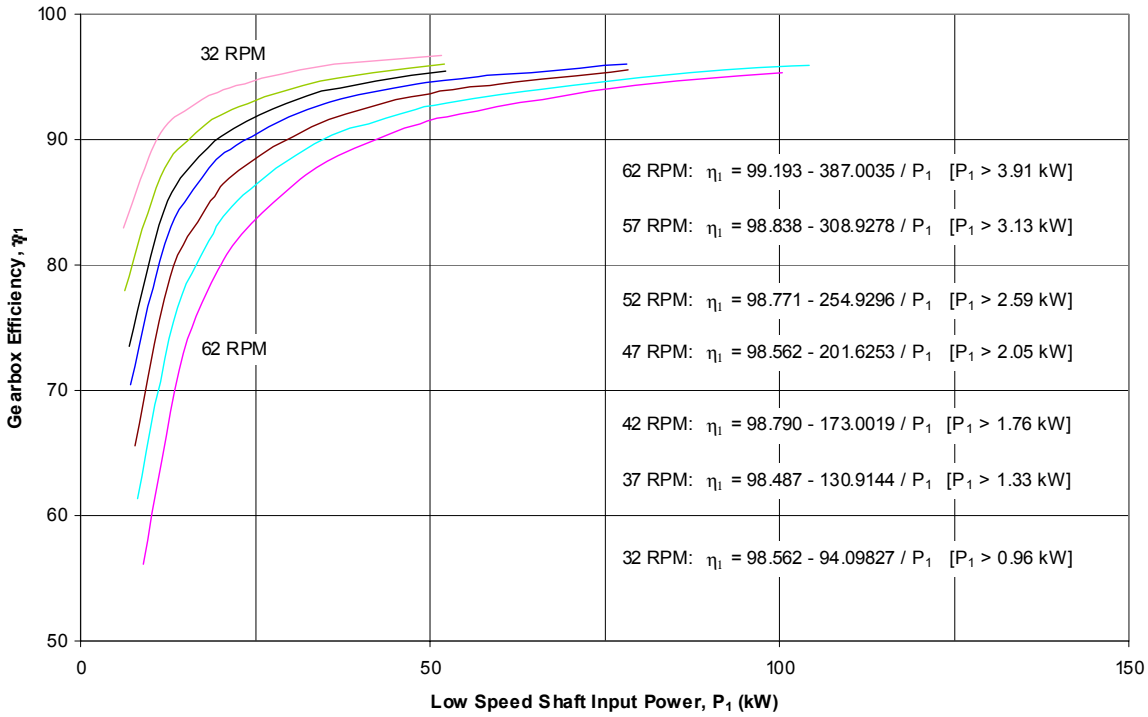

Figure 4.8 Family of gearbox efficiency curves (operation at rated temperature)

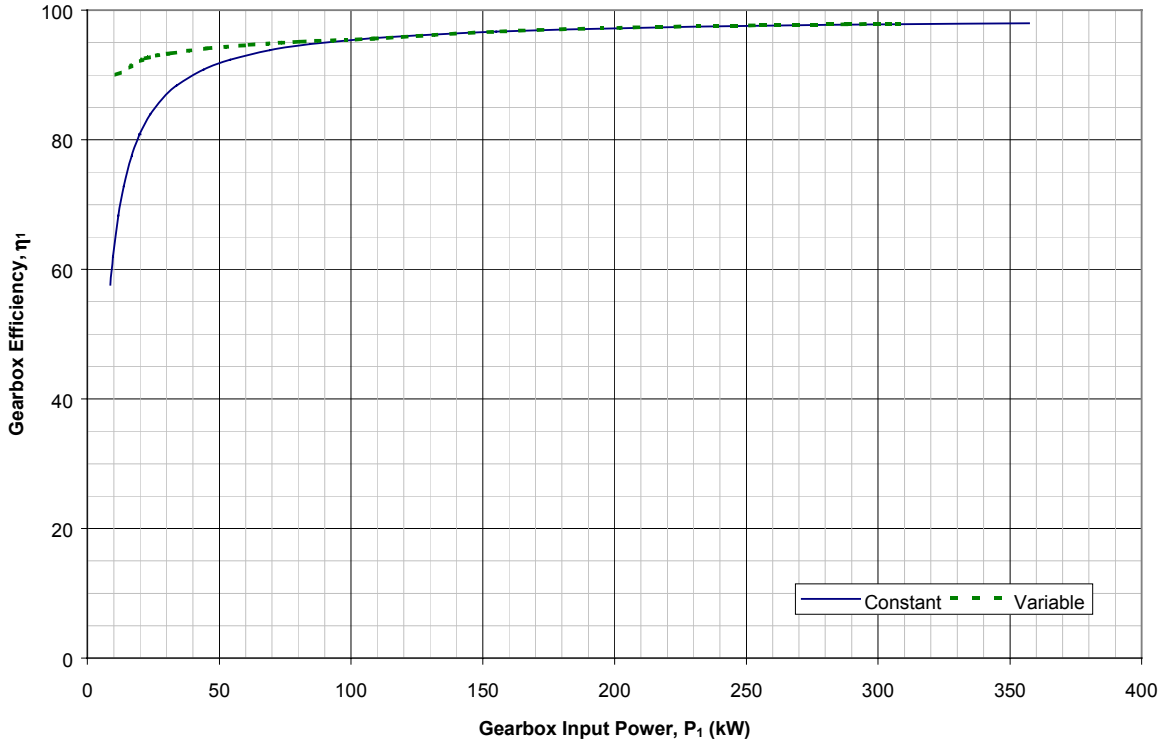

Figure 4.9 Gearbox efficiency for constant- and variable-speed operation

5.0 VSGS Field Testing

5.1 Z-40M VSGS Field Test

5.1.1 Test Set-Up

We conducted VSGS field tests on the Zond Z-40M prototype turbine between April and August of 1996. Because the turbine was commissioned at the same time as the VSGS was installed and brought on line, some start-up difficulties with the turbine, the turbine controller, and the VSGS were expected. The following difficulties were related to the VSGS:

- Because of seasonally high winds, it was not possible to adhere to the wind speed limitations of the start-up procedure.

- Although the VSGS synchronized consistently every time the turbine was brought on line, the reactive power controller (Q-controller) was not stable until a proportional term was added to the existing integral feedback controller. This problem was unexpected because the Q-controller operated stably throughout the preliminary field tests that were performed on a Vestas V-15 turbine. It also operated stably during the VSGS efficiency tests that we conducted on this doubly fed generator at Marathon Electric Company a few months earlier.

- The existing pitch-control algorithm (which controlled pitch using turbine output power as input) caused the turbine output power to oscillate at a frequency of approximately 0.2 Hz, finally driving the turbine output power so high that the VSGS lost synchronism. The oscillation stopped as soon as the wind died down, to the point where the pitch-controller action was no longer needed (output power less than pitch set-point). Only with the pitch-controller inactive were we able to operate the turbine indefinitely. We were able to see under this condition that the normally existent 3p power-oscillations (as seen from instantaneous output power plots of a similar fixed-speed turbine) were eliminated by the VSGS controls. Adjustment of the operating RPM according to power-output of the turbine was not very successful. In particular, while operating close to rated wind speed (just prior to where the pitch-controller started to limit output power), excessive over-shoots in output power were observed.

After a series of discussions and dynamic simulations performed by NREL, we determined that the following approach to control the turbine is optimal:

- Implement generator torque control using field-oriented control for the doubly fed generator
- In Region II (output power less than rated power), control the generator torque according to a predetermined target-power curve as function of operating RPM
- In Region III (output power equal to rated power), maintain rated generator torque and control RPM to be constant at rated RPM using a proportional/integral/differential-(PID-)controller for blade-pitch.

This approach decouples generator and pitch control, and makes use of the fact that RPM can change only slowly due to the large rotor inertia; nevertheless, the pitch controller, which also can move only relatively slowly, is still able to maintain tight RPM-control. Because EPC had not yet developed field-oriented control for the doubly fed generator, and given Zond's immediate controller needs, this solution was never implemented.

5.1.2 Test Matrix

A detailed description of the tests, the testing methods, and the test equipment used can be found in the Z-40M VSGS Test-Plan [8]. The following is a brief summary of the planned tests for the VSGS:

- Perform a scan of the entire RPM-range and visually check turbine for any vibrations (tower or blades)
- Acquire discrete-RPM power curves between 17 and 33 RPM in 2-RPM intervals. Develop optimum target-RPM curve from the results.
- Acquire variable-speed power-curve based on the previously developed optimum target-RPM curve
- Determine Total Demand Distortion (TDD) of voltages and currents, both on the 480 VAC and 12 kV side of the utility transformer over the full output power range (0 to 750 kW).
- Perform acoustic measurements in accordance with American Wind Energy Association (AWEA) standards.

5.1.3 Test Results

A RPM-scan with visual observation did not reveal any dynamic activity of the turbine between 17 and 33 RPM. In particular, we observed no tower motion in this RPM-range.

Because of the difficulties that we encountered with the RPM-based generator-control algorithm, Zond Energy Systems elected to terminate testing with EPC's controller at that point. No additional test results are available.

5.2 AWT-26 VSGS Field Test

5.2.1 Test Set-up

The components of the optimized VSGS (gearbox, doubly fed generator, and VSGS controller) were installed on the AWT-26 turbine at the National Wind Technology Center in July, 1997 (see Figure 1, [6]). A mainframe stiffener was added for increased structural strength of the nacelle mainframe. This modification was deemed necessary for all turbines of this type, and was unrelated to the variable-speed test. We provided a fiber-optic link for increased electrical noise immunity in order to replace the electrical communication link between the nacelle programmable logic controller (PLC) and the PLC located in the turbine controller cabinet. We found, however, that the existing electrical communication link was not affected by the VSGS. Additional fiber-optic cables were installed to connect the outputs of the generator RPM-encoder to the VSGS and the data acquisition system at the tower base. Electrical connections were added between the VSGS and the turbine controller for automated VSGS operation and for fault communication.

We encountered the following problems during installation and initial checkout:

- The conduits for both the power and control cables connecting the VSGS with the turbine controller were found destroyed due to improper refilling of the trench after their original installation (approximately 1994), and, subsequently, heavy equipment passing over the area. We found this damage because it was impossible to add control cables in the otherwise almost empty conduit.

- Wiring inside the VSGS suffered shipping damage from being shipped laying on its back due to improper wire routing in the far back of the VSGS enclosure. We discovered this problem while attempting to start up the VSGS; we found that the USRC output was shorted out.

- The VSGS was unable to synchronize without the blades mounted to the rotor hub. After motoring up to synchronous RPM, the gearbox caused so much drag that the generator RPM dropped below the minimum synchronization RPM before the VSGS was able to synchronize. After the blades were mounted, the VSGS synchronized reliably.

- The USRC faulted out frequently during motor-up. We found a dynamic hunting problem where the rotating system oscillates between motoring and generating. This problem was caused by the control algorithm that we had originally implemented (linear increase of operating frequency). We were able to correct this problem by implementing a constant-slip algorithm that uses generator RPM as the feedback signal. This change allowed us to increase the rotor acceleration rate significantly.

- We observed that the closed-loop feedback control of the stator reactive power controller was unstable when first activated. We found that the polarity of the stator reactive power signal was reversed due to the reverse phase sequence of the utility grid at the test site (compared to EPC's utility grid). A sign reversal in the controller software corrected this problem.

- We observed a tower resonance at approximately 32 rotor RPM (866 generator RPM). This observation agrees with the predicted first tower mode of the Campbell-diagram. A complete scan of the operating RPM-range (32 RPM to 62 RPM) revealed additional resonant points at 38 and 48 rotor RPM. However, no adverse motion of the turbine could be observed at these RPM set-points. Consequently, we decided to raise the minimum operating RPM to 34 rotor RPM, and—for the final variable-speed control algorithm—allow the controller to skip over 38 and 48 rotor RPM.

- A failure of an MOV on the output of the USRC combined with a "hung"-condition of the VSGS user interface resulted in a fire inside the VSGS controller that caused some damage. This resulted in major modifications of the fault protection and emergency shutdown system of the VSGS controller [13].

- After the retrofit for true variable-speed operation (which included the implementation of field-oriented control for the doubly fed generator), we found that the USRC faulted out frequently on output over-voltage. We found that the rotor-current reference waveforms were highly distorted. We traced the distorted reference waveforms back to an imbalance of the measured line-to-neutral grid-voltages. An investigation of the 480-VAC mains of the turbine site revealed that a grid-transformer with a delta-connected 480-VAC secondary was installed. Because the 480-VAC system was floating relative to earth-ground, an arbitrary relationship existed between the legs of the utility grid and earth ground. The generator controller, however, references its measured grid voltages relative to earth ground. The result was that the measured line-to-neutral grid-voltages were unequal in magnitude and not 120 degrees out of phase, as the control algorithm expects. NREL site engineers decided to exchange this transformer with a wye-connected transformer from another site.

- After implementing field-oriented control, we found that the USRC faulted consistently on output over-voltage after approximately 45 minutes of operating time. We found that the USRC reference waveforms became increasingly distorted after about 15 minutes during every trial run. Because we were unable to investigate this problem further, we had to assume that this distortion is due to the gradual build-up of a numerical error in the field-oriented control algorithm (DC-offset) which results in the reference waveforms becoming distorted.

5.2.2 Test Matrix

A detailed description of the tests, the testing methods, and the test equipment used can be found in the AWT-26 VSGS Test-Plan [9]. The following is a brief summary of the tests that we conducted:

- In RPM-control mode, complete a dynamic effects analysis of the turbine over the entire RPM-range to determine potentially dangerous critical RPM-points,
- In RPM-control mode, obtain turbine power curves at 32, 50, and 57 RPM (the 57 RPM power-curve is the fixed-speed power-curve of the turbine which was obtained before the VSGS retrofit)
- In RPM-control mode, perform acoustics tests with modified blade tips
- In variable-speed mode of operation, find a soft-stall target-power curve that results in maximum energy output of the turbine while minimizing power and RPM excursions beyond their rated values.
- For this target-power curve, find the variable-speed power curve of the retrofitted turbine.

- In variable-speed mode of operation using the maximum energy-capture approach, find the actual power vs. RPM characteristic and the resulting power curve.

5.2.3 Test Results

5.2.3.1 Data Acquisition Systems [6]

Two data acquisition systems were used to collect test information. A low-frequency system recorded one-minute averages of important power-performance and meteorological data. A high-frequency system recorded power-performance transients and turbine structural responses for use in evaluating variable-speed control strategies and making comparisons to constant-speed operation. The data acquisition systems were independent of each other.

Low-frequency data were acquired using a Campbell Scientific 21X data logger mounted on the meteorological tower approximately two rotor-diameters upstream of the turbine in the prevailing wind direction. There were no obstructions in this direction for 18.75 rotor diameters. The data logger sampled at 1 Hz and recorded one-minute averages with statistics of all data. Information was stored on a Campbell Scientific M1 module and downloaded to a programmable computer on a weekly basis. The recorded data included atmospheric temperature and pressure, generator speed, power output, gearbox temperature, and hub-height wind speed and direction. The methods of data reduction and analysis are discussed in detail in Appendix A.5.

High-frequency data were acquired using an Analog Devices 5B01 back plane with signal conditioning devices. A National Instruments DAQCard-AI-16XE-50, installed in a laptop computer PCMCIA slot, was connected to the 5B01 back plane for analog-to-digital conversion of the signals. Data were sampled at 20 Hz and stored in files of ten-minute length. The sampling rate of 20 Hz was more than twice the Nyquist frequency for all signals of interest. The data recorded were hub-height wind speed, generator speed, power output, and nacelle acceleration in two orthogonal directions. No rotating frame measurements were recorded because of the limited scope of this study, the primary objective of which was the evaluation of the converter and control methodologies for fixed-pitch stall-regulated turbines.

5.2.3.2 Dynamic Effects Analysis

A complete account of the dynamic effects testing can be found in [10]. Figures 5.1 and 5.2 show the results of these tests. As expected, the turbine showed some pitch- and yaw-motion around 32 rotor RPM. Because power production was negligible at that operating point, we decided to raise the minimum operating RPM to 34 rotor RPM, thus avoiding this critical RPM.

Additional operating points that showed some indication of dynamic activity were found at 38 and 48 rotor RPM. However, no tower or teeter motion was visible. To avoid any potential problems during variable-speed operation later on, we inserted flat spots in the target-power curve so the VSGS would skip over rather than dwell on either one of these operating points.

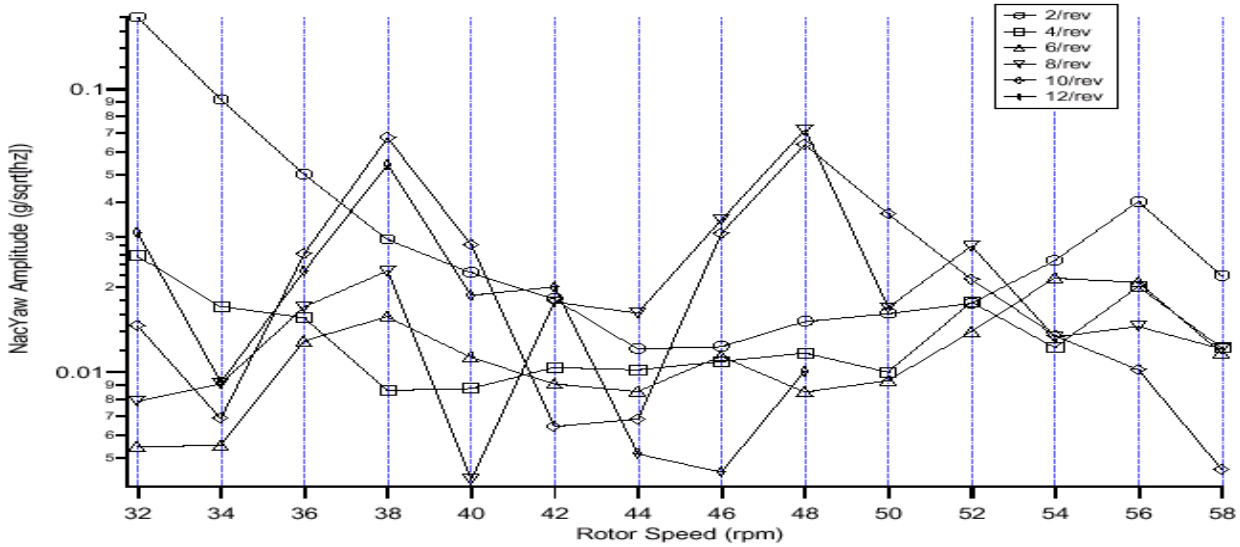

Figure 5.1 Nacelle yaw amplitude

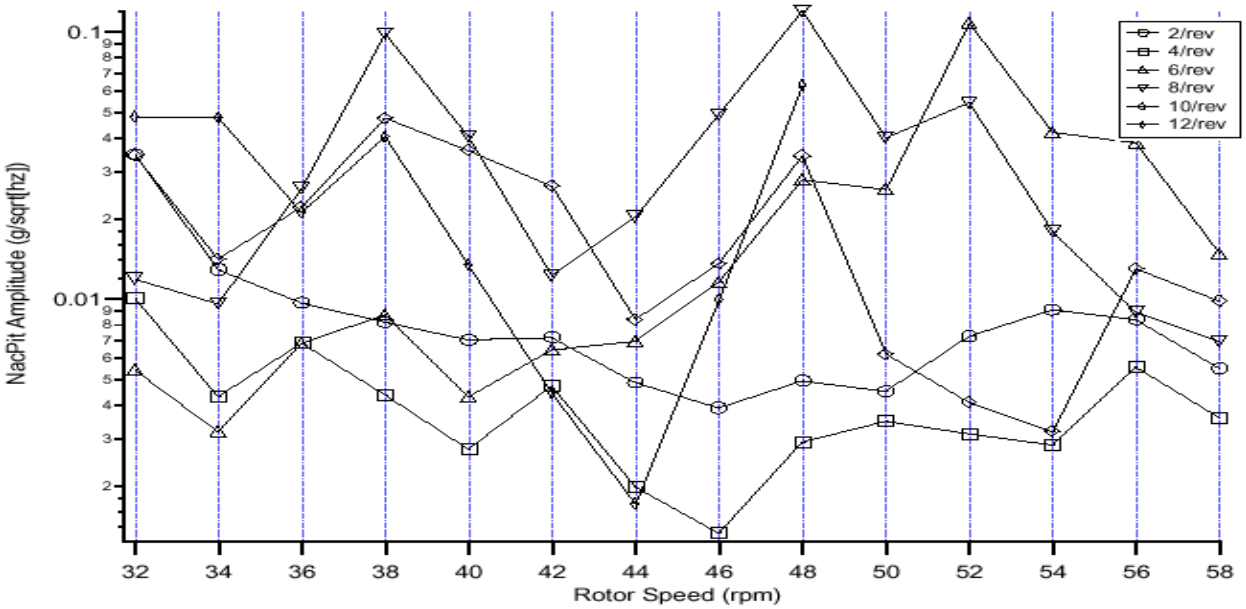

Figure 5.2 Nacelle pitch amplitude

5.2.3.3 Constant-RPM Operation

After completing the dynamic effects tests, we operated the turbine over extended periods of time to obtain power curves at 32 and 50 RPM. Figure 5.3 shows the measured discrete RPM power curves at 32, 50, and 57 RPM. The power curve at 57 RPM is the original power curve of the fixed-speed AWT-26 and was obtained before the VSGS retrofit. At low wind-speeds, we expected greater output power at lower RPM, but from these curves we see that this expected improvement did not materialize. These phenomena may be attributable to larger than expected converter losses at low power, or Reynolds-number effects as discussed in [6].

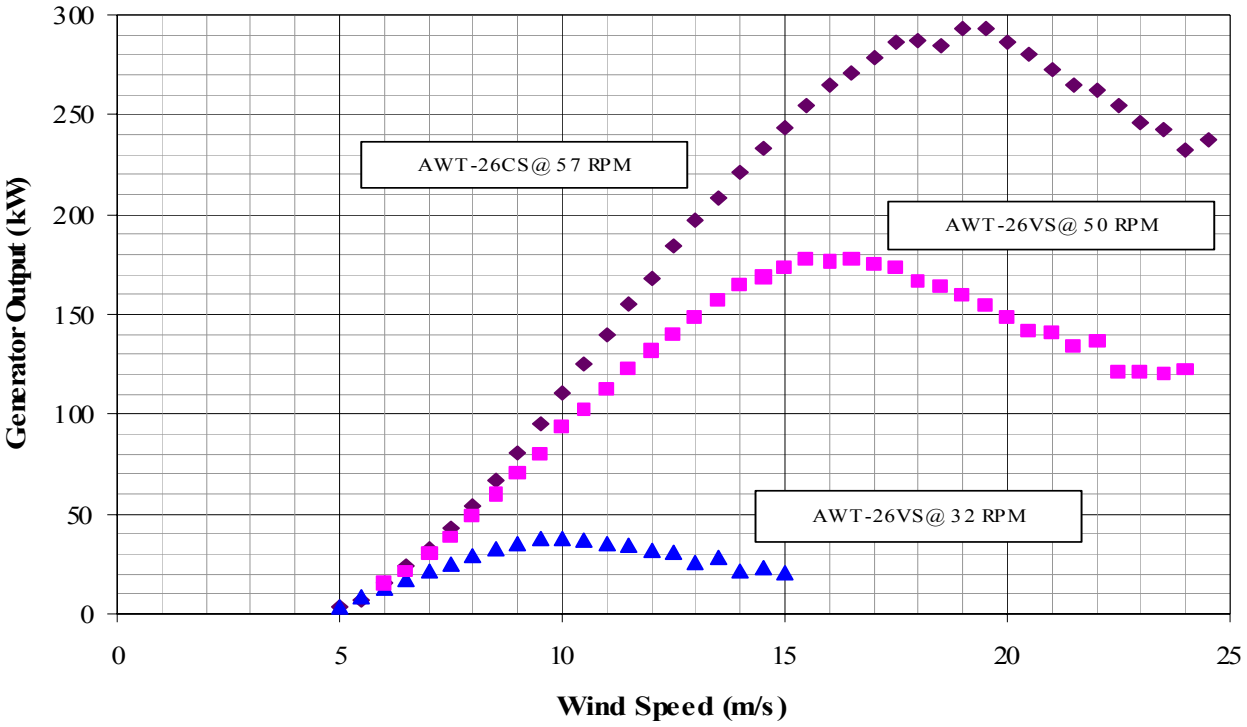

Figure 5.3 Constant and discrete-RPM power curves of the AWT-26

5.2.3.4 Soft-Stall Operation

After completing the discrete-RPM power curves, we converted the VSGS controller to operate in a true variable-speed mode using torque-control for the generator. The torque-reference for the generator is calculated from the momentary operating RPM. The algorithm maintains peak-C_p operation of the turbine rotor for as long as the turbine output power is below rated output power and the rotor RPM is below point A of Figure 2.6. (This is operator adjustable; however, for safety reasons, it is not adjustable to higher than 60 RPM.) Figure 5.4 shows the turbine output power as a function of RPM for a power-RPM schedule, which maintained peak-C_p operation up to 48 RPM and then progressively forces the rotor into stall to limit the turbine output power to below 300 kW. Figure 5.5 shows the AWT-26 variable-speed power curve obtained for the soft-stall control algorithm [6].

Besides the one-minute average data, which we obtained for the previous graphs, we collected 20 Hz data to examine the effectiveness of the instantaneous torque-control. Figure 5.6 shows turbine output power during start-up, both in constant-speed and variable-speed operating mode. Although these data were collected one

year apart, both events have been recorded using the same measuring equipment and in similar wind conditions. Clearly, most of the adverse dynamic effects of constant-speed operation have been eliminated. In particular, the 450 kW power spike, which occurs in constant-speed mode as the soft-starter connects the generator across the grid, no longer occurs in variable-speed operation. Figure 5.7 shows the turbine output power during steady-state operation, both in constant-speed and variable-speed operation. The 2p-oscillations of the turbine output power in constant-speed mode no longer exist in variable-speed operation. As expected, this result shows that the drivetrain components of the turbine can be substantially downsized if the turbine is operated with a generator that allows instantaneous torque-control.

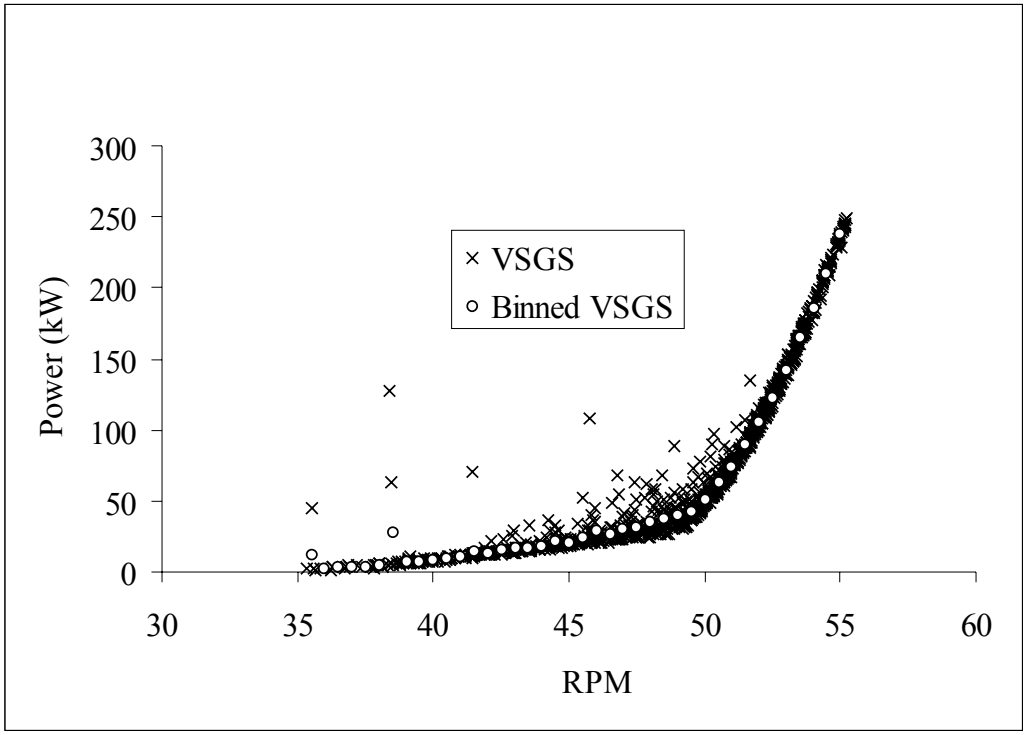

Figure 5.4 AWT-26 soft-stall operating characteristic (Power vs. RPM)

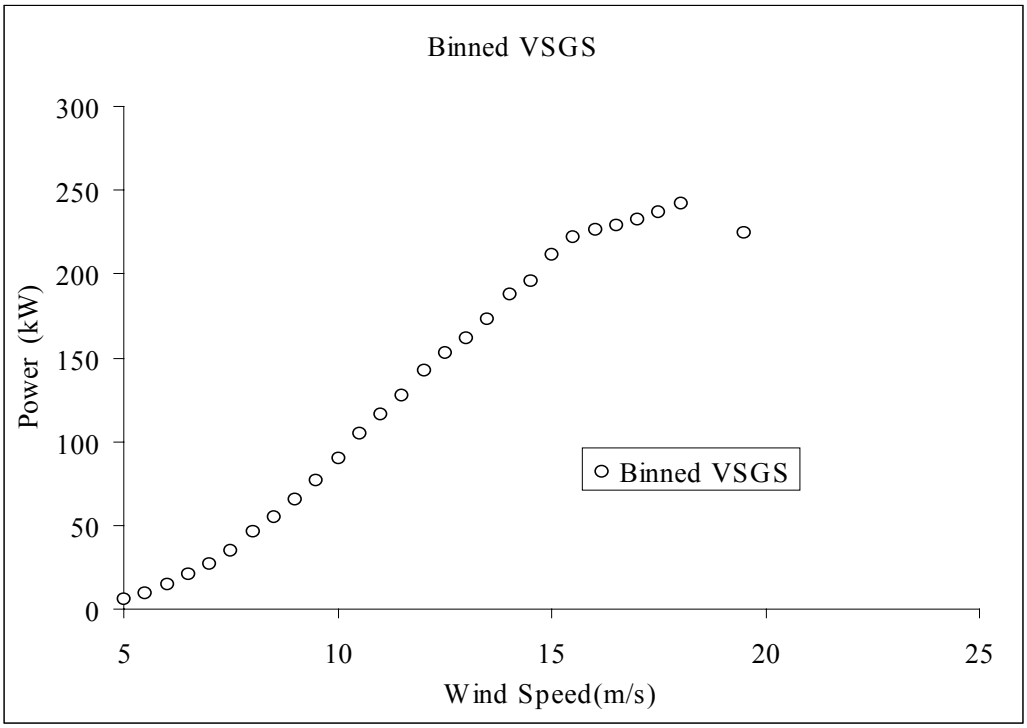

Figure 5.5 AWT-26 variable-speed power curve (soft-stall)

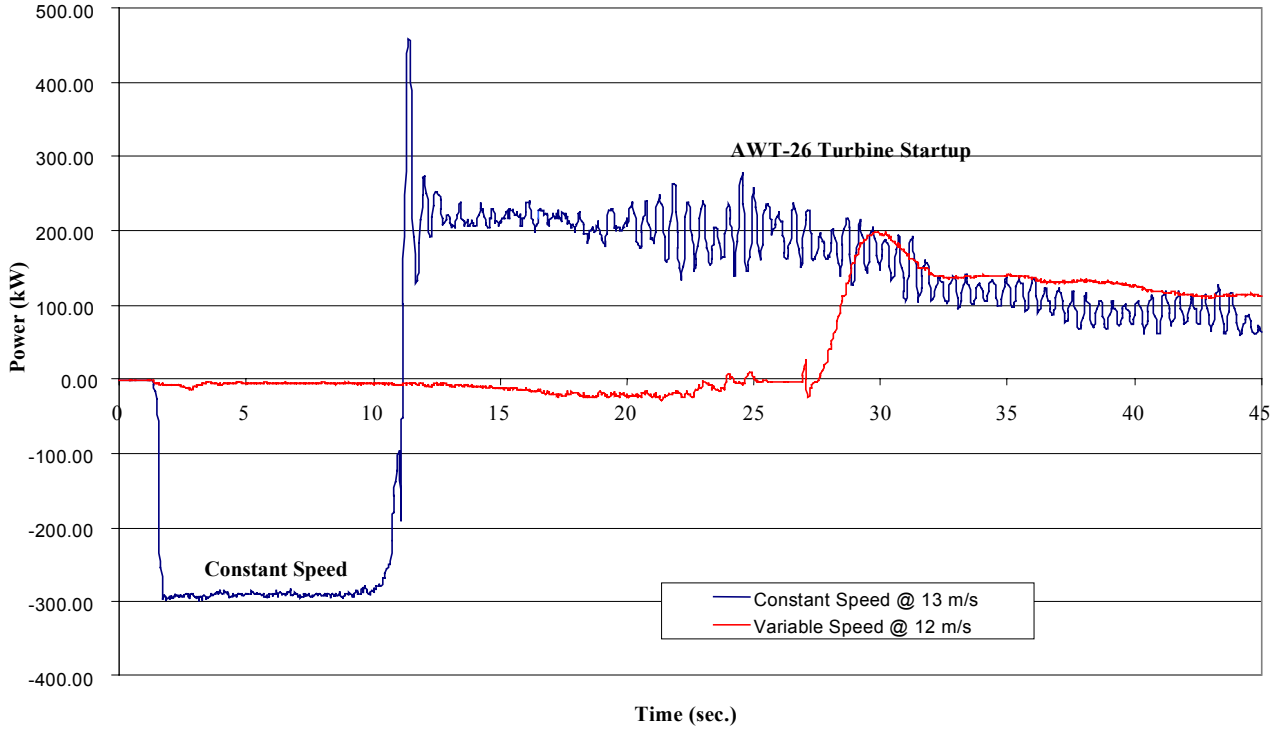

Figure 5.6 AWT-26 constant-speed and variable-speed output power during start-up

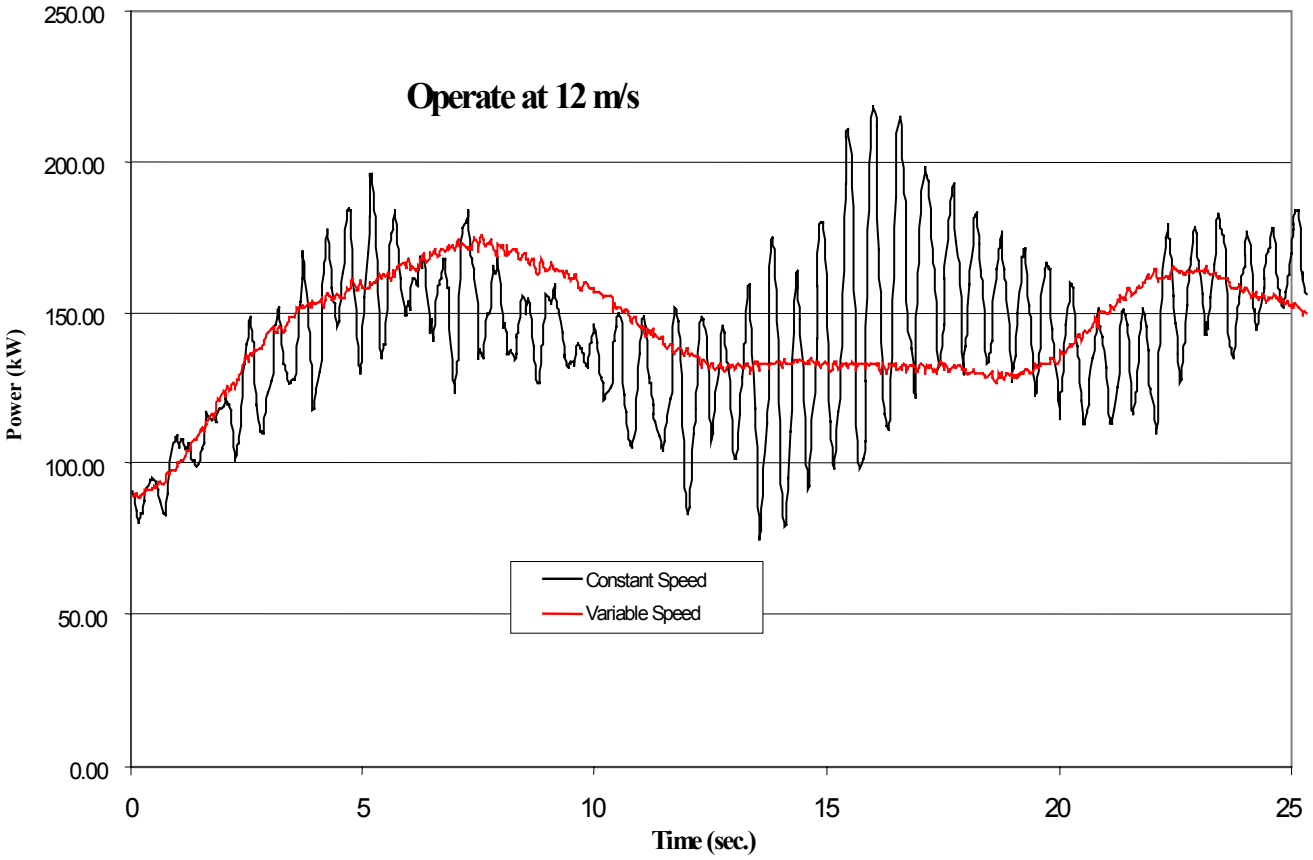

Figure 5.7 AWT-26 constant-speed and variable-speed output power (steady-state)

5.2.3.5 Maximum Energy Capture Operation

Finally, we implemented the algorithm for maximum energy capture operation and operated the turbine in this mode to collect power-curve data. Figures 5.8 and 5.9 show the power vs. RPM characteristic and the power-curve for this approach in comparison to the soft-stall approach. Figure 5.8 clearly shows that it is possible to tightly limit RPM and power to the desired maximum values.

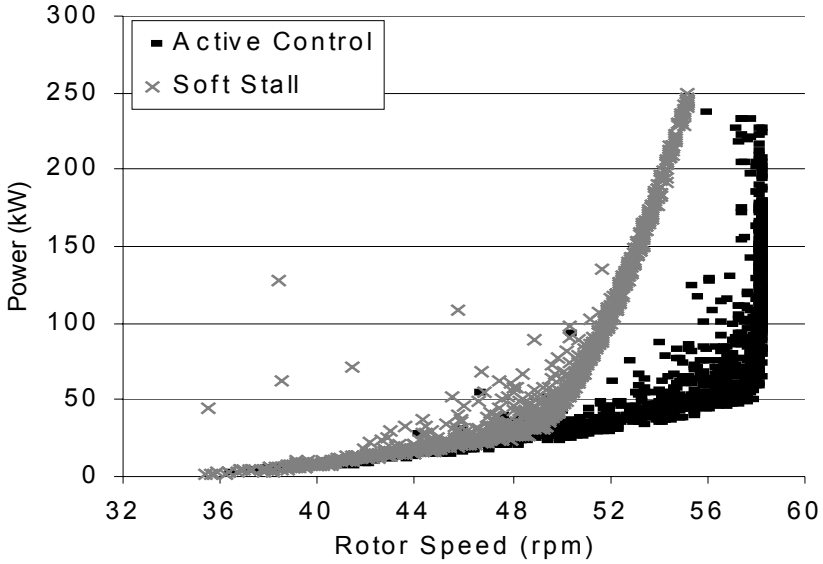

Figure 5.8 Power vs. RPM characteristic of maximum energy capture approach (Compared to soft-stall operation).

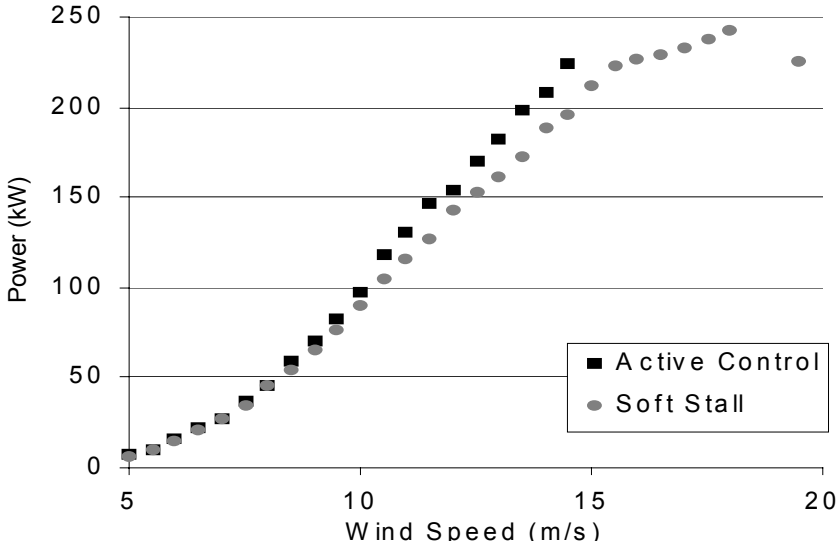

Figure 5.9 Comparison of power-curves of maximum energy capture approach and soft-stall Approach.

Figure 5.10 compares the rotor power coefficient (deduced from measured electrical power and drivetrain component efficiencies) for the three operating modes tested: (a) fixed-speed operation of the original AWT-26 turbine at 57 RPM, (b) discrete-speed operation of the AWT-26 VSGS turbine at 32 and 52 RPM, (c) soft-stall operation, and (d) maximum-energy-capture operation. Power Coefficient is plotted against wind speed, rather than tip-speed-ratio, to better illustrate how rotor efficiency is affected by the three control strategies over the operating range of the turbine. C_p curves can be found in [6]. The data from this figure can be found in Appendix A.3 in tabular form.

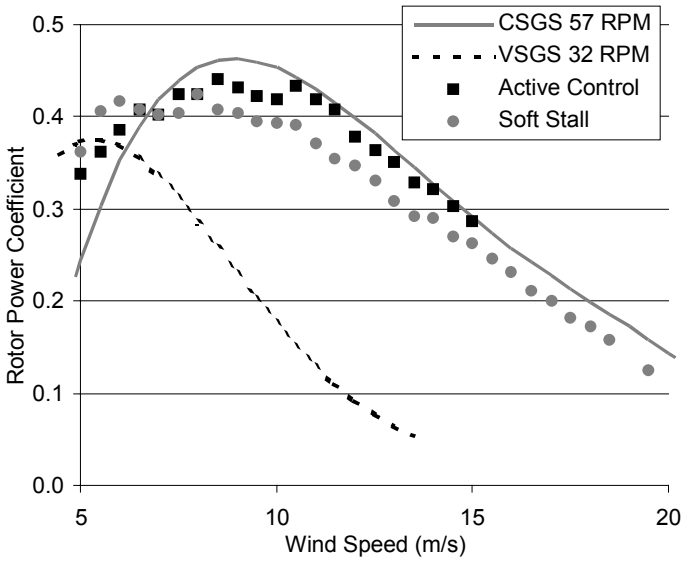

Figure 5.10 Coefficient of rotor performance for three different control strategies.

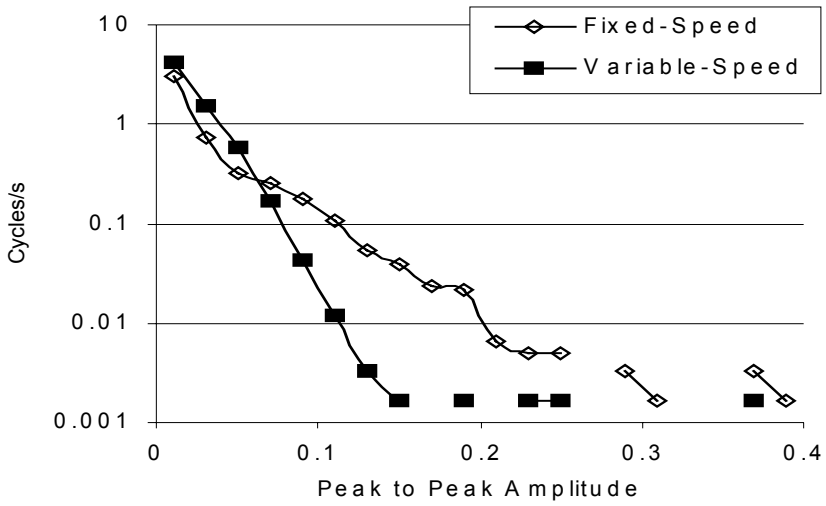

Figure 5.11 Rainflow cycle counts for fixed- and variable-speed drivetrain torque

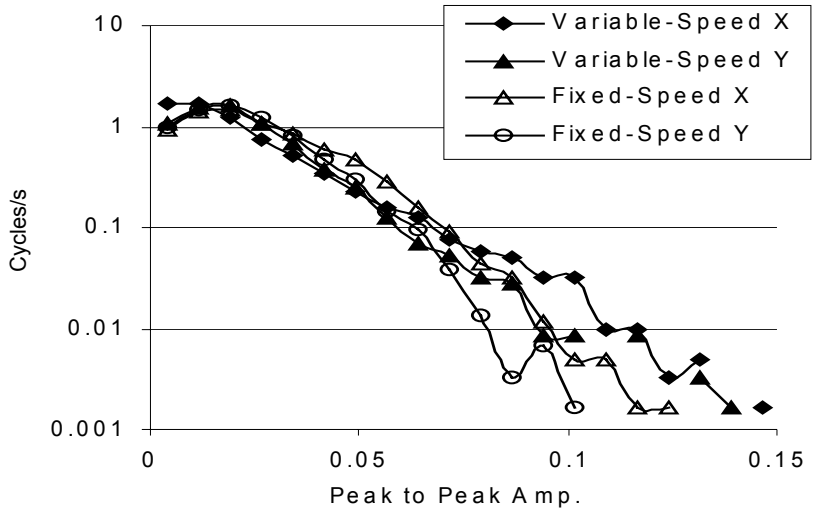

Figure 5.12 Rainflow cycle counts of nacelle acceleration for variable-speed and fixed-speed operation

5.2.3.6 Data Reduction [6]

For developing power curves, the one-minute-average wind speed, rotor speed, and generator power were downloaded from the Campbell 21X data-logger, along with atmospheric temperature and pressure, and turbine status. These data were "filtered" by removing points that did not meet the acceptance criteria, which were:

- Wind directions from 165^{o} to 332^{o}
- Turbine not off-line due to grid or turbine faults
- Sensors and data system functioning properly
- Turbine not in start-up, manual, standby, or shutdown.

The filtered data were normalized to a site-average air density of 1.0 kg/m^3, then sorted and tabulated in wind-speed bins of 0.5 m/s (4.75–5.25 m/s, 5.25–5.75 m/s, and so forth). Typical data presentation is a scatter-plot of power versus wind speed (or rpm) and superimposed power curve of median wind speed versus mean generator power for the data in the bins.

A similar approach was used to develop C_p-TSR curves, where the power coefficient (C_p) and tip-speed ratio (TSR) were calculated for each one-minute-average data point, then normalized, binned, and plotted. Because our interest was in rotor C_p, the measured generator power was converted to rotor power by correcting for gearbox, generator, and converter efficiencies (for the VSGS) measured in the laboratory. High-frequency power data were smoothed and filtered to remove data spikes caused by the self-powered OSI power transducer.

5.2.3.7 Acoustic Measurements

In September 1998, engineers of AeroAcoustics, Inc., performed acoustic measurements on the AWT-26 VSGS turbine. These tests were to quantify the reduction in sound pressure level at reduced rotor speed, thereby confirming the claimed noise benefit of variable-speed turbines.

Two different blade-tip geometries were tested: the rotating tip-vane (aerodynamic brake) of the original AWT-26, as shown in Figure 5.13, and a conventional tip which was designed by NREL engineers to produce a more benign acoustic signature, as shown in Figure 5.14.

Because the prevailing wind-speeds were low during the available test period, data for high wind speeds were not obtained. However, the expected strong relationship between sound pressure level and blade tip-speed (RPM) is clearly demonstrated by the test data of Figure 5.15. AeroAcoustics engineers assured us that the obvious scatter in sound-pressure-level data is very typical of this test procedure, and is observed frequently in measurements of aircraft noise.

Figure 5.15 also shows that in typical operation (at 57-58 RPM) in low wind speeds, the rotating tip vanes of the AWT-26 have a sound pressure level approximately 1.5 dB higher than the conventional tips. No attempt was made to extrapolate these results to higher wind speeds.

Figure 5.13 Original AWT-26 Tip-brake

Figure 5.14 AWT-26 Conventional blade-tip

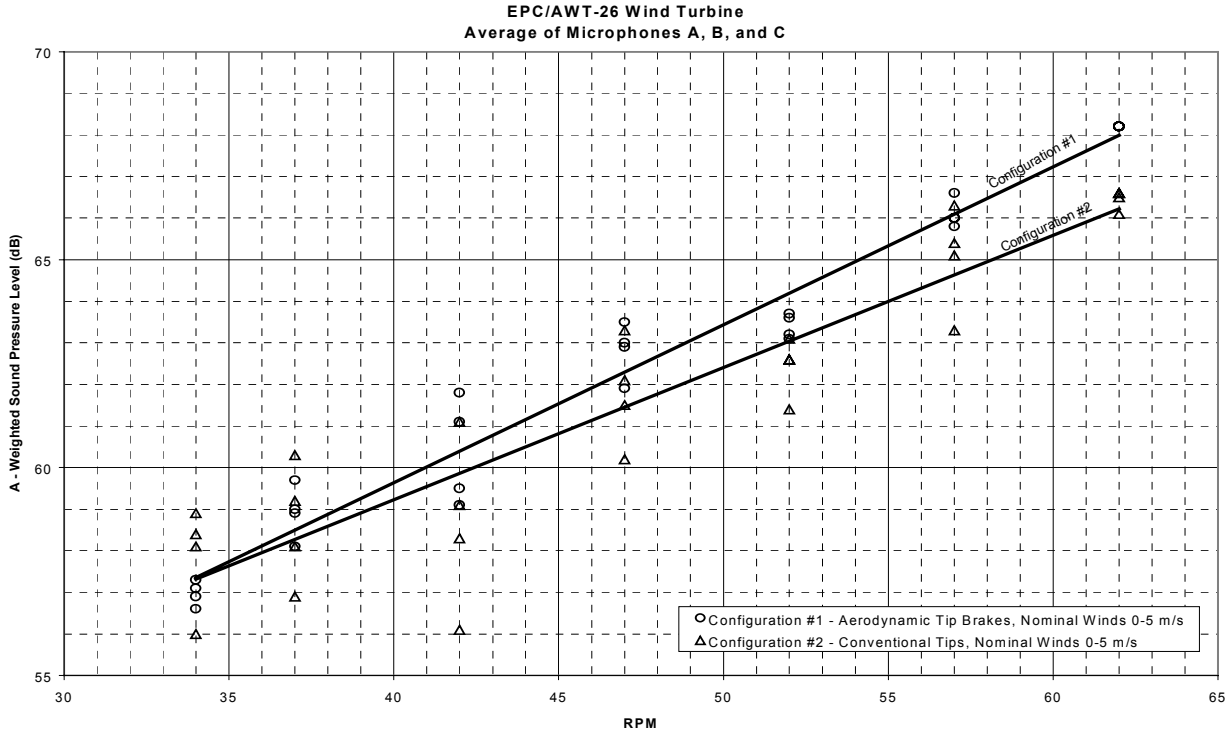

Figure 5.15 AWT-26VS rotor sound pressure levels

5.2.4 Discussion of Results

We operated the AWT-26 turbine at the National Wind Technology Center in three variable-speed operating modes for extended periods to collect mechanical and electrical data that would sufficiently characterize the steady-state and dynamic behavior of this turbine in variable-speed operating mode. The test results of the variable-speed operation have to be viewed in light of the two following operating limitations that we knew would have a detrimental impact in particular on the measured power-curves and, thus, AEP:

- The maximum operating RPM was limited to approximately 58 rotor RPM, because we would have otherwise exceeded the safety margins of the existing mechanical brake. We knew that, in order to show significant gains in AEP, operation of up to at least 63 rotor RPM would be necessary. Obviously, this was not possible.
- For safety reasons, we limited the maximum output power setting for both the soft-stall and maximum-energy capture operating modes to 240 kW, compared to the 275 kW setting for fixed-speed operation.

The power-curves from discrete-speed operation (see Figure 5.3) show no gain in output power at wind speeds below 7 m/sec despite the fact that the rotor C_p (see Figure 5.10) is higher at these wind-speeds. This means that the increased rotor output power is lost in higher electrical losses of the generator and power converter (The fixed-speed system obviously has no power converter). A potential remedy for this shortcoming would be a different 4-quadrant power converter, which leaves the grid-side inverter-bridge inoperative during operation at sub-synchronous generator RPM. (Power flow through the converter is from the grid to the generator under this operating condition). During sub-synchronous generator operation, this would cut the electrical losses of the power converter approximately in half.

This modification would result in:

- A considerable improvement of the power curve at low wind-speeds due to the high sensitivity of this curve to any kind of mechanical or electrical losses in Region II, and
- An improved AEP due to the large number of operating hours spent in Region II.

The relative drop of peak-C_p from 57 RPM down to 32 RPM in Figure 5.10 is attributed to Reynolds number effects [6], even though some loss of accuracy in the measured data for the drive-train efficiencies may account for some of the difference.

Furthermore, the C_p-curve data show that rotor performance using the maximum energy-capture method is superior to rotor performance using the soft-stall method, keeping in mind that we did not attempt to push the soft-stall approach to its limits (again due to safety concerns). This may have resulted in better rotor performance. The data points of maximum energy-capture follow quite closely the fixed-speed curve; however, we would have expected this curve above the 57 RPM fixed-speed curve because the turbine operated at 58 RPM.

Next to improvements in power output, a very important aspect in evaluating variable-speed operation was the ability of any variable-speed control approach to reduce mechanical stresses on the turbine, thus giving future turbine designers needed guidelines for applying lower absolute limits to their designs with the resulting reduction in cost of mechanical components. We considered the following performance aspects as crucial in evaluating variable-speed operation:

- Limitation of 1-second peak-power output:
  In fixed-speed operation, the highest recorded overshoot was 458 kW, corresponding to 167% rated power. In general, stall-controlled turbines may experience overshoots of up to 200 % of rated power. The highest peak-power reading for the maximum-energy capture approach was 323 kW, corresponding to 130% of the peak-power setting. However, we have not attempted to reduce this overshoot through control parameter optimization. Using the soft-stall control method, the maximum output power did not exceed 240 kW. Because of lack of experience and the requirement to proceed with extreme caution, we did not attempt to push the capabilities of this approach any closer to its limits. From a cost standpoint, a

reduction in peak-power output benefits both the mechanical and electrical designs. The cost of the power-electronic converter is largely driven by its peak-current requirement.

- Reduction of drive-train peak-torque:
  Figure 5.11 clearly shows that the number of low-frequency, high-amplitude cycles on the drive-train are reduced as the generator torque becomes a controlled quantity. The data for both fixed- and variable-speed curves were taken for winds with similar mean speeds and turbulence intensity.

An additional parameter that we were able to quantify was noise emissions of the turbine in both fixed and variable-speed modes of operation. Most important was our comparison of turbine sound-pressure levels of the original fixed-speed version with the variable-speed version, with both operating in low-wind conditions. We found that under these conditions the turbine sound pressure level during variable-speed operation was more than 10.5 dB lower than for the original fixed-speed version. Although this result does not affect COE, it will have an increasingly stronger impact on wind-farm siting decisions.

6.0 Conclusions

6.1 General

We performed trade-off studies on various variable-speed generation system topologies that we deemed feasible for wind-turbine application. Based on the results of these studies, we designed and prototyped variable-speed generation systems for doubly fed generators rated at 275 kW and 750 kW. Both systems were tested in the laboratory and on actual wind turbines in the field. In addition, an efficiency test of a commercial 275 kW wind-turbine gearbox was performed.

The results of the VSGS trade-off studies were clearly in favor of the doubly fed generator topology, both in terms of system efficiency and in terms of projected manufacturing cost. For the purpose of good power quality—both on the grid and on the DFG rotor—we selected the USRC as power converter of choice. We had prototyped this type of power converter at lower power levels before; however, implementation at current levels of 125 and 300 Amps, respectively, meant that we had to cover some new ground, both in terms of sourcing appropriately rated components and physical layout.

We encountered difficulties finding instrumentation that allowed us to measure the electrical rotor quantities of the doubly fed generator accurately. This was crucial for the determination of the component efficiencies of the VSGS. In the end, we did collect credible, averaged data that allowed us to completely characterize the 275 kW VSGS overall and its components (generator and power converter).

During field-testing on the 750-kW wind turbine, we found that the original VSGS control algorithm ran into conflicts with the turbine control algorithm and was not suitable for steady-state turbine control. However, we were able to show that this algorithm was capable of eliminating 3p-oscillations normally encountered with fixed-speed systems.

We were able to characterize a 275 kW VSGS on a turbine at NREL in three different operating modes. Two of these operating modes incorporated a new control algorithm (vector control) for the doubly fed generator. Though we were not able to completely eliminate all control irregularities the VSGS showed good dynamic stability in sometimes challenging operating conditions. Overall, turbine operation was dynamically much smoother than in its original fixed-speed mode.

6.2 Projected Commercial System Performance

Both the laboratory and field test results show clearly that the originally chosen electrical system operated at less-than-expected overall efficiency, with the result that in low-wind conditions the gain in aerodynamic efficiency was lost in increased VSGS losses. Whereas it would be not economical to attempt to reduce the already low generator losses (both rotor and stator), a different topology and operating strategy for the power-electronic converter may yield significant improvements. During field-testing, it quickly became apparent that operating the VSGS in connection with the USRC resulted in excellent power quality. The requirements of IEEE Standard 519-1992 for the overall system were exceeded by far. However, this came at the cost of converter losses that had considerable impact on VSGS efficiency at low output power.

The USRC utilizes a soft-switched DC current-link to synthesize the desired output voltage waveforms. At fractional output power, the DC-current in the link cannot be reduced to less than approximately 60% of rated. This results in unacceptably high semiconductor conduction losses at minimum or zero output power. The challenge, therefore, is to devise a 4-quadrant converter topology that combines the desired effect of soft-switching and acceptable voltage-rise (dV/dt) on the rotor of the doubly fed generator with very high conversion efficiency over the entire operating range, acceptable harmonic levels, and controllable power-factor on the utility-grid side.

Over the past several years, EPC has developed, prototyped, and manufactured a parallel-resonant power converter (PRC) at current ratings of 50, 100, and 300 Amps that applies a pseudo-PWM signal against its load at a high modulation frequency with low dV/dt. The PRC topology utilizes two buses, a DC-bus and a resonant bus. This topology can be linked at the DC-bus with a standard PWM Insulated-Gate Bipolar Transistor (IGBT) bridge that is connected to the utility grid through a three-phase AC-inductor. In parallel with the PRC technology EPC has developed a PWM hard-switched inverter using state-of-the-art, highly integrated power-electronic building blocks for the same application. Figure 6.1 shows the power-circuit of this hybrid topology.

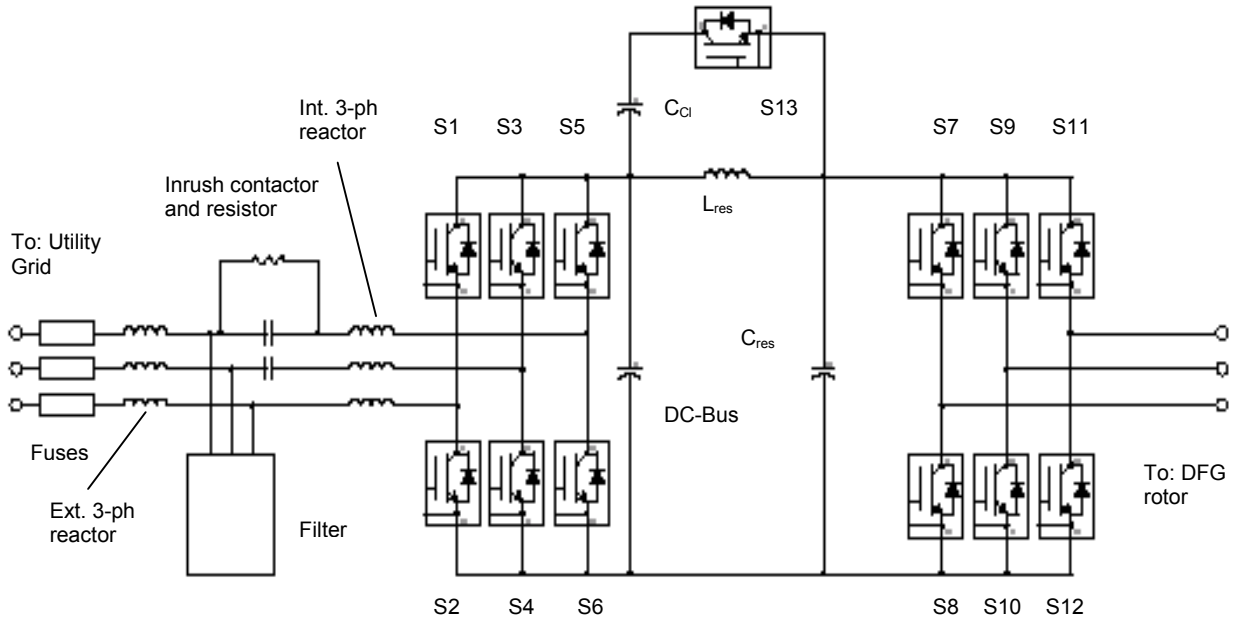

Figure 6.1 Hybrid PWM/soft-switching 4-quadrant power converter

As the generator operates at sub-synchronous RPM and very low power and as power flows through the converter from the utility grid to the generator rotor, the grid-side PWM-bridge is kept inactive and acts like a diode-rectifier at almost zero power loss. The resulting harmonic currents injected into the grid from the diode-rectifier are negligible compared to the limits allowed by IEEE 519–1992. Only the generator-side, soft-switching bridge is active. The grid-side IGBT-bridge would be activated by the rising DC bus voltage once power flows from the rotor to the converter at super-synchronous RPM. The grid-side PWM bridge will then be controlled to maintain the DC bus voltage at a set value by injecting sinusoidal currents into the utility grid while also maintaining a desired grid power factor. Injection of substantial amounts of reactive current would result in additional losses incurred by this bridge, however. Table 6.1 shows measured power loss figures for three characteristic VSGS operating points and the resulting overall VSGS efficiencies, both for the original USRC and for the proposed hybrid topology.

Table 6.1 System Efficiencies with Proposed New Hybrid Converter

RPM	P_{mech} [kW]	P_{rotor} [kW]	I_{rotor} [A]	P_{grid} [kW]	USRC loss [kW]	Hybrid loss [kW]	VSGS eff. (with USRC)	VSGS eff. (with Hybrid)
836	10.2	-5.1	54.8	3.6	2.8	1.6	35.5	47.1
1,356	125.9	12.8	78.3	114.4	4.3	2.2	90.9	92.5
1,618	249.6	59.2	111.8	232.1	5.9	4.0	93.0	93.8

The results clearly indicate the impact that converter efficiency has on overall VSGS efficiency at low VSGS output power.

6.3 Electrical System Cost Update

Because the USRC technology was never commercialized, no reliable manufacturing cost figures were available to enable a turbine designer to determine the overall cost of the turbine, nor determine a reliable COE figure.

EPC has manufactured both sides of the hybrid power converter and, therefore, has reliable manufacturing cost figures for both parts of this hybrid 4-quadrant power converter. The strong advantage of the hard-switching IGBT-bridge on the grid-side is that it can be purchased as one highly integrated block—including DC bus, IGBT drivers, and very sophisticated protection logic. This reduces the manufacturing cost considerably. Quantity cost figures for the 275-kW VSGS (including a 100 Amp rated 4-quadrant hybrid converter) are provided in Volume 2, Chapter 4.

7.0 Recommendations

During the course of this project, technical and patent-protection issues came up that needed to be addressed.

As previously mentioned, the USRC technology overshot the goal of good power-quality at the cost of efficiency at fractional load and estimated manufacturing cost. As a result, we proposed a different power converter topology—one that is technically mature, addresses all the requirements of a VSGS based on the doubly fed generator, and has a competitive manufacturing cost. We therefore recommend implementing such a topology in a doubly fed, variable-speed generation system in the future.

Much attention was paid to the patent-protection issue of variable-speed wind generation systems by Electronic Power Conditioning, Inc., and others. Kenetech Windpower successfully protected its legal rights for the patent protection of any VSGS topology for wind-power generation applications against a European competitor attempting to import its product into the United States. The broad interpretation of U.S. patent No. 5,083,039 [11] of the International Trade Commission (ITC) was unexpected at the onset of this project. Kenetech Windpower, however, went into bankruptcy shortly after the issuing of this ruling. Meanwhile, the electronics section of Kenetech Windpower was purchased by Trace and became Trace Technologies, Inc. The rights to this and other (less important) patents were purchased by Zond Systems (now Enron Wind). Enron has implemented a 750-kW variable-speed wind turbine based on the doubly fed generation system, with Trace Technologies supplying the controls and power electronic converter. The patent expires in 2009. Unless the applicability of the patent for the doubly fed topology is legally challenged, it will remain protected until its expiration.

8.0 References

[1] Muljadi, E.; Pierce, K.; and Migliore, P. *A Conservative Control Strategy for Variable-Speed Stall-Regulated Wind Turbines.* AIAA-2000-0031, ASME Conference, Reno, NV. NREL/CP-500-24791, January 2000.

[2] Lawlor, S.; McCoy, T.; Robertson, I.; and Weigand, C. *Variable-Speed Generation Subsystem using the Doubly-Fed Generator. Design Review Package,* Advanced Wind Turbines, Inc., and Electronic Power Conditioning, Inc. Prepared for National Renewable Energy Laboratory, February 1995

[3] Wright, A.; Osgood, R.; and Malcolm, D. *Analysis of a Two-Bladed, Teetering-Hub Turbine Using the ADAMS Software.* Presented at Windpower '94, Minneapolis, MN, May 1994

[4] Christenson, C.; Mikhail, A.; and Weigand, C. *Advanced Wind Turbine Next Generation Innovative Subsystems Project, Lower Tier Subcontract Support. 2nd Design Review Meeting,* Zond Energy Systems Inc., October 1995

[5] Muljadi, E. *Variable Speed Implementation of EPC Generating Systems with RLA-AWT26 Wind Turbine and the Associated Control Systems.* National Renewable Energy Laboratory, Wind Technology Division, January 1994

[6] Pierce, K. and Migliore, P. *Maximizing Energy Capture of Fixed-Pitch Variable-Speed Wind Turbines.* AIAA-2000-0032, ASME Conference, Reno, NV. NREL/CP-500-27551, January 2000

[8] Christenson, C. and Mikhail, A. *Zond Z-40M Field Experiment Test Plan.* Zond Energy Systems, Inc. Prepared for National Renewable Energy Laboratory, April 1996

[9] McCoy, T. and Griffin, D. *EPC/AWT-26 Variable Speed Turbine Test Plan.* Advanced Wind Turbines Inc. Seattle, WA, November 1997

[10] Larwood, S.M. *Dynamic Characterization of the AWT-26 Turbine for Variable Speed Operation.* NREL/TP-500-24919, Golden, CO. National Renewable Energy Laboratory, July 1998

[11] Richardson, R.D. and Erdman, W.L., U.S. Patent No. 5,083,039. *Variable Speed Wind Turbine.* U.S. Windpower, Inc. Livermore, California, January 21, 1992.

[12] Vas, P. *Vector Control of AC Machines.* Oxford University Press, Monographs in Electrical and Electronic Engineering, 1990

[13] Migliore, P. Memorandum to NWTC Site 3.2 Incident Review Team, Subject: *Activities Related to Electrical Cabinet Fire at NWTC Site 3.2 on November 3, 1997,* dated January 26, 1998.

Appendix A.1

ID	Name
1	NREL Variable-Speed Wind Generation Project
2	Start of NREL Project
3	Task 1.0 Project Planning
4	Task 1.1 Project Work Plan (Deliverable #1)
5	Task 1.2 Technical Review Meeting (Meeting #1)
6	Task 1.3 Kick-off Meeting (Meeting #2)
7	Task 2.0 VSGS Preliminary Design
8	Task 2.1 Trade-off Studies
9	Task 2.2 Performance and Cost Analyses
10	Task 2.3 O&M Analysis
11	Task 2.4 Special Considerations for Baseline Turbine
12	Task 2.5 Design Review Package (Deliverable #3)
13	Task 2.6 Design Review Meeting (Meeting #3)
14	
15	
16	
17	
18	
19	
20	
21	
22	
23	
24	
25	
26	

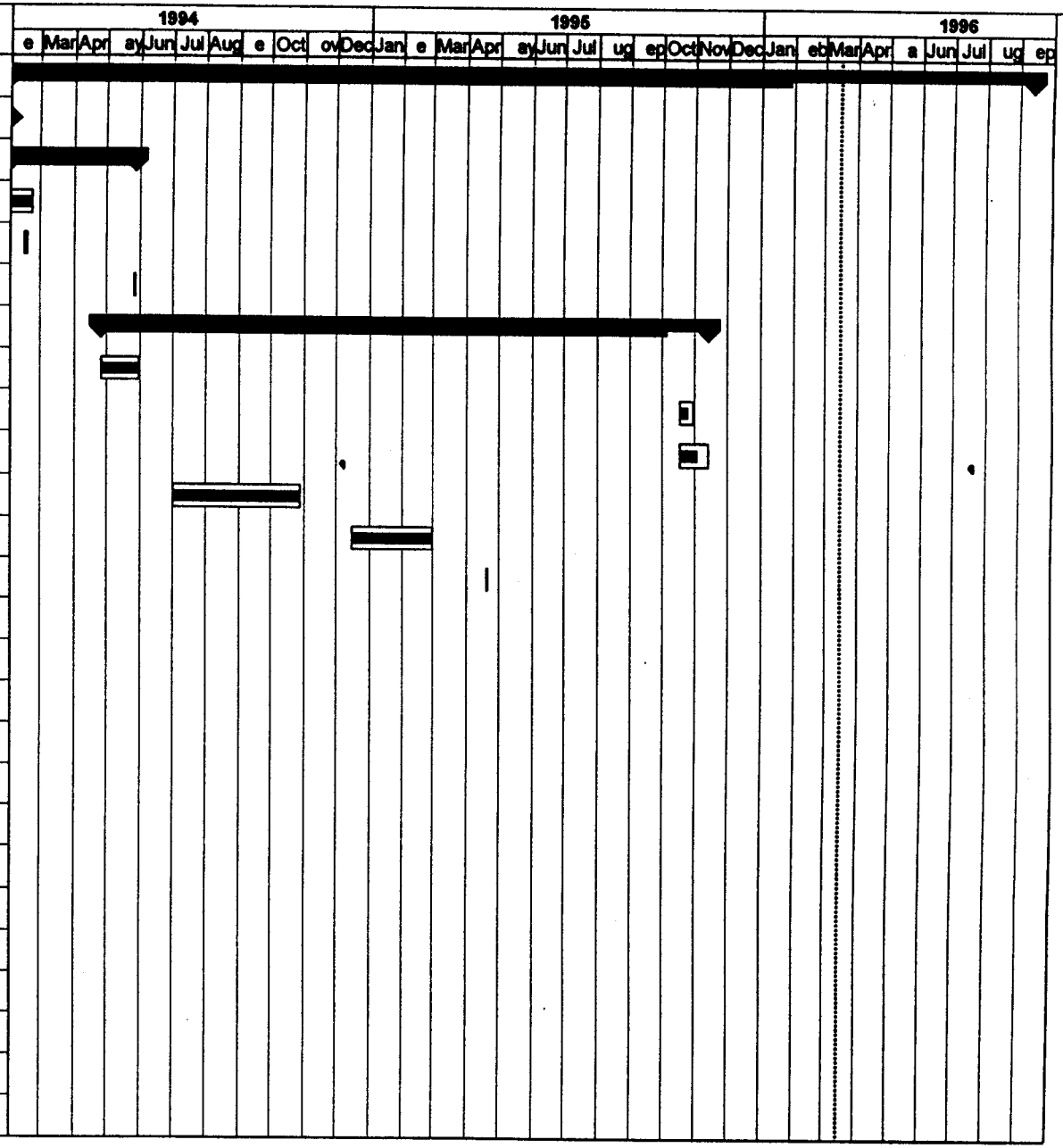

Project: NREL VSGS Project
Date: 3/14/96

Critical
Noncritical
Percent complete
Milestone
Summary

NREL PROJECT SCHEDULE

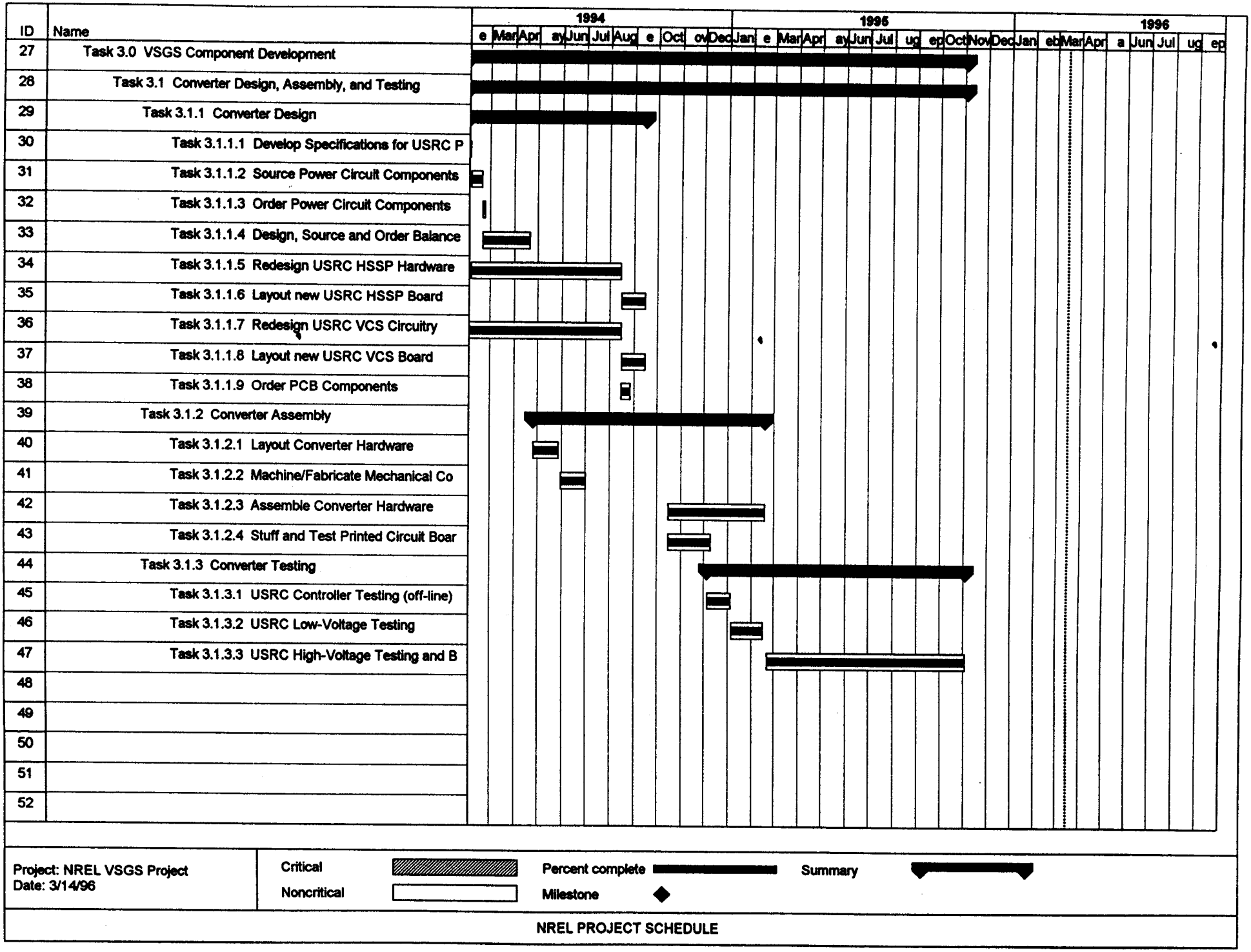
ID
Name
1994
1995
1996
27 Task 3.0 VSGS Component Development
28 Task 3.1 Converter Design, Assembly, and Testing
29 Task 3.1.1 Converter Design
30 Task 3.1.1.1 Develop Specifications for USRC P
31 Task 3.1.1.2 Source Power Circuit Components
32 Task 3.1.1.3 Order Power Circuit Components
33 Task 3.1.1.4 Design, Source and Order Balance
34 Task 3.1.1.5 Redesign USRC HSSP Hardware
35 Task 3.1.1.6 Layout new USRC HSSP Board
36 Task 3.1.1.7 Redesign USRC VCS Circuitry
37 Task 3.1.1.8 Layout new USRC VCS Board
38 Task 3.1.1.9 Order PCB Components
39 Task 3.1.2 Converter Assembly
40 Task 3.1.2.1 Layout Converter Hardware
41 Task 3.1.2.2 Machine/Fabricate Mechanical Co
42 Task 3.1.2.3 Assemble Converter Hardware
43 Task 3.1.2.4 Stuff and Test Printed Circuit Boar
44 Task 3.1.3 Converter Testing
45 Task 3.1.3.1 USRC Controller Testing (off-line)
46 Task 3.1.3.2 USRC Low-Voltage Testing
47 Task 3.1.3.3 USRC High-Voltage Testing and B
48
49
50
51
52
Project: NREL VSGS Project
Date: 3/14/96
Critical
Noncritical
Percent complete
Milestone
Summary
NREL PROJECT SCHEDULE

ID	Name
53	Task 3.2 DFG Design, Assembly, and Testing
54	Task 3.2.1 Supply DFG Specifications to Selected Ma
55	Task 3.2.2 Study DFG Designs as Proposed By Man
56	Task 3.2.3 Request Design Changes
57	Task 3.2.4 DFG Assembly
58	Task 3.2.5 DFG Witness Test at Factory
59	Task 3.2.6 DFG Shipping to EPC
60	Task 3.3 Controller Design, Assembly, and Testing
61	Task 3.3.1 Controller Architecture Design
62	Task 3.3.2 Controller Hardware Schematics
63	Task 3.3.3 Controller PCB Layout
64	Task 3.3.4 Order Controller PCB Components
65	Task 3.3.5 Controller PCB Stuffing and Testing
66	Task 3.3.6 Controller PCB Programming
67	Task 3.4 Power System Integration
68	Task 3.4.1 Design, Source, and Order Power System
69	Task 3.4.2 Layout Power System Hardware
70	Task 3.4.3 Assemble Power System Hardware
71	
72	
73	
74	
75	
76	
77	
78	

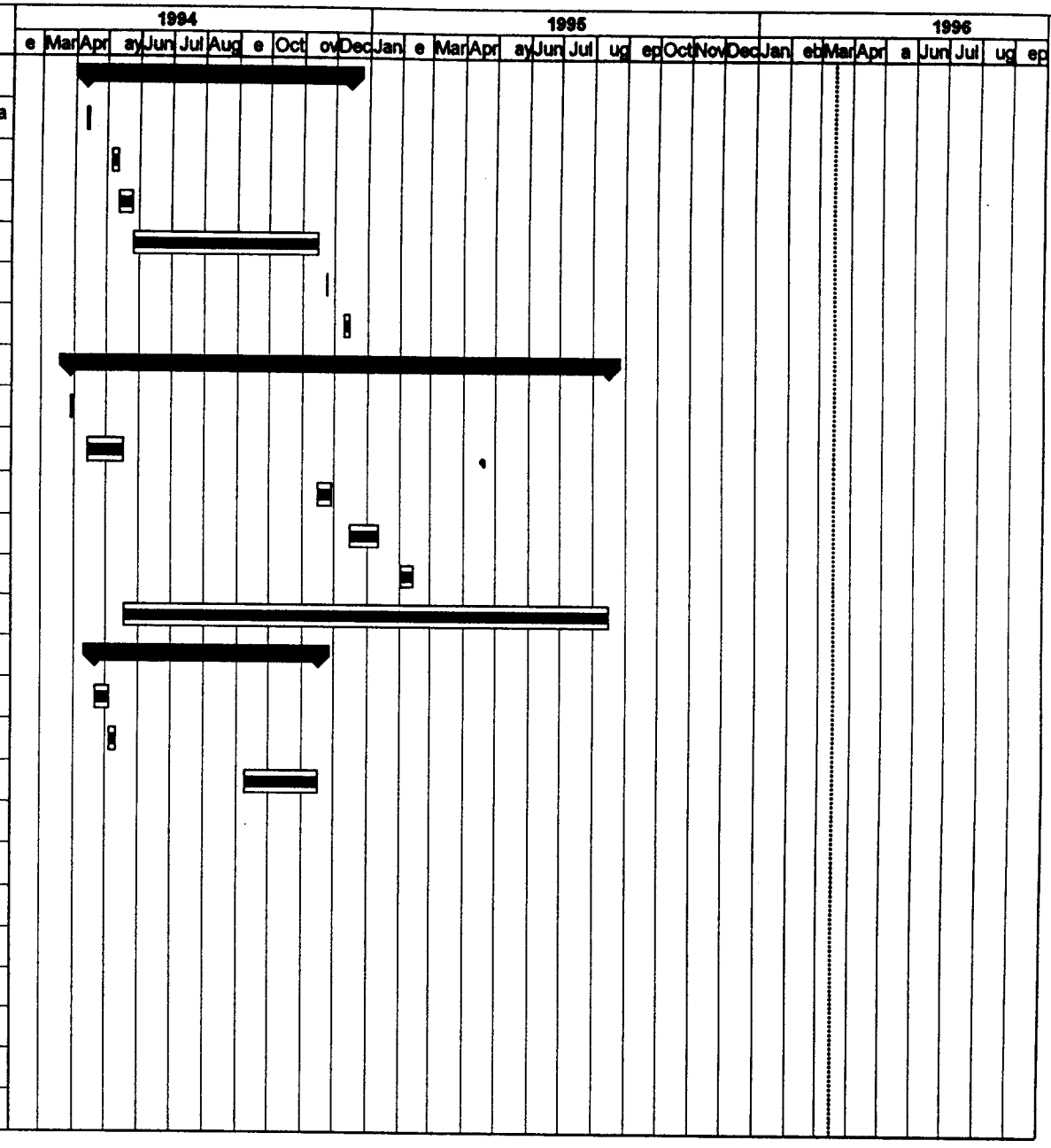

Project: NREL VSGS Project
Date: 3/14/96

Critical
Noncritical
Percent complete
Milestone
Summary

NREL PROJECT SCHEDULE

ID	Name
79	Task 4.0 VSGS Laboratory Testing
80	Task 4.1 Laboratory Test Plan (Deliverable #4)
81	Task 4.2 Laboratory Test Equipment
82	Task 4.3 Laboratory Test Set-up
83	Task 4.4 Laboratory Testing
84	Task 4.4.1 VSG System Start-up and Debugging
85	Task 4.4.2 Integrated VSG System Test and Docume
86	Task 4.4.2.1 Set-Up of Data Acquisition System
87	Task 4.4.2.2 Implementation of Turbine Drive-Tr
88	Task 4.4.2.3 Static and Dynamic System Test
89	Task 4.5 Laboratory Test Results
90	Task 5.0 VSGS Field Testing
91	Task 5.1 Turbine Test Plans (Deliverable #5)
92	Task 5.2 Turbine Retrofit and Restoration
93	Task 5.2.1 V-15 Turbine Retrofit
94	Task 5.2.2 V-15 Turbine Restauration
95	Task 5.2.3 Z-40 Turbine Retrofit
96	Task 5.2.4 Z-40 Restauration
97	Task 5.2.5 AWT-26 (P3) Retrofit
98	Task 5.2.6 AWT-26 (P3) Restauration
99	Task 5.3 Field-Test Equipment
100	Task 5.4 Test Readiness Review Meeting (Meeting #4)
101	Task 5.5 Turbine Testing
102	Task 5.5.1 V-15 Turbine Testing
103	Task 5.5.2 Z-40 Turbine Testing
104	Task 5.5.3 AWT-26 (P3) Testing

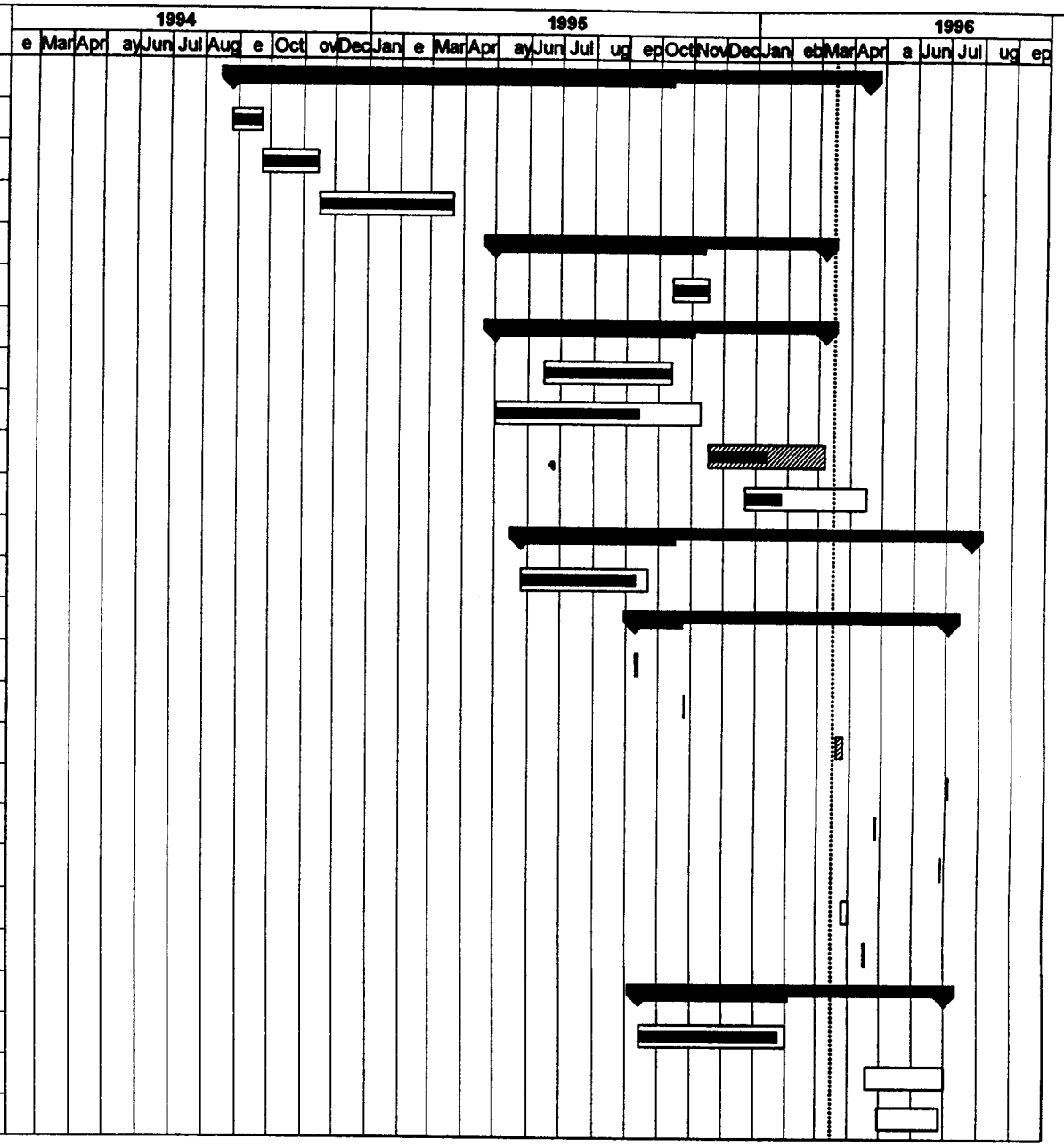

Project: NREL VSGS Project
Date: 3/14/96

Critical
Noncritical
Percent complete
Milestone
Summary

NREL PROJECT SCHEDULE

ID	Name
105	Task 5.6 Field Test Results
106	Task 6.0 Summary Analysis of VS Turbine Operation
107	Task 7.0 Final Report (Deliverable #6)
108	Task 8.0 Final Review Meeting (Meeting #5)
109	End of NREL Project

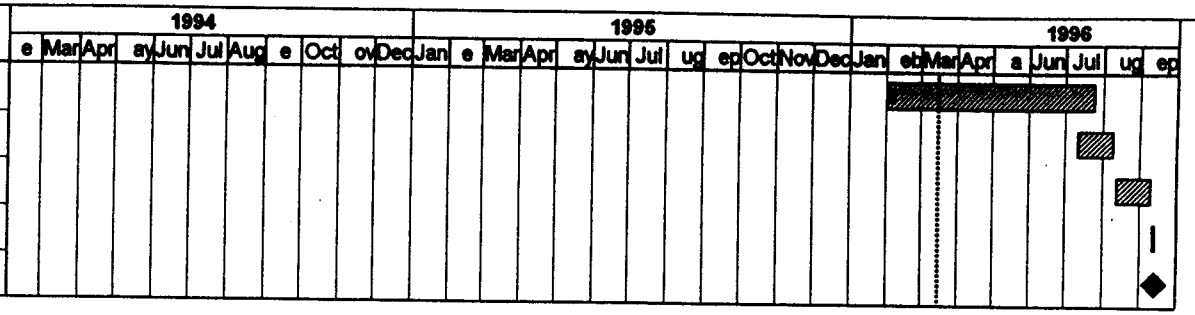

Project: NREL VSGS Project
Date: 3/14/96

Critical
Noncritical
Percent complete
Milestone
Summary

NREL PROJECT SCHEDULE

Appendix A.2

275KW VSGS

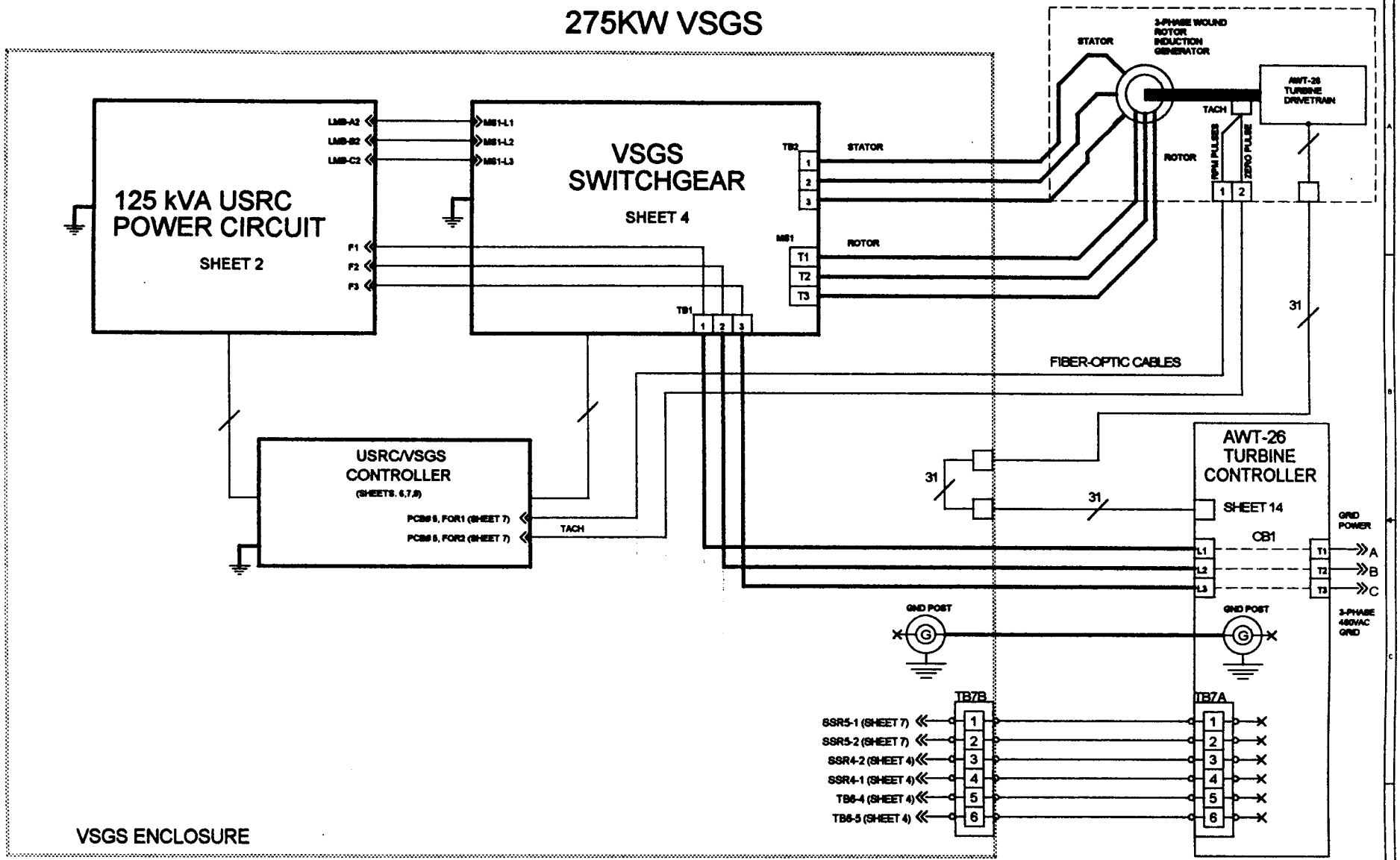

FILE: 434B.SCH

NOTES:

NOTE 1: EARTH GROUND IS TO BE 1 AWG INSULATED WIRE AND ISOLATED FROM ALL OTHER GROUNDING SYSTEMS.

NOTE 2:
ALL POWER CABLE SHOWN IS 3/0 AWG OR 2 EACH 1 AWG COPPER.

APPROVALS		DATE
Engineer:	CW	
Drawn:	JBN	
Checked:	CHW	

Sunday, April 18, 1993

Electronic Power Conditioning Inc.

275KW VSGS MAIN POWER SCHEMATIC

Size	CAGE CODE	DWG NO	Rev
B		00434	A

SCALE

Sheet 1 of 14

4-18-97 JBN

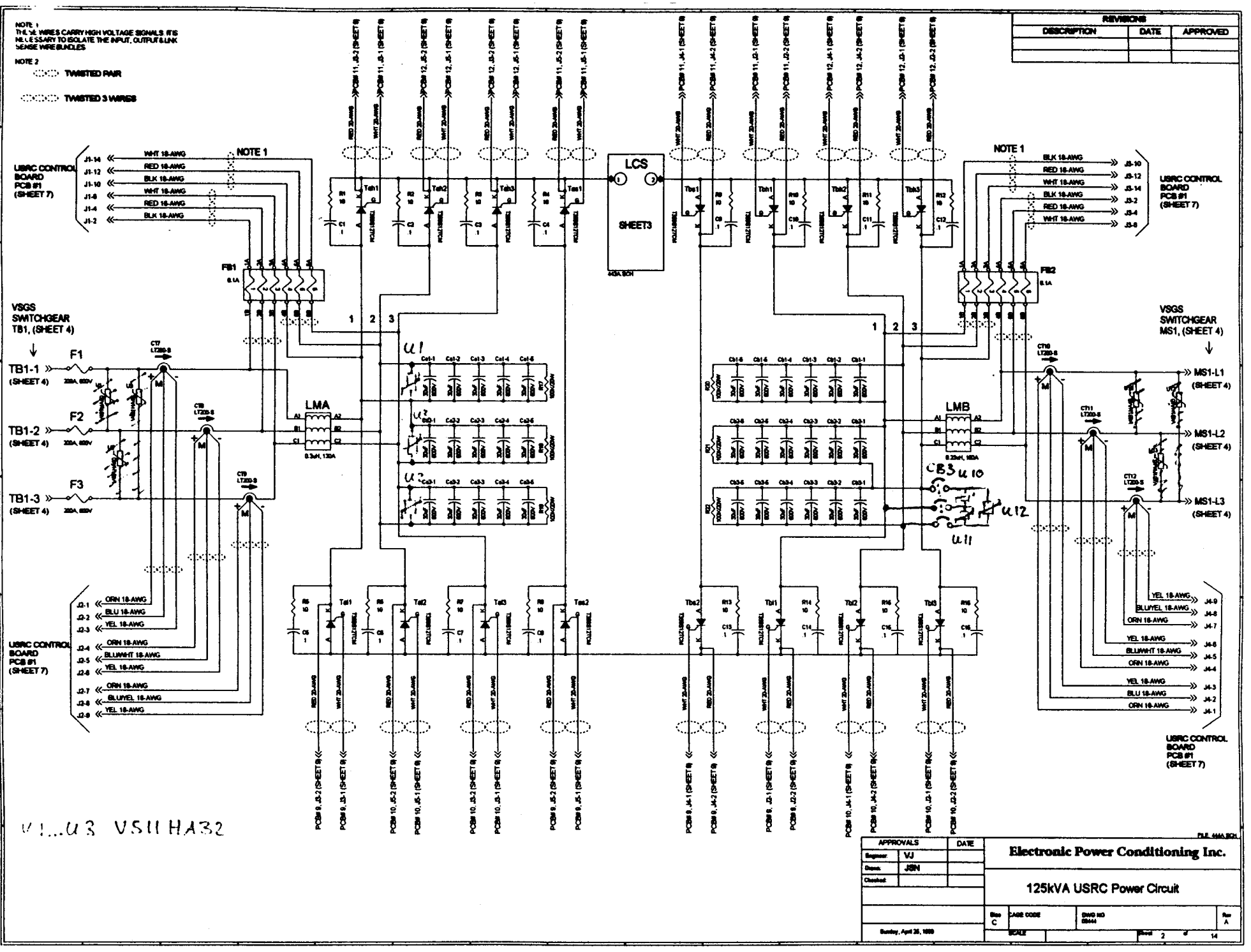
NOTE 1
THESE WIRES CARRY HIGH VOLTAGE SIGNALS. IT IS NECESSARY TO ISOLATE THE INPUT, OUTPUT & LINK SENSE WIRE BUNDLES
NOTE 2
TWISTED PAIR
TWISTED 3 WIRES
REVISIONS
DESCRIPTION
DATE
APPROVED
USRC CONTROL BOARD PCB #1 (SHEET 7)
VSGS SWITCHGEAR TB1, (SHEET 4)
VSGS SWITCHGEAR MS1, (SHEET 4)
LCS
SHEET3
LMA
LMB
TB1-1
TB1-2
TB1-3
MS1-L1
MS1-L2
MS1-L3
F1
F2
F3
V1...U3 VS11HA32
Electronic Power Conditioning Inc.
125kVA USRC Power Circuit

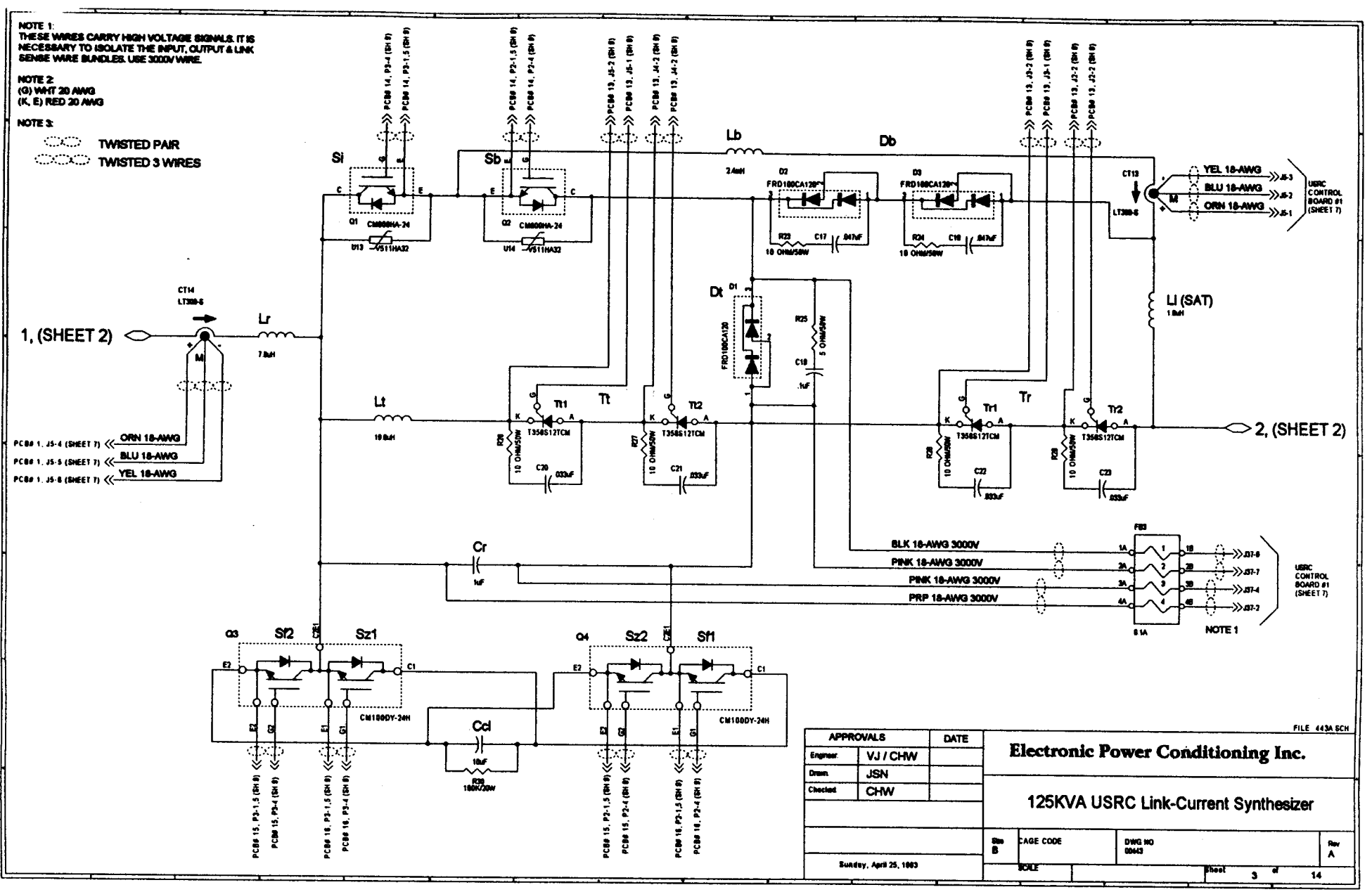
NOTE 1:
THESE WIRES CARRY HIGH VOLTAGE SIGNALS. IT IS NECESSARY TO ISOLATE THE INPUT, OUTPUT & LINK SENSE WIRE BUNDLES. USE 3000V WIRE.
NOTE 2:
(G) WHT 20 AWG
(K, E) RED 20 AWG
NOTE 3:
TWISTED PAIR
TWISTED 3 WIRES
Si
Sb
Lb
2.4mH
Db
D2
FRD180CA120
D3
FRD180CA120
CT13
LT308-S
YEL 18-AWG
BLU 18-AWG
ORN 18-AWG
J5-3
J5-2
J5-1
USRC CONTROL BOARD #1 (SHEET 7)
Q1
CM800HA-24
Q2
CM800HA-24
U13
V511HA32
U14
V511HA32
R23
10 OHM/50W
C17
.047uF
R24
10 OHM/50W
C18
.047uF
CT14
LT308-S
1, (SHEET 2)
Lr
7.8uH
Dt
D1
FRD180CA120
R25
5 OHM/50W
C19
.1uF
Ll (SAT)
1.8uH
Lt
10.8uH
Tt1
T358S127CM
Tt
Tt2
T358S127CM
R26
10 OHM/50W
C20
.033uF
R27
10 OHM/50W
C21
.033uF
Tr1
T358S127CM
Tr
Tr2
T358S127CM
R28
10 OHM/50W
C22
.033uF
R29
10 OHM/50W
C23
.033uF
2, (SHEET 2)
PCB# 1, J5-4 (SHEET 7)
ORN 18-AWG
PCB# 1, J5-5 (SHEET 7)
BLU 18-AWG
PCB# 1, J5-6 (SHEET 7)
YEL 18-AWG
Cr
1uF
BLK 18-AWG 3000V
PINK 18-AWG 3000V
PINK 18-AWG 3000V
PRP 18-AWG 3000V
FB3
61A
J37-6
J37-7
J37-4
J37-2
USRC CONTROL BOARD #1 (SHEET 7)
NOTE 1
Q3
Sf2
Sz1
CM100DY-24H
Q4
Sz2
Sf1
CM100DY-24H
Ccl
10uF
R30
100K/20W
PCB# 15, P3-1,5 (SH 9)
PCB# 15, P3-4 (SH 9)
PCB# 16, P3-1,5 (SH 9)
PCB# 16, P3-4 (SH 9)
PCB# 15, P2-1,5 (SH 9)
PCB# 15, P2-4 (SH 9)
PCB# 16, P2-1,5 (SH 9)
PCB# 16, P2-4 (SH 9)
FILE 443A.SCH
APPROVALS
DATE
Engineer VJ / CHW
Drawn JSN
Checked CHW
Sunday, April 25, 1993
Electronic Power Conditioning Inc.
125KVA USRC Link-Current Synthesizer
Size B
CAGE CODE
DWG NO 00443
Rev A
SCALE
Sheet 3 of 14

VSGS SWITCHGEAR

REVISIONS		
DESCRIPTION	DATE	APPROVED

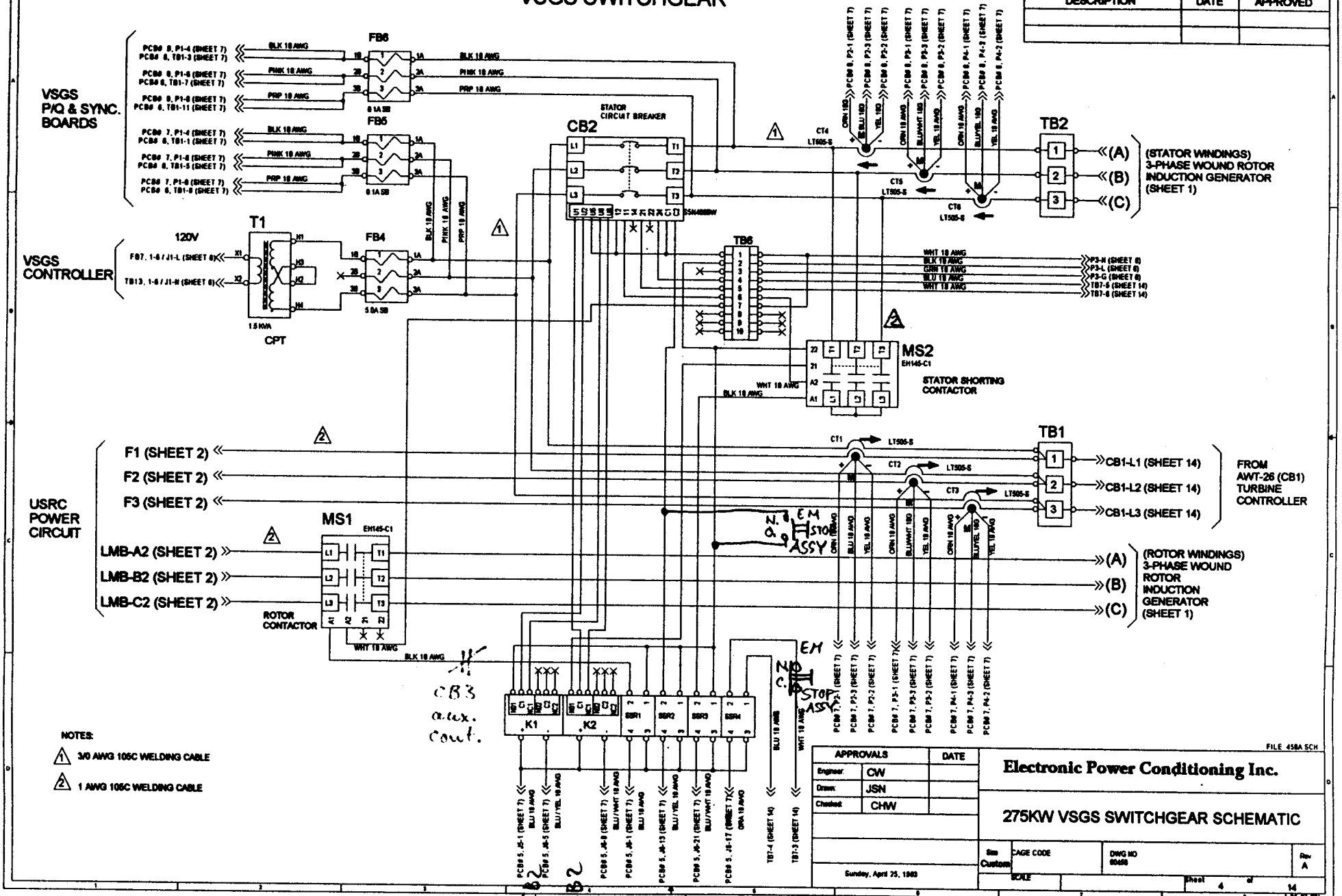

APPROVALS		DATE
Engineer	CW	
Drawn	JSN	
Checked	CHW	

Sunday, April 25, 1993

Electronic Power Conditioning Inc.

275KW VSGS SWITCHGEAR SCHEMATIC

Size	CAGE CODE	DWG NO	Rev
Custom		80458	A

SCALE | Sheet 4 of 14

FILE 458A.SCH

4-25-97 JSN

Open CB2 Close CB2 MS1 MS2 Trip CB2 Touch

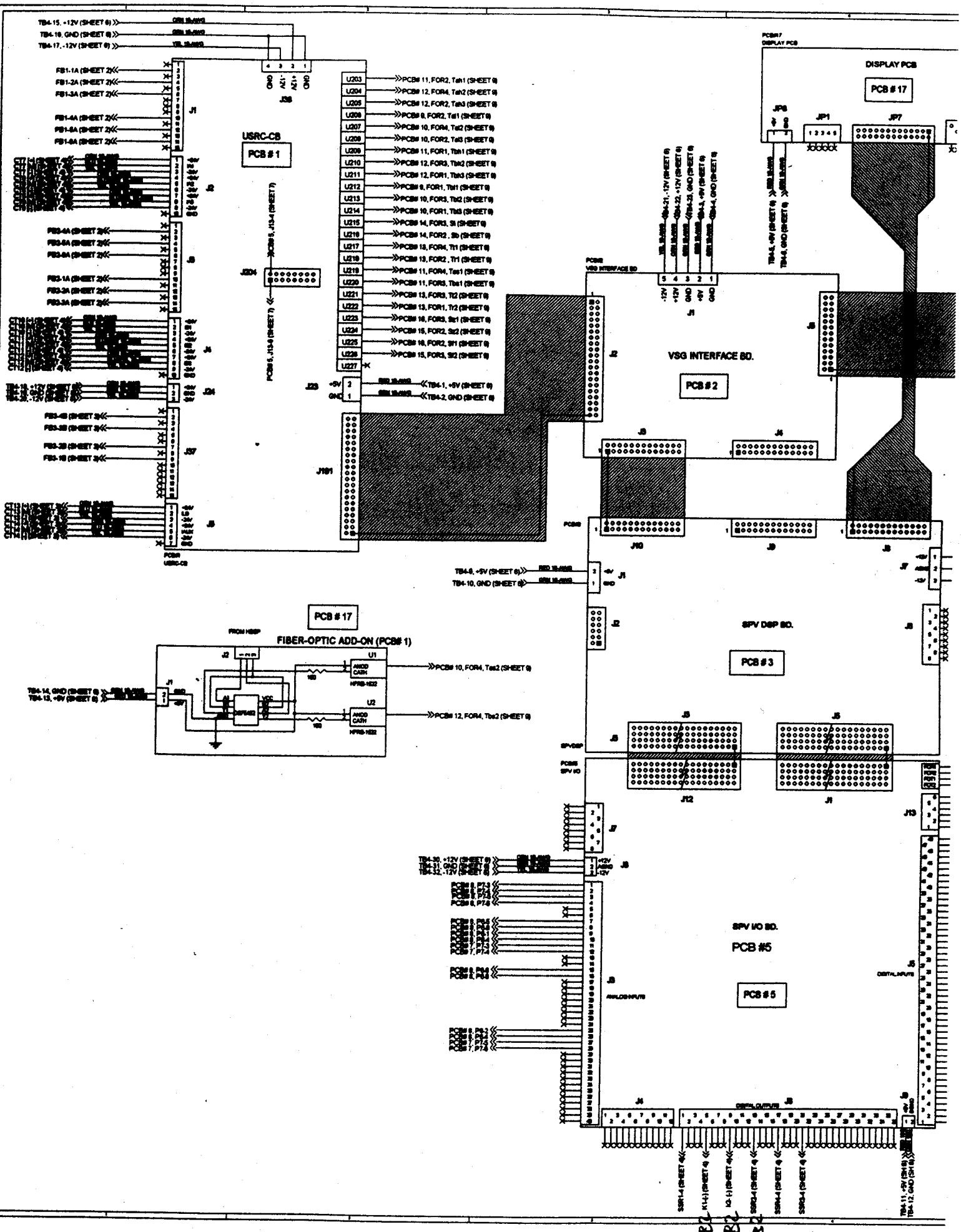

MS1 open CB2 close CB2 in it fan it MS2

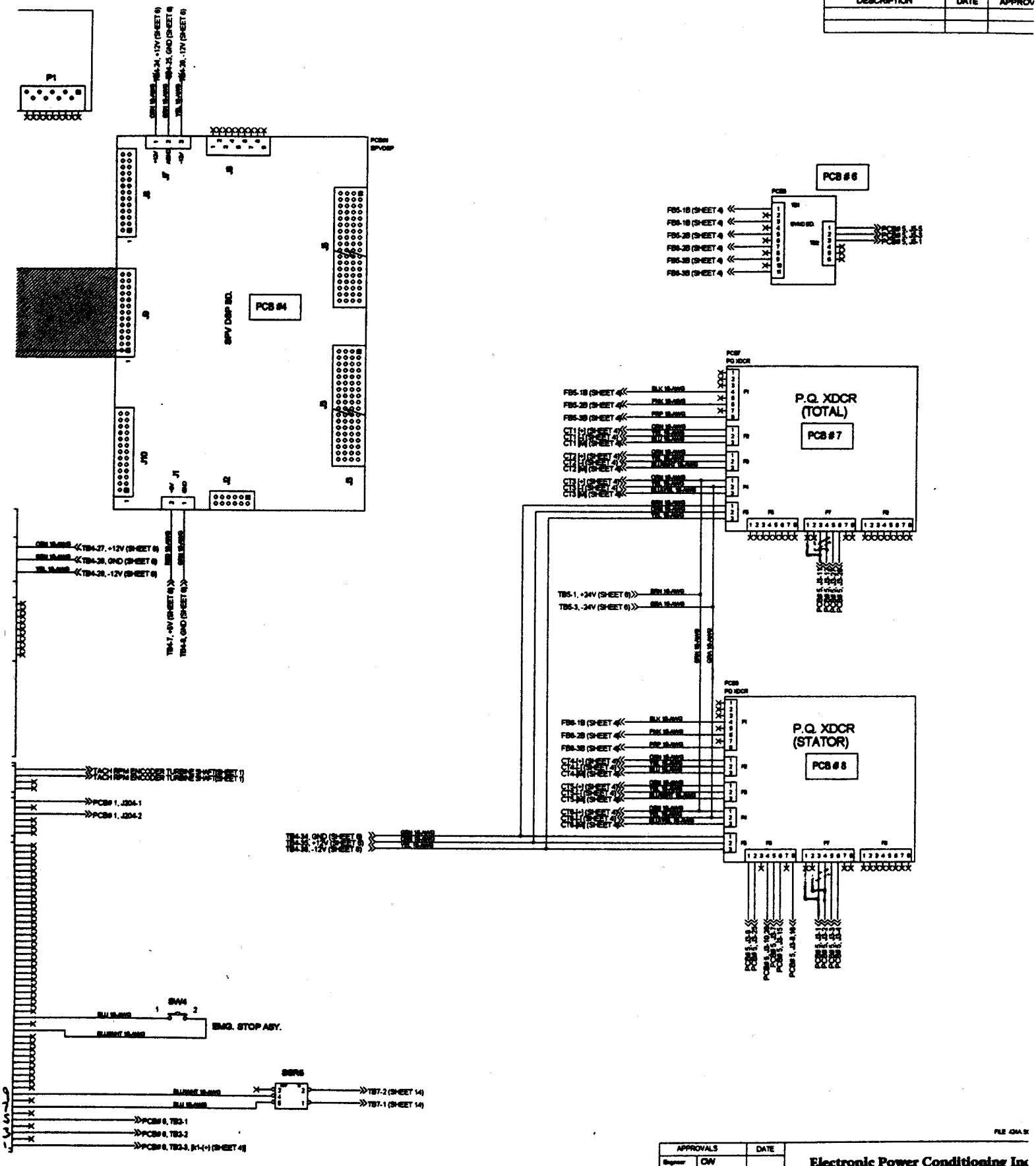
REVISIONS
DESCRIPTION
DATE
APPROV
P1
PCB#4
SPV DSP BD.
PCB#6
PCB#7
P.Q. XDCR
(TOTAL)
PCB#8
P.Q. XDCR
(STATOR)
SW4
EMG. STOP ASY.
SSR6
APPROVALS
DATE
Engineer
CW
Drawn
JBN
Checked
Electronic Power Conditioning Inc
VSGS CONTROL BOARDS
SIZE
D
CAGE CODE
DWG NO
SCALE
Sheet 7 of 14

VSGS CONTROLLER SCHEMATIC

REVISIONS		
DESCRIPTION	DATE	APPROVED

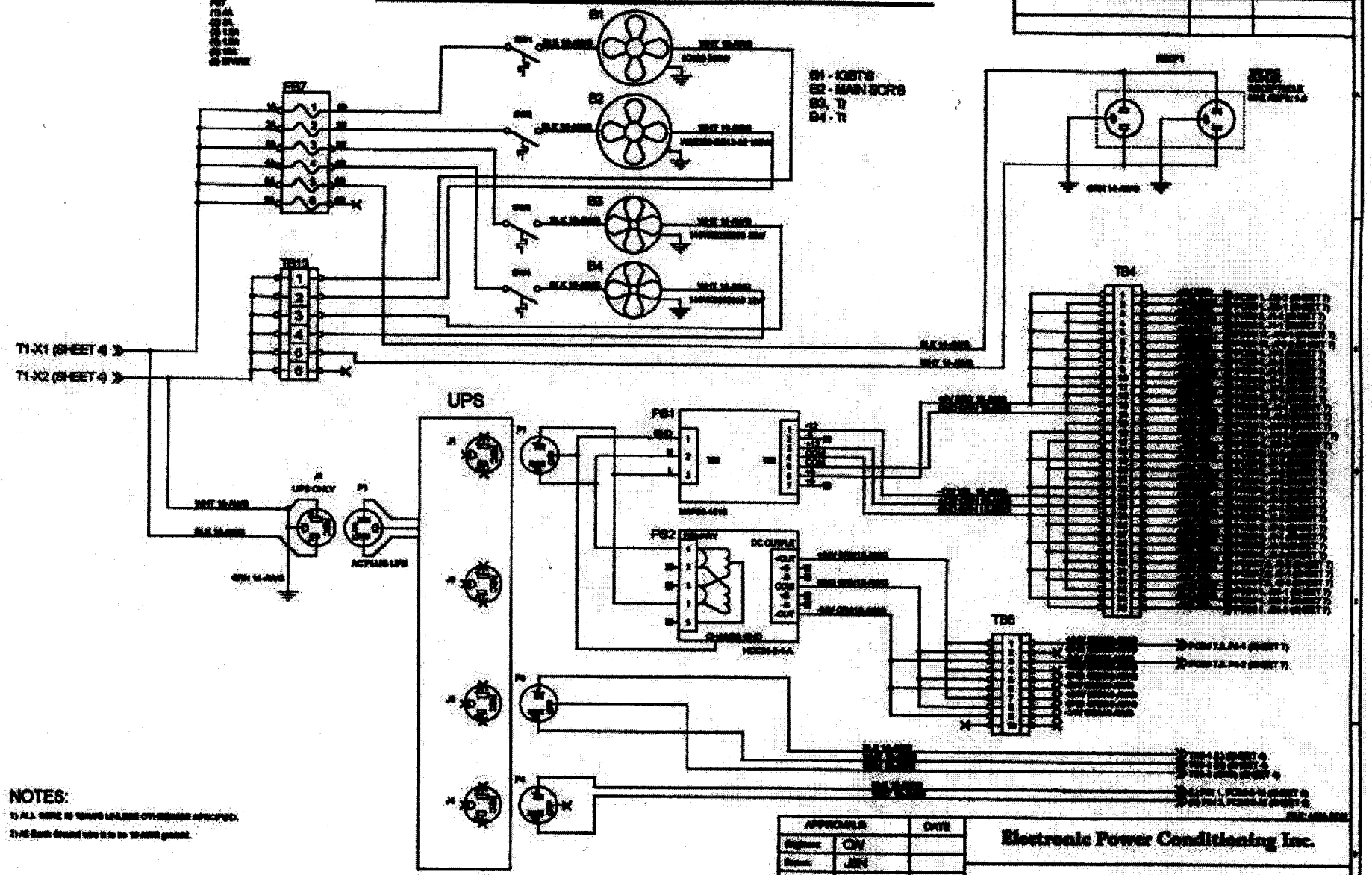

NOTES:

1) ALL WIRE IS 16 AWG UNLESS OTHERWISE SPECIFIED.

2) All Earth Ground wire is to be 10 AWG gauge.

APPROVALS		DATE
	CW	
	JEN	

Electronic Power Conditioning Inc.

VSGS CONTROLLER SCHEMATIC

Size B	DWG NO	REV A
SCALE		SHEET 6 OF 14

REVISIONS		
DESCRIPTION	DATE	APPROVED

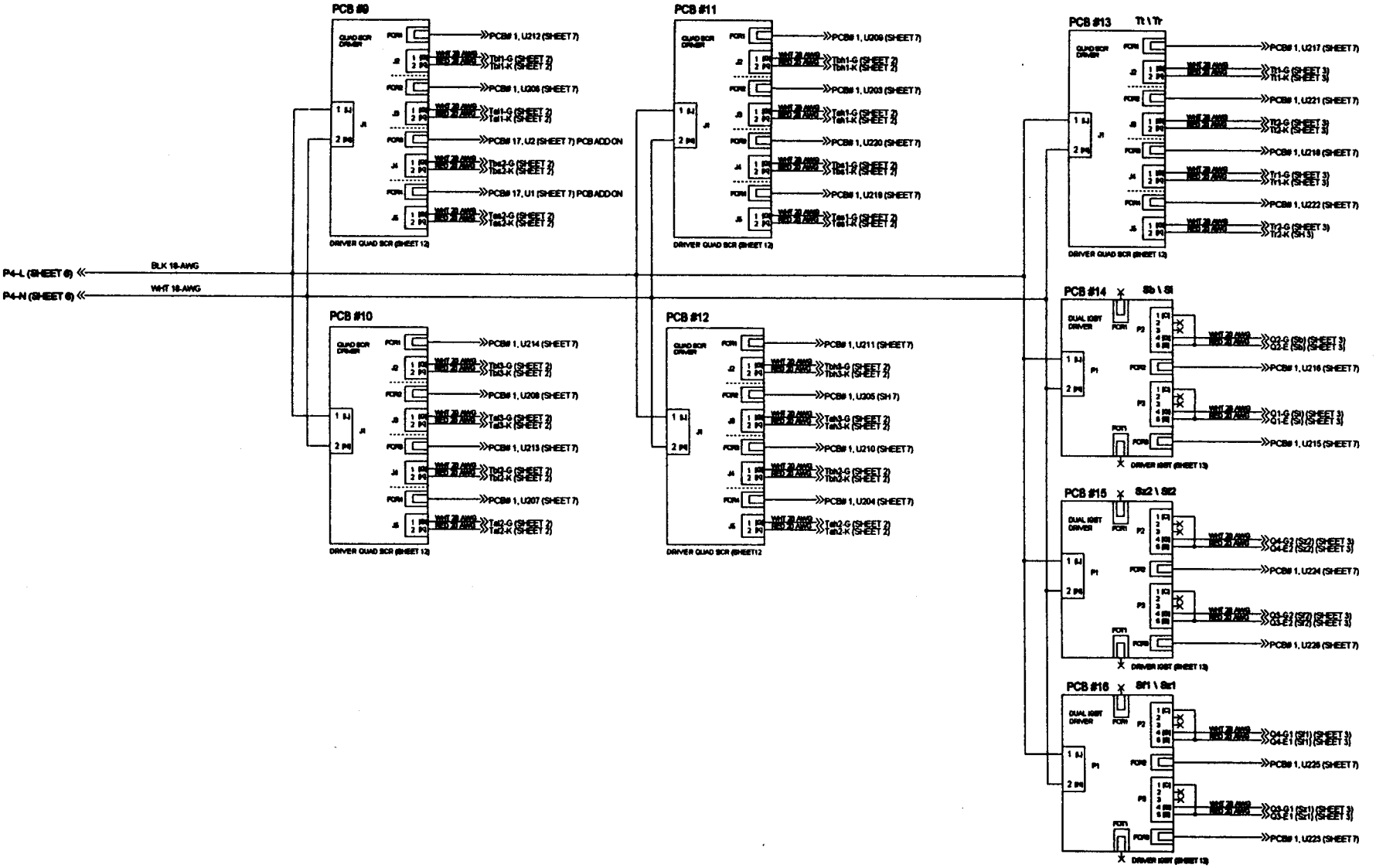

APPROVALS		DATE
Engineer		
Drawn	JBN	
Checked	CHW	

Sunday, April 10, 2022

Electronic Power Conditioning Inc.

DRIVER BOARDS WIRING DIAGRAM

Size	CAGE CODE	DWG NO	Rev
C		60000	A

SCALE

Sheet 9 of 14

REVISIONS		
DESCRIPTION	DATE	APPROVED

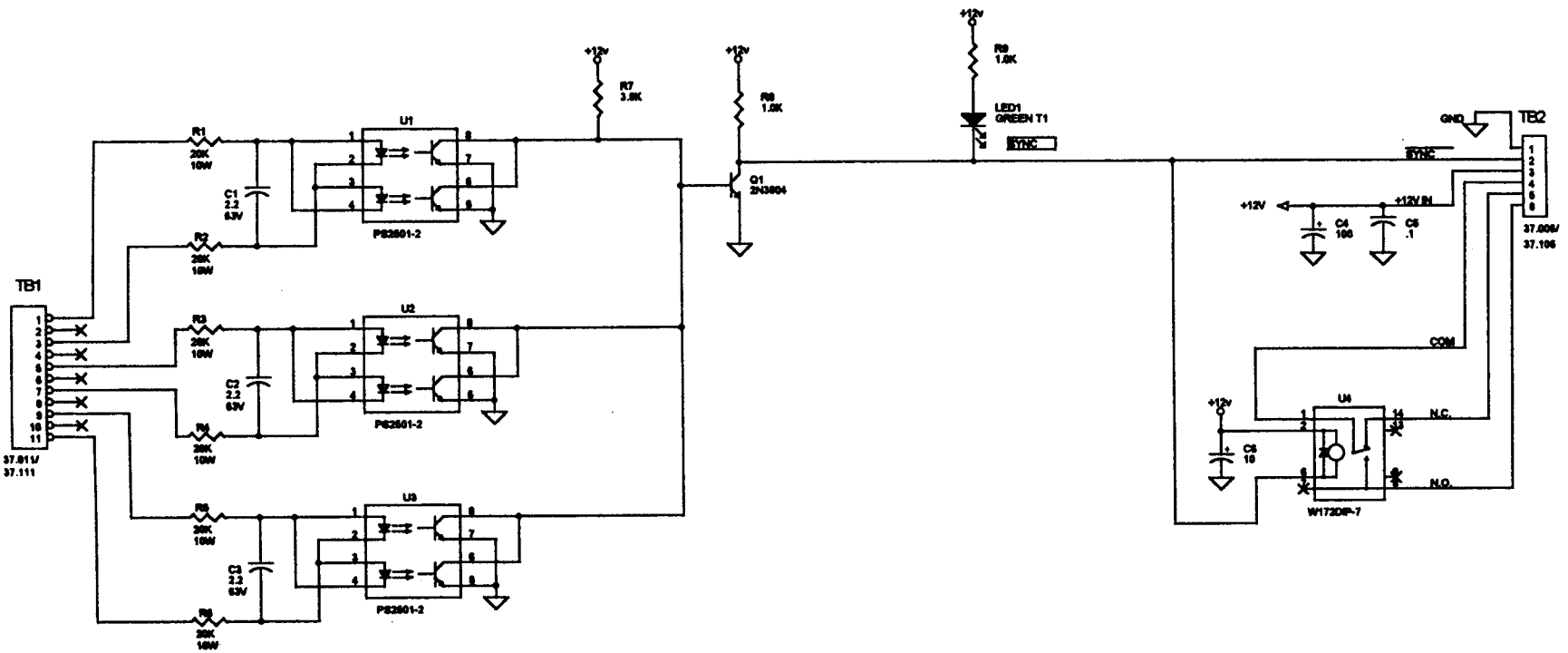

APPROVALS		DATE
Engineer:	CHW	
Drawn:	JBN	
Checked:	CHW	

Tuesday, April 02, 1996

Electronic Power Conditioning Inc.

SYNCHRONIZER BOARD SCHEMATIC

Size B	CAGE CODE	DWG NO 06448	Rev B
SCALE	FILE: 4488.SCH	Sheet 10 of 14	

2-13-97 JBN

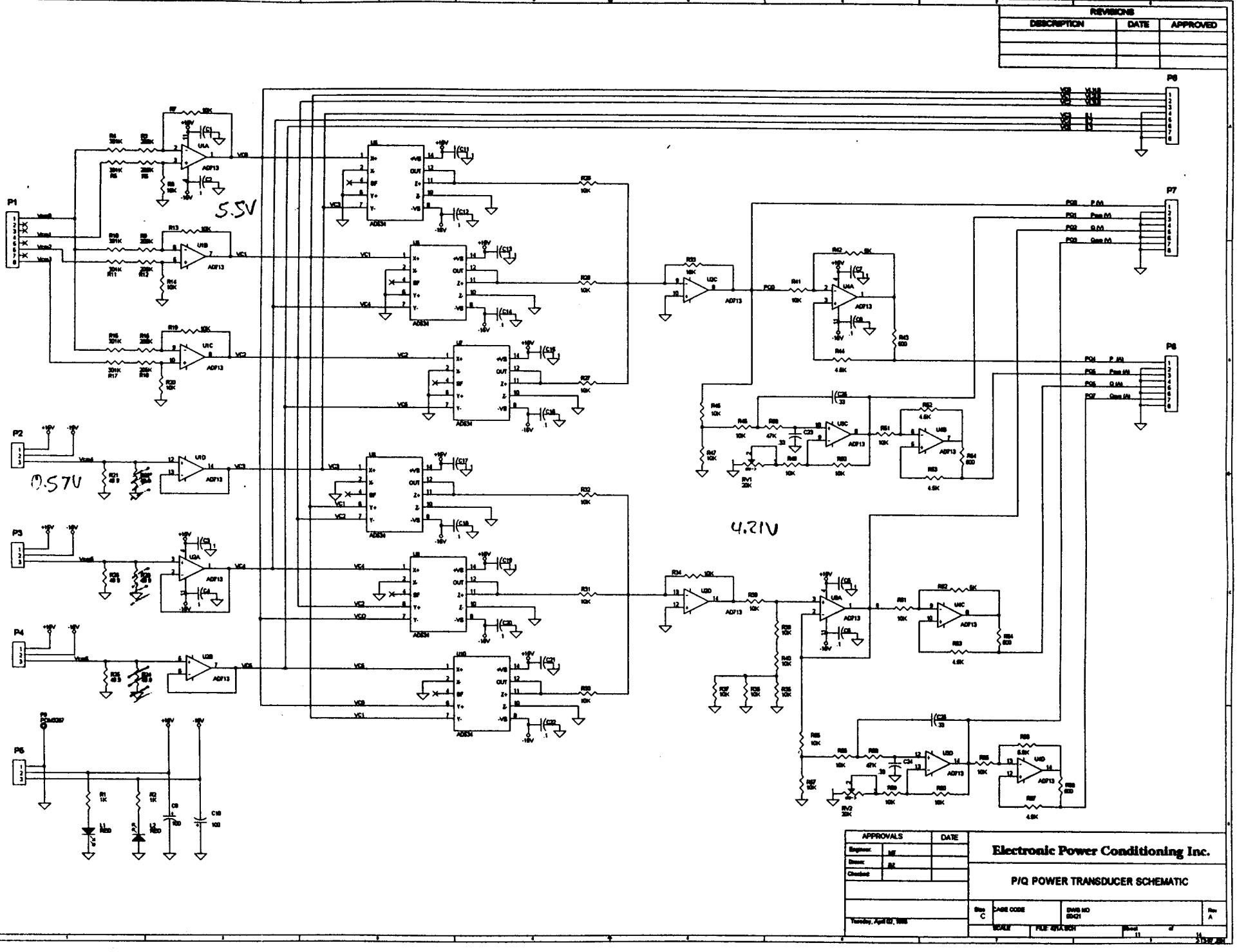
REVISIONS
DESCRIPTION
DATE
APPROVED
5.5V
0.57V
4.21V
APPROVALS
DATE
Electronic Power Conditioning Inc.
P/Q POWER TRANSDUCER SCHEMATIC

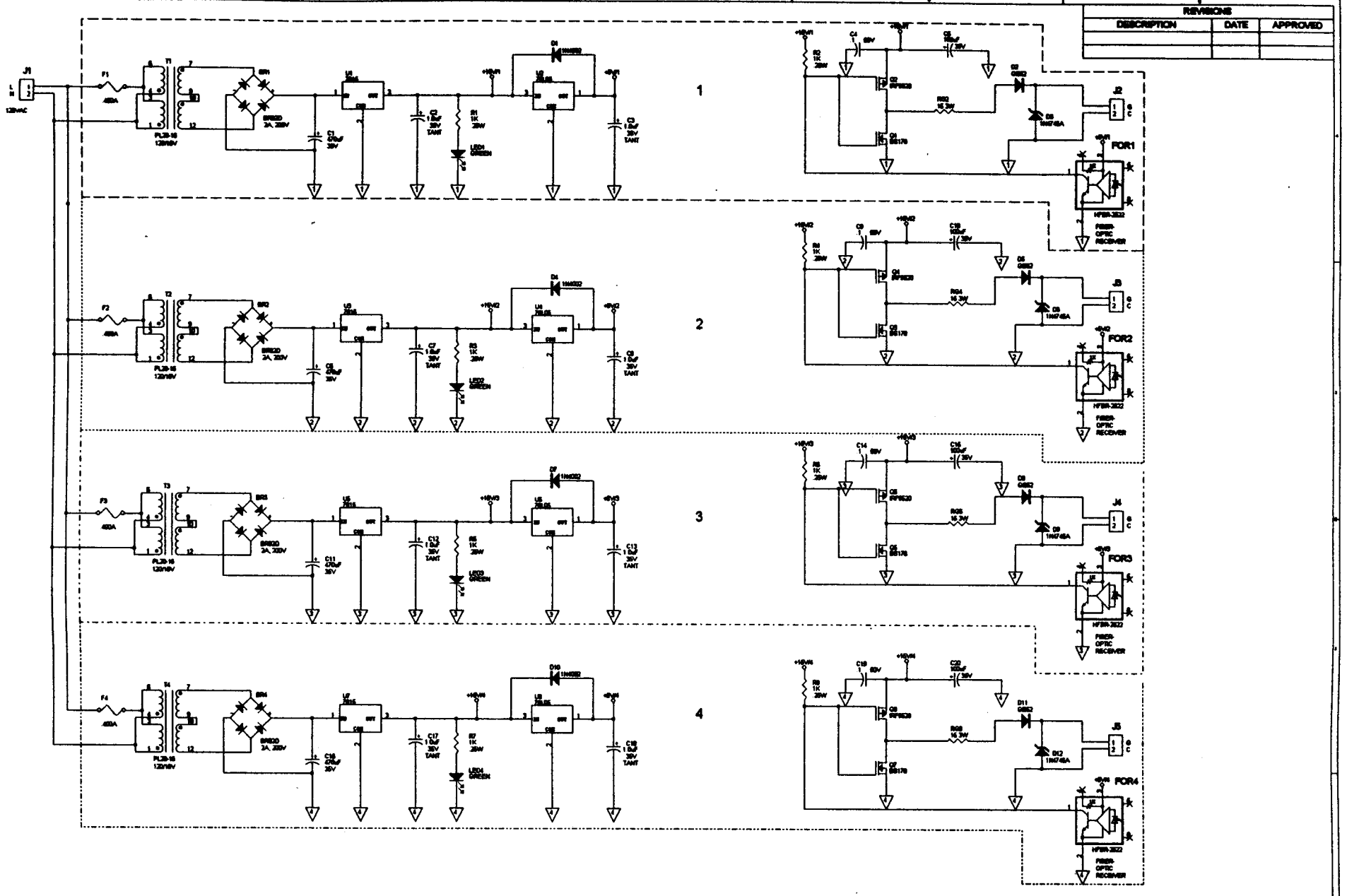
REVISIONS
DESCRIPTION
DATE
APPROVED
1
2
3
4
FOR1
FOR2
FOR3
FOR4
THIS DOCUMENT CONTAINS INFORMATION AND NEITHER IT NOR ANY INFORMATION THEREIN SHALL BE DISCLOSED WITHOUT WRITTEN CONSENT OF ELECTRONIC POWER CONDITIONING
APPROVALS
DATE
Electronic Power Conditioning Inc.
QUAD SCR DRIVER BOARD SCHEMATIC

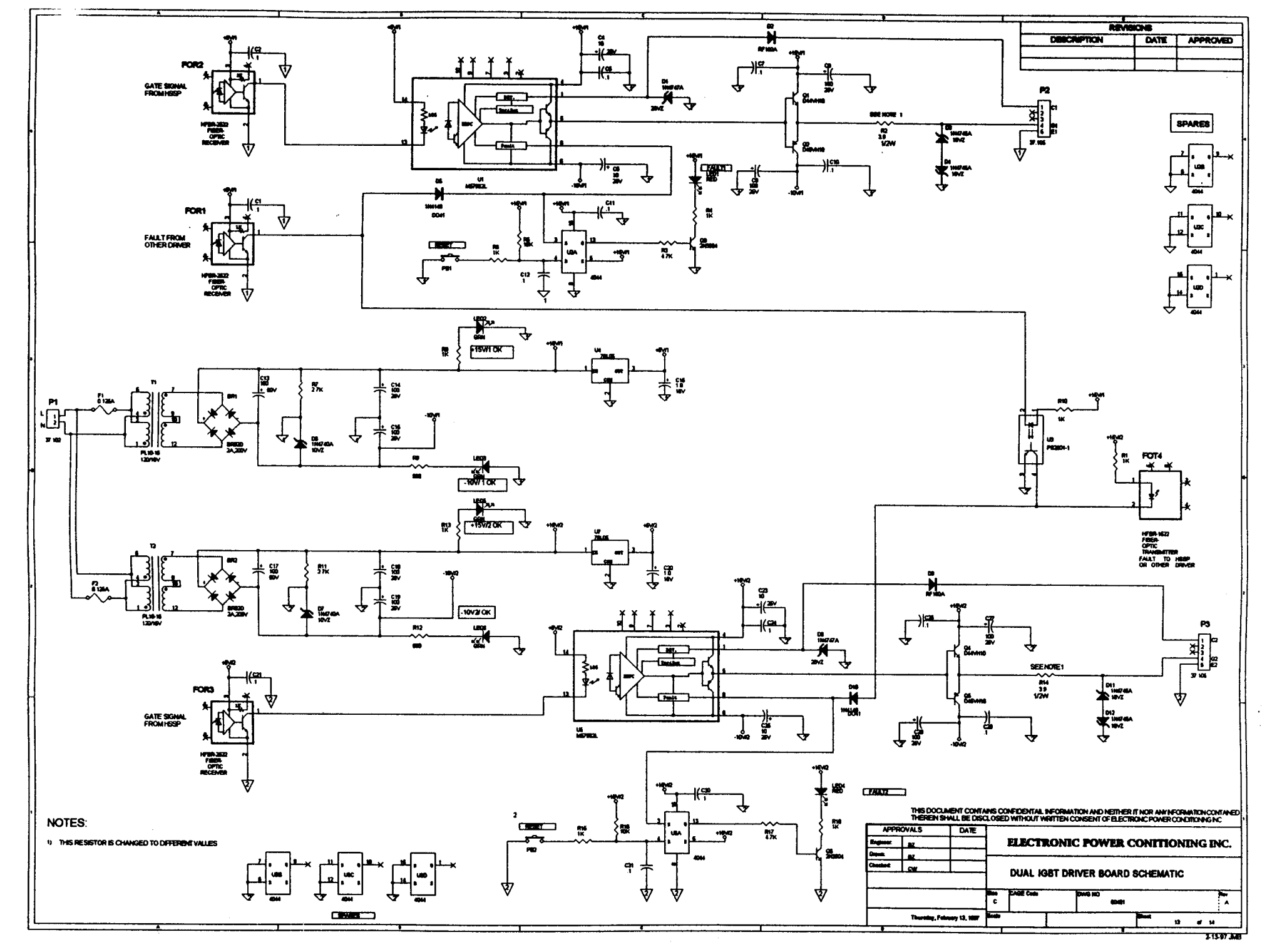
REVISIONS
DESCRIPTION
DATE
APPROVED
GATE SIGNAL FROM HSSP
FAULT FROM OTHER DRIVER
HFBR-2522 FIBER OPTIC RECEIVER
SPARES
+15V1 OK
-10V1 OK
+15V2 OK
-10V2 OK
SEE NOTE 1
HFBR-1522 FIBER OPTIC TRANSMITTER
FAULT TO HSSP OR OTHER DRIVER
NOTES:
1) THIS RESISTOR IS CHANGED TO DIFFERENT VALUES
THIS DOCUMENT CONTAINS CONFIDENTIAL INFORMATION AND NEITHER IT NOR ANY INFORMATION CONTAINED THEREIN SHALL BE DISCLOSED WITHOUT WRITTEN CONSENT OF ELECTRONIC POWER CONDITIONING INC
APPROVALS
DATE
Engineer
Drawn
Checked
ELECTRONIC POWER CONDITIONING INC.
DUAL IGBT DRIVER BOARD SCHEMATIC
Size C
CAGE Code
DWG NO
60401
Rev A
Thursday, February 13, 1997
Sheet 13 of 14
2-13-97 JMB

REVISIONS		
DESCRIPTION	DATE	APPROVED

AWT-26 CONTROL ENCLOSURE (PARTIAL)

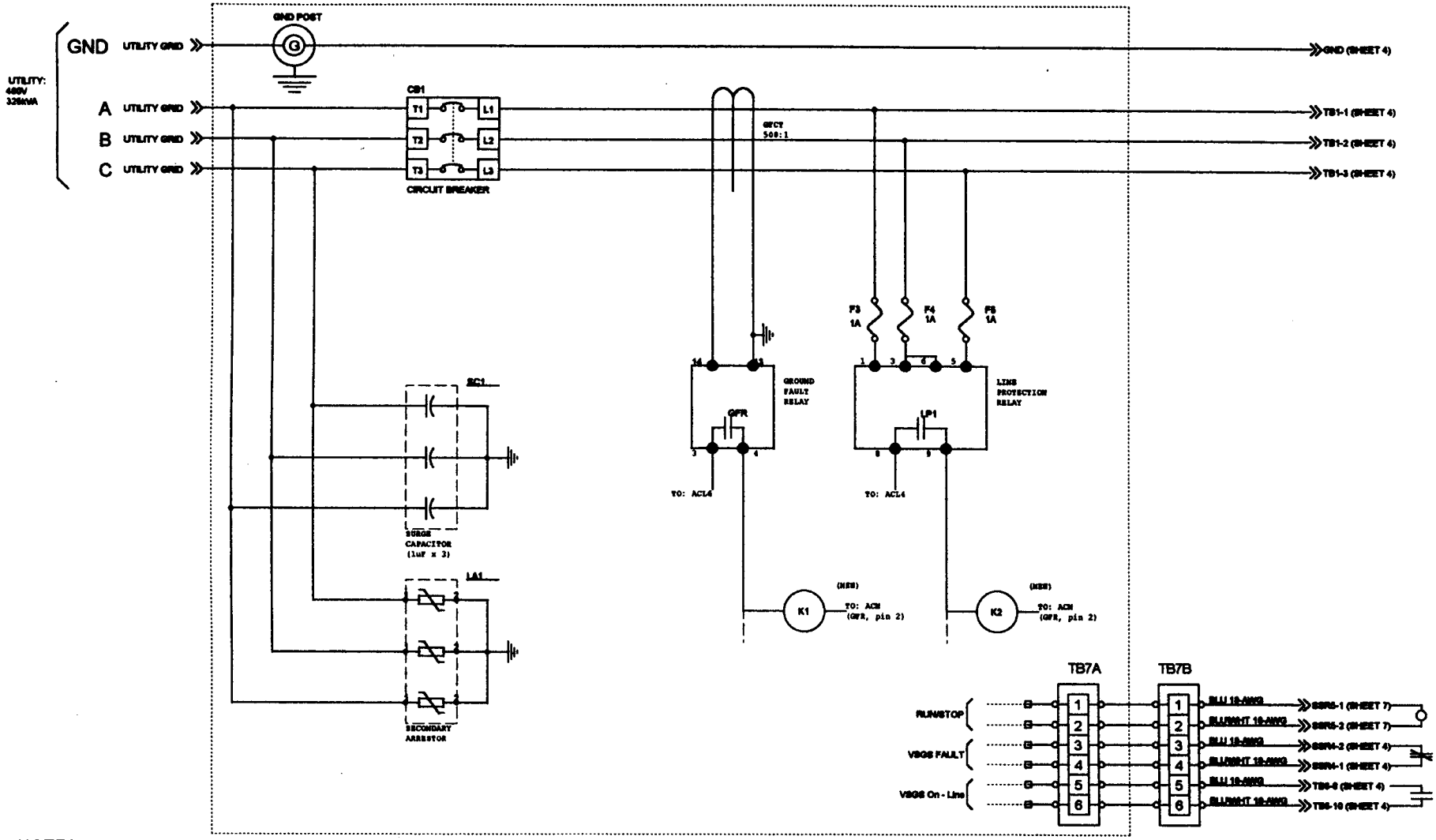

NOTES:

SC1: 3 x 1.0uF, 600VAC

LA1: Secondary Arrester

GFR: Ground Fault Relay

LP1: Line Protection Relay

K_{GFR} Relay, SPDT, 120VAC Coil

K_{LP1} Relay, SPDT, 120VAC Coil

APPROVALS		DATE
Engineer:	RVRLA	
Drawn:	CW	
Checked:		

Thursday, April 22, 1993

Electronic Power Conditioning Inc.

AWT-26 TURBINE CONTROLLER

Size	CAGE CODE	DWG NO	Rev
B		00447	A

SCALE

Sheet 14 of 14

FILE: 447A.SCH

4-21-97 JSN

Appendix A.3

Rotor Power Coefficient Data for Variable Speed Methods

EPC Final Report Figure 5.10

wind speed	TSR	CSGS 57 RPM	wind speed	TSR	VSGS 50 RPM	wind speed	TSR	VSGS 32 RPM	Wind Speed (m/s)	Binned VSGS (2)	Wind Speed (m/s)	Binned VSGS (1)
4.5	17.24	-0.10	4.5	15.1	0.117	4.5	9.7	0.3030	4.5	0.274	4.5	0.30
5	15.52	0.20	5	13.6	0.215	5	8.7	0.3667	5.0	0.339	5	0.36
5.5	14.11	0.26	5.5	12.4	0.308	5.5	7.9	0.3822	5.5	0.363	5.5	0.41
6	12.93	0.35	6	11.3	0.367	6	7.3	0.3731	6.0	0.387	6	0.42
6.5	11.94	0.39	6.5	10.5	0.402	6.5	6.7	0.3594	6.5	0.408	6.5	0.41
7	11.09	0.42	7	9.7	0.421	7	6.2	0.3338	7.0	0.402	7	0.40
7.5	10.35	0.44	7.5	9.1	0.433	7.5	5.8	0.3057	7.5	0.426	7.5	0.40
8	9.70	0.45	8	8.5	0.443	8	5.4	0.2804	8.0	0.424	8	0.42
8.5	9.13	0.46	8.5	8.0	0.436	8.5	5.1	0.2565	8.5	0.440	8.5	0.41
9	8.62	0.46	9	7.6	0.425	9	4.8	0.2323	9.0	0.431	9	0.41
9.5	8.17	0.46	9.5	7.2	0.414	9.5	4.6	0.2056	9.5	0.423	9.5	0.40
10	7.76	0.46	10	6.8	0.404	10	4.4	0.1785	10.0	0.419	10	0.39
10.5	7.39	0.44	10.5	6.5	0.381	10.5	4.1	0.1547	10.5	0.434	10.5	0.39
11	7.05	0.43	11	6.2	0.361	11	4.0	0.1280	11.0	0.419	11	0.37
11.5	6.75	0.42	11.5	5.9	0.344	11.5	3.8	0.1094	11.5	0.409	11.5	0.35
12	6.47	0.40	12	5.7	0.324	12	3.6	0.0898	12.0	0.379	12	0.35
12.5	6.21	0.38	12.5	5.4	0.306	12.5	3.5	0.0779	12.5	0.364	12.5	0.33
13	5.97	0.36	13	5.2	0.286	13	3.4	0.0603	13.0	0.352	13	0.31
13.5	5.75	0.34	13.5	5.0	0.268	13.5	3.2	0.0570	13.5	0.329	13.5	0.29
14	5.54	0.33	14	4.9	0.251	14	3.1	0.0406	14.0	0.322	14	0.29
14.5	5.35	0.31	14.5	4.7	0.232	14.5	3.0	0.0390	14.5	0.303	14.5	0.27
15	5.17	0.29	15	4.5	0.215	15	2.9	0.0334	15.0	0.287	15	0.26
15.5	5.01	0.28	15.5	4.4	0.201	15.5	2.8	0.0351	15.5	0.269	15.5	0.25
16	4.85	0.26	16	4.3	0.181	16	2.7	0.0251	16.0		16	0.23
16.5	4.70	0.24	16.5	4.1	0.166	16.5	2.6	0.0000	16.5	0.220	16.5	0.21
17	4.56	0.23	17	4.0	0.149	17	2.6	0.0202			17	0.20
17.5	4.43	0.22	17.5	3.9	0.135						17.5	0.18
18	4.31	0.20	18	3.8	0.119						18	0.17
18.5	4.19	0.18	18.5	3.7	0.109						18.5	0.16
19	4.08	0.17	19	3.6	0.097						19	
19.5	3.98	0.16	19.5	3.5	0.088						19.5	0.13
20	3.88	0.15	20	3.4	0.079						20	
20.5	3.79	0.13	20.5	3.3	0.069						20.5	0.10
21	3.70	0.12	21	3.2	0.065							
21.5	3.61	0.11	21.5	3.2	0.058							
22	3.53	0.10	22	3.1	0.054							
22.5	3.45	0.09	22.5	3.0	0.045							
23	3.37	0.08	23	3.0	0.043							
23.5	3.30	0.07	23.5	2.9	0.040							
24	3.23	0.07	24	2.8	0.039							
24.5	3.17	0.07	24.5	2.8	0.034							
			25	2.7	0.029							
			25.5	2.7	0.027							

Appendix A.4

AEROACOUSTICS, INC.
22125 17th Avenue SE., Suite 113, Bothell, WA 98021
(425) 483-5173 Fax (425) 483-4057

DOCUMENT AA1381

ACOUSTIC TEST RESULTS OF AWT-26 WIND TURBINE WITH EPC VARIABLE SPEED GENERATION SYSTEM

Prepared By: Gus Freitag

Approved By: Gary Gorder

Date: 1/5/99

REVISIONS

REV	DESCRIPTION	DATE	BY
IR	Initial Release	01/05/99	G. Gorder

LIST OF ACTIVE PAGES

ORIGINAL		ADDED PAGES						ORIGINAL		ADDED PAGES					
PAGE	REV	PAGE	REV	PAGE	REV	PAGE	REV	PAGE	REV	PAGE	REV	PAGE	REV	PAGE	REV
Title															
ii															
iii															
iv															
1															
2															
3															
4															
5															
6															
7															
8															
9															
10															
11															
Ap A															

TABLE OF CONTENTS

1.0 SUMMARY

This document describes the conduct and results of the acoustics tests on the AWT-26 wind turbine with the EPC Variable Speed Generation System. The tests were conducted at the National Wind Technology Center in Boulder, Colorado, from September 22 to September 25, 1998. These acoustics tests were intended to validate the claimed noise benefit of variable speed wind turbines and to quantify the reduction in sound power level at reduced rotor speeds. An additional goal of the tests was to compare the noise level of aerodynamic tip brakes with the noise level of conventional tips.

The results obtained clearly show that at nominal wind speeds of up to 5 m/s the average noise pressure level emitted by the turbine increases with increasing rotor RPM. Because of the lack of strong winds during the test days, no conclusions can be made on how noise pressure levels vary with higher wind speeds and rotor RPM. The turbine equipped with the aerodynamic tip brakes was determined to be noisier than the turbine equipped with the conventional tips at nominal wind speeds of up to 5 m/s. The average sound pressure level difference between the two configurations was about zero dB at a rotor speed of 34 RPM, and increased to about 1.8 dB at a maximum rotor speed of 62 RPM.

2.0 INTRODUCTION

The field test program for the EPC/AWT-26 wind turbine included acoustic tests intended to verify the noise benefit of variable speed wind turbines and to quantify the reduction in sound power level at reduced rotor speeds. The AWT-26 is equipped with tip vanes for aerodynamic braking, a configuration claimed to be noisy. Therefore, an additional goal of the test program was to compare the noise signature of the tip vanes to that of a more conventional tip, so that engineers can have better information when evaluating future design choices.

The turbine was operated at various discrete rotor speeds in the desired wind speed range in order to determine the noise signature of the turbine installed with the conventional tips and the aerodynamic tip brakes. The sound pressure levels were recorded for each configuration using one-minute averages.

The noise test was conducted at the National Wind Technology Center in Boulder, Colorado from September 22 to September 25, 1998.

3.0 TEST DESCRIPTION

3.1 Test Site

The tests were conducted at the National Wind Technology Center near Boulder, CO. As shown in the diagram below, the three microphones were positioned at prevailing downwind locations approximately 125 feet from the base of the wind turbine. Each microphone was placed on a mounting board flat on the ground pointing towards the wind turbine.

Microphone Setup for EPC/AWT-26 Noise Measurements

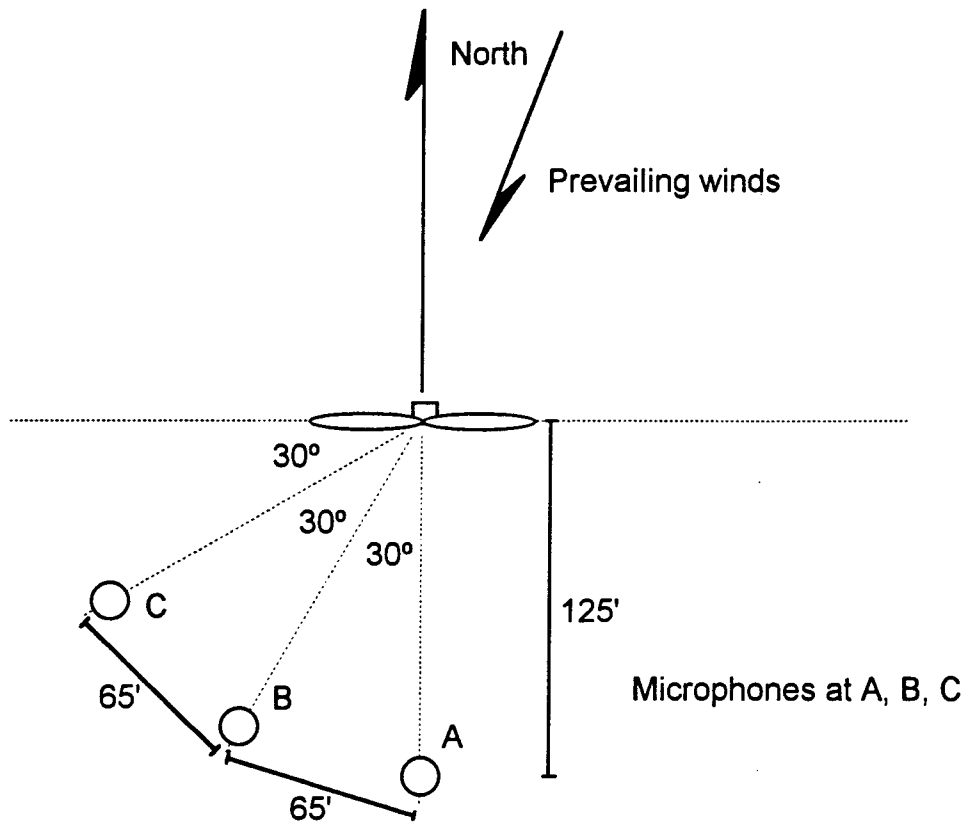

3.2 Test Instrumentation

3.2.1 Noise Measuring Equipment

The noise measurement equipment consisted of the components illustrated in the diagram below. The system consists of three Larson Davis Labs (LDL) model 2559, ½-inch condenser microphones, a LDL Model 812 Sound Level Meter (SLM), a LDL Model 2900 Real Time Analyzer and Precision Sound Level Meter (RTA) set to the 'slow' response. The signals from each microphone were recorded on a Teac RD-135T Digital Audio Tape (DAT) Data Recorder. A laptop computer controlled the system. Low impedance cables connected the microphones to the SLM and RTA. Each microphone was placed on a 1-meter diameter mounting plate with the diaphragm of the microphone in a plane normal to the board and with the axis of the microphone pointing towards the turbine. Windscreens were placed on the microphones. The windscreens consist of one half of an open foam sphere centered on the diaphragm of the microphone. Two LDL model EC 100 cables of approximately 100-ft length connected the microphones to the SLM.

Noise Measurement Stations

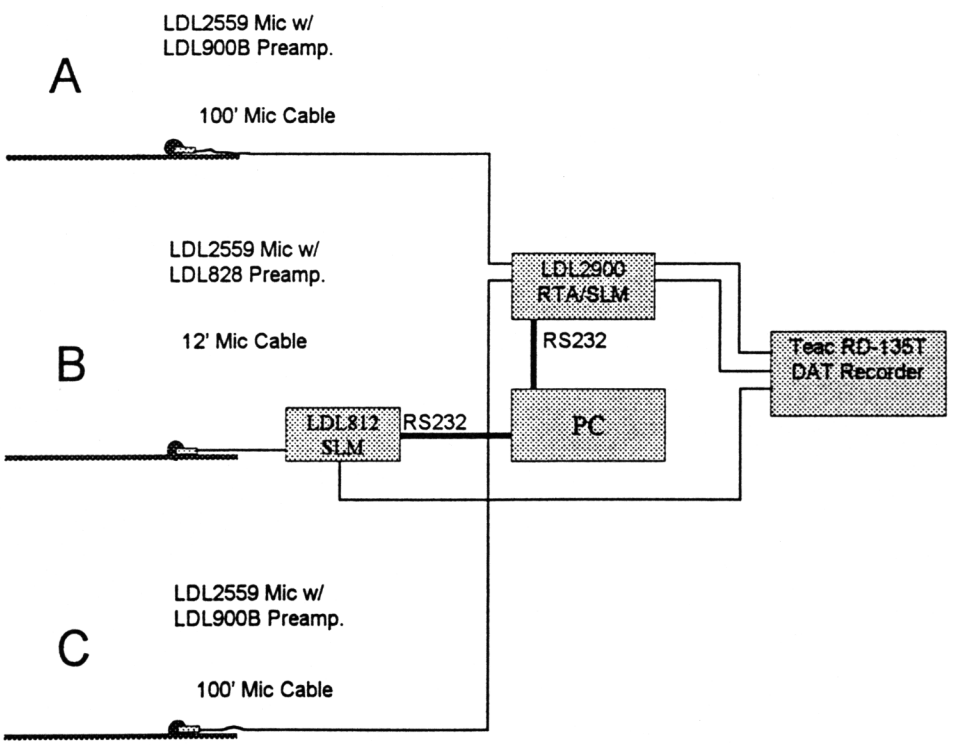

Microphones A and C were coupled with LDL Model 900B preamplifiers and connected to the analyzer by over 75 feet of low impedance cable. Absolute sensitivity of the condenser microphone is provided in the manufacturer's documentation. The system was calibrated in the field using a LDL CA250 sound level meter calibrator/pistonphone. LDL Model WS-1 windscreens were employed for all measurements on the microphones.

The LDL Model 812 SLM and Model 2900 RTA employed in the field measurement system provided a direct read-out of the sound exposure level (SEL) recorded. Field calibrations were performed using the LDL CA250 calibrator at the beginning and end of each test series and during any breaks in testing.

3.2.2 Meteorological Equipment

Meteorological test equipment was located behind microphone B and with the sensors mounted on a tripod at a height of approximately 5 feet. The temperature and relative humidity of the atmosphere were measured using a Pacer Model HTA4200 Hygro-Thermometer Anemometer DataLogger. The meter is a digital indicator using a capacitance element sensor accurate to ±2% RH and a platinum resistance element accurate to ±0.4° F. Wind speed and direction were recorded through the HTA4200 from a Digitar Model TWR-3 anemometer and wind vane. Additional weather data were obtained from the NREL anemometer stationed near the wind turbine.

METEOROLOGICAL DATA ACQUISITION SYSTEM COMPONENTS			
Description	**Manufacturer**	**Model**	**S/N**
Digital Hygro-Thermometer Anemometer DataLogger	Pacer	HTA4200	4200-9511785
Anemometer and Wind Vane	Digitar	TWR-3	91219060

3.2.3 Wind Turbine Performance

The EPC converter was used to set the rotor speed for this test.

3.3 Test Conduct

The target number of measurements for each configuration used in conducting the test are presented in the tables below.

EPC/AWT-26 Wind Turbine Test Sequence #1 Aerodynamic Tip Brakes Installed			
	Wind Speed (m/s)		
RPM	0-5	5-9	9-13
34	4	3	3
37	4	3	3
42	4	3	3
47	4	3	3
52	4	3	3
57	4	3	
62	4	3	

EPC/AWT-26 Wind Turbine Test Sequence #2 Conventional Tips Installed	
	Wind Speed (m/s)
RPM	0-5
34	4
37	4
42	4
47	4
52	4
57	4
62	4

EPC/AWT-26 Wind Turbine Test Sequence #3 One Aerodynamic Tip Brake and One Conventional Tip Installed			
	Wind Speed (m/s)		
RPM	0-5	5-9	9-11
34	4	3	3
37	4	3	3
42	4	3	3
47	4	3	3
52	4	3	3
57	4	3	
62	4	3	

In order to ensure that sufficient data were recorded, at least four valid runs were performed for every test configuration. Manual notes taken during the test by the acoustics engineer were used in subsequent data analysis and are presented in Appendix A. Note that these manual notes allow the reader to correlate test runs with test configuration and time of day.

Test data were acquired for each run using one-minute averages.

3.4 Test Condition Acceptability

No runs were repeated due to meteorological conditions. Precipitation occurred just before run 22 of test sequence 2, during which data acquisition was temporarily stopped. Lack of stronger winds hindered the completion of the test matrix for winds above 5 m/s. Even though all microphones recorded noise data for each run, only the data from the microphone within ± 15° from the downwind direction was used in the analysis.

4.0 TEST RESULTS

As seen on page 10, the average noise pressure levels for configuration #1 (aerodynamic tip brakes installed) are higher than configuration #2 (conventional tips installed) at nominal wind speeds of up to 5 m/s. Configurations #1 and #2 emit about equal sound levels at a rotor speed of 34 RPM. At higher rotor RPM's, however, configuration #1 is louder than configuration #2. At the maximum rotor speed of 62 RPM, the noise difference between the two configurations is about 1.8 dB. Winds were slight and variable during the test days for configurations #1 and #2; therefore, no data points for these configurations were taken at higher wind speeds.

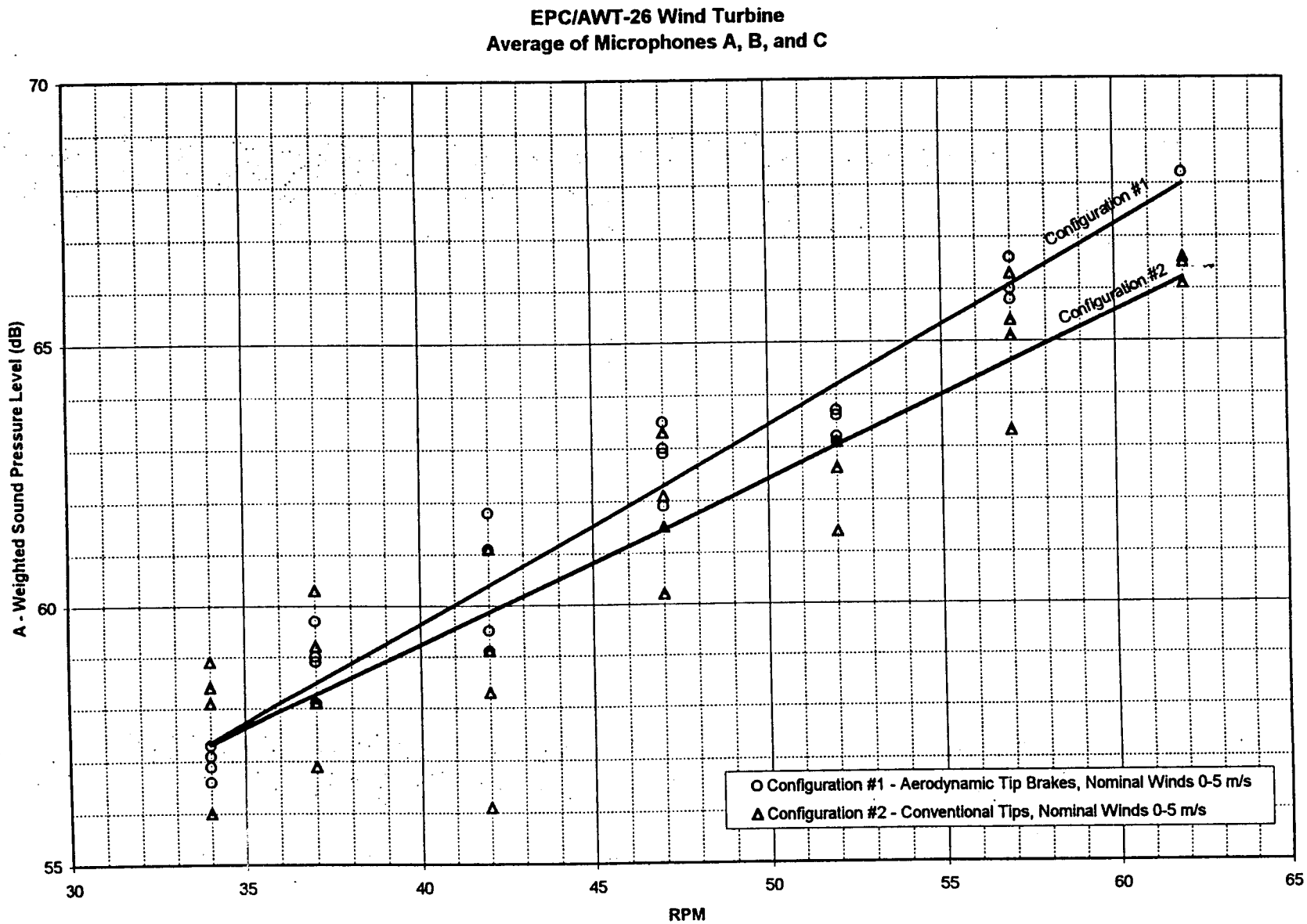

ResultsAnalysis All (2) One mic
11/25/98 7:01 AM

5.0 REFERENCES

1. Addendum #1 – Acoustics Test, "AWT-26 Wind Turbine with EPC Variable Speed Generation System", Paul Migliore, September 21, 1998.

2. IEC Document 88/48/CDV, "Wind Turbine Generator Systems – Part 10: Acoustic Noise Measurement Techniques", D. Bakker, January 1995.

3. National Wind Technology Center web page, "Advanced Wind Turbines – AWT-26", http://nwtc.nrel.gov/nwtc_tour/awt-26.html.

Appendix A
Test Notes

WIND TURBINE SYSTEMS - ACOUSTICAL DATA ACQUISITION LOG

TURBINE	AWT-26	LOCATION:	NREL, Golden, CO
TEST PLAN:	88/48/CDV	DATE:	9/22/98
TEST TYPE/REF #	1 - AERODYNAMIC TIP BRAKES	ACOUSTICAL ENGINEER:	G. Freitag

ACOUSTICAL SYSTEM COMPONENTS

Mic	Color Code	Microphone		Preamplifier		Wind Screen		Amplifier			Real Time Analyzer / SLM			DAT Recorder			Pistonphone	
		Model	S/N	Model	S/N	Model	S/N	Model	S/N	Channel	Model	S/N	Channel	Model	S/N	Channel	Model	S/N
C1	Green	2559	2226	828	847	WS-1	A				812	200		135	723752	1	CA250	1983
S1	Red	2559	1810	900B	1681	WS-1	B				2900	227	1	135	723752	2	CA250	1983
S2	Blue	2559	1844	900B	1682	WS-1	C				2900	227	2	135	723752	3	CA250	1983

TEST LOG

AA-1 DATA

RUN / RECORD TYPE*	COND NO / RPM	TIME OF DAY	~~AMP RX GAIN~~ (dB)	RTA RANGE (dB)	DAT RECORDER TAPE	DAT RECORDER ID	DAT RECORDER RANGE (V)	NOISE LEVEL (dB) C1 ~~MAX~~ SEL	NOISE LEVEL (dB) S1 ~~MAX~~ EPNL	NOISE LEVEL (dB) S2 ~~MAX~~ EPNL	PISTONPHONE CAL PRE / POST	PISTONPHONE CAL LEVEL (dB)	PISTONPHONE CAL Pamb (mb)	WIND NOM	WIND AVE	NOTES DIR	NOTES RH	NOTES
R		415 R				7	120		✓		PRE	114.0						S1 = 180°
		416 R				8	120	✓			PRE	114.0						C1 = [redacted] 210°
		417 R				9	120			✓	PRE	114.0						S2 = [redacted] 240°
		1620				10	80	AMBIENT										
		1622		70		11	~~75~~	AMBIENT							2	14	50.0	High freq @ S1
AERO	TIP BRAKES,	1625		70		12		AMBIENT						0-5	0	32		High freq @ S2
1	1/34	1646	~~RX~~	70		13		OVERLOAD							4	34	48.7	N#1
2		1648		90		14		~~56.5~~	56.7	57.3				0-5	4	34	48.7	
3		1653		90		15		56.2	56.9	57.6				0-5	0	344	50.8	
4		1656		90		16		56.0	56.3	56.6				0-5	3	344	50.2	
5		1659		80		17		57.1	56.3	58.5				0-5	3	26	49.8	
6	1/37	1703		~~90~~ 80		18		59.0	59.5	59.4				0-5	4	340	49.7	
7		1705		80		19		58.1	58.2	58.6				0-5	4	340	51.2	
8		1707		80		20		59.7	60.0	58.7				0-5	3	338	50.3	
9		1709		80		21		58.9	58.9	59.1				0-5	1	344	51.7	
10	1/42	1713		80		22		59.1	59.3	59.2				0-5	3	344	50.7	
11		1715		80		23		61.8	63.7	63.5				0-5	2	342	50.3	
12		1718		80		24		59.5	59.9	60.2				0-5	4	342	50.0	
13		1720		80		25		61.1	62.0	60.1				0-5	2	6	50.6	
14	1/47	1723		80		26		62.7	62.9	62.2				0-5	2	6	51.6	
15		1725		80		27		62.3	63.0	61.2				0-5	3	336	50.8	
16		1728		80		28		62.7	63.5	63.4				0-5	3	334	51.2	
17		1730		80		29		61.5	61.9	61.7				0-5	2	4	50.9	

*LOG AS RUN NUMBER FOR TEST TURBINE NOISE, OR RECORD TYPE FOR AMBIENT NOISE, PINK NOISE, OR PISTONPHONE CAL

Test flapping on one blade at lower speeds

WIND TURBINE SYSTEMS - ACOUSTICAL DATA ACQUISITION LOG

TURBINE	AWT-26	LOCATION:	NREL
TEST PLAN:	88/48/CDV	DATE:	9/22/98
TEST TYPE/REF #	1° AERO TIP BRAKES	ACOUSTICAL ENGINEER:	G. Freitag

ACOUSTICAL SYSTEM COMPONENTS

Mic	Color Code	Microphone		Preamplifier		Wind Screen		Amplifier			Real Time Analyzer / SLM			DAT Recorder			Pistonphone	
		Model	S/N	Model	S/N	Model	S/N	Model	S/N	Channel	Model	S/N	Channel	Model	S/N	Channel	Model	S/N
C1	Green	2559	2226	828	847	WS-1	A				812	200		135	723752	1	CA250	1983
S1	Red	2559	1810	900B	1681	WS-1	B				2900	227	1	135	723752	2	CA250	1983
S2	Blue	2559	1844	900B	1682	WS-1	C				2900	227	2	135	723752	3	CA250	1983

TEST LOG

RUN / RECORD TYPE*	COND NO / RPM	TIME OF DAY	AMP GAIN (dB)	RTA RANGE (dB)	DAT RECORDER TAPE	DAT RECORDER ID	DAT RECORDER RANGE (V)	NOISE LEVEL (dB) C1 SEL	NOISE LEVEL (dB) S1 EPNE	NOISE LEVEL (dB) S2 EPNE	PISTONPHONE CAL PRE / POST	PISTONPHONE CAL LEVEL (dB)	PISTONPHONE CAL Pamb (mb)	AAI DATA WIND NOM	AAI DATA WIND AVG	AAI DATA NOTES DIR	AAI DATA RH	
18	1/52	1734		80		30		63.6	63.6	63.4				0-5	2	4	52.3	
19		1737		80		31		63.7	64.1	64.3				0-5	3	344	50.9	
20		1739		80		32		63.1	63.6	61.2				0-5	1	344	51.6	
21		1741		80		33		63.4	63.2	63.3				0-5	2	344	52.2	
22	1/57	1744		80		34		66.6	66.7	66.5				0-5	3	344	52.0	Airplane OH
23		1746		80		35		65.7	65.8	65.6				0-5	2	342	53.3	
24		1748		80		36		65.9	66.0	66.2				0-5	2	342	52.1	
25		1750		80		37		66.4	66.0	66.3				0-5	2	338	52.8	Airplane OH
26	1/62			80		38		OVERLOAD						0-5	0	338	52.7	Not Valid
27		1754		90		39		68.9	68.2	68.1				0-5	0	338	53.2	
28		1757		90		40		68.1	68.2	67.6				0-5	2	338	53.5	
29		1759		90		41		68.4	68.2	65.4				0-5	3	342	53.6	
30		1801		90		42		67.9	68.2	67.2	POST			0-5	3	342	53.8	
PISTON		1806		120		43		✓			PRE	113.8						
"		1808		120		44				✓	POST	114.1						
"		1810		120		45			✓		POST	114.0						
END OF AERO TIP BRAKES TEST																		

*LOG AS RUN NUMBER FOR TEST TURBINE NOISE, OR RECORD TYPE FOR AMBIENT NOISE, PINK NOISE, OR PISTONPHONE CAL

WIND TURBINE SYSTEMS - ACOUSTICAL DATA ACQUISITION LOG

TURBINE	AWT-26	LOCATION:	NREL
TEST PLAN:	88/48/CDV	DATE:	9/23/98
TEST TYPE/REF #	2 CONVENTIONAL TIPS	ACOUSTICAL ENGINEER:	G. Freitag

ACOUSTICAL SYSTEM COMPONENTS

Mic	Color	Microphone		Preamplifier		Wind Screen		Amplifier			Real Time Analyzer / SLM			DAT Recorder			Pistonphone	
	Code	Model	S/N	Model	S/N	Model	S/N	Model	S/N	Channel	Model	S/N	Channel	Model	S/N	Channel	Model	S/N
C1	Green	2559	2226	828	847	WS-1	A				812	200		135	723752	1	CA250	1983
S1	Red	2559	1810	900B	1681	WS-1	B				2900	227	1	135	723752	2	CA250	1983
S2	Blue	2559	1844	900B	1682	WS-1	C				2900	227	2	135	723752	3	CA250	1983

TEST LOG

RUN / RECORD TYPE*	COND NO/ RPM	TIME OF DAY	AMP GAIN (dB)	RTA RANGE (dB)	DAT RECORDER TAPE	DAT RECORDER ID	DAT RECORDER RANGE (V)	NOISE LEVEL (dB) Lamax C1 dBA Max SEL	NOISE LEVEL (dB) Lamax S1 dBA Max EPNL	NOISE LEVEL (dB) Lamax S2 dBA Max EPNL	PISTONPHONE CAL PRE / POST	PISTONPHONE CAL LEVEL (dB)	PISTONPHONE CAL Pamb (mb)	AAI DATA WIND NOM	AAI DATA WIND (MPH) AVE	NOTES DIR	NOTES RH	
PISTON		1410				46				✓	PRE	114.0						
✓		1412				47		✓			PRE	114.0						
✓		1413				48			✓		PRE	114.0						
1	2/34			70		49	OVERLOAD											Not Valid
2		1520		80		50	56.5	56.0	56.6					0-5	0	358	47	Rain
3		1522		80		51	54.2	58.9	57.5					0-5	2	308	48.1	Rain
4		1524		80		52	56.7	58.4	58.3					0.5	3	308	49.3	Rain/Pwr drive
5		1527		80		53	55.8	58.1	56.5					0-5	1	308	49.3	Pwr drive mode
6	2/37	1530		80		54	57.7	58.1	60.6					0-5	1	308	47.6	
7		1533		80		55	57.9	57.9	59.5					0-5	0	308	46.7	
8		1535		80		56	56.00	56.9	57.1					0-5	1	308	45.5	
9		1537		80		57	55.6	60.3	58.3					0-5	0	308	45.3	
10	2/42	1540		80		58	59.3	59.1	61.7					0-5	0	308	45.8	
11		1542		80		59	58.6	56.1	58.6					0-5	0	308	46.7	
12		1545		80		60	59.3	56.9	58.3					0.5	0	308	47.6	
13		1547		80		61	59.0	61.1	60.4					0.5	0	308	46.9	
14	2/47	1550		80		62	60.4	61.5	61.6					0-5	0	308	46.1	
15		1552		80		63	59.3	60.9	60.2					0-5	0	308	46.9	
16		1554		80		64	61.9	62.8	63.3					0-5	0	308	44.9	
17		1556		80		65	61.0	61.5	62.1					0-5	0	308	43.3	
18	2/52	1559		80		66	62.6	63.1	63.6					0-5	1	308	46.3	
19		1601		80		67	62.5	62.4	63.8					0-5	1	308	47.6	
20		1603		80		68	61.8	62.6	62.6					0-5	0	308	47.8	
21		1605		80		69	60.7	61.4	62.2					0-5	0	308	47.7	

*LOG AS RUN NUMBER FOR TEST TURBINE NOISE, OR RECORD TYPE FOR AMBIENT NOISE, PINK NOISE, OR PISTONPHONE CAL

WIND TURBINE SYSTEMS - ACOUSTICAL DATA ACQUISITION LOG

TURBINE	AWT-26	LOCATION:	
TEST PLAN:	88/48/CDV	DATE:	
TEST TYPE/REF #	2 (ONVENTIONAL TIP)	ACOUSTICAL ENGINEER:	

ACOUSTICAL SYSTEM COMPONENTS

Mic	Color	Microphone		Preamplifier		Wind Screen		Amplifier			Real Time Analyzer / SLM			DAT Recorder			Pistonphone	
	Code	Model	S/N	Model	S/N	Model	S/N	Model	S/N	Channel	Model	S/N	Channel	Model	S/N	Channel	Model	S/N
C1	Green	2559	2226	828	847	WS-1	A				812	200		135	723752	1	CA250	1983
S1	Red	2559	1810	900B	1681	WS-1	B				2900	227	1	135	723752	2	CA250	1983
S2	Blue	2559	1844	900B	1682	WS-1	C				2900	227	2	135	723752	3	CA250	1983

TEST LOG

RUN / RECORD TYPE*	COND NO/ RPM	TIME OF DAY	AMP GAIN (dB)	RTA RANGE (dB)	DAT RECORDER TAPE	DAT RECORDER ID	DAT RECORDER RANGE (V)	NOISE LEVEL (dB) C1 SEL	NOISE LEVEL (dB) S1 EPNL	NOISE LEVEL (dB) S2 EPNL	PISTONPHONE CAL PRE / POST	PISTONPHONE CAL LEVEL (dB)	PISTONPHONE CAL Pamb (mb)	AA DATA WIND NOM	AA DATA WIND (MPH) AVE	AA DATA DIR	AA DATA NOTES RH	
22	2/57			80		70									2	303	Inc 3	Downpour/Not Valid
23		1640		80		71		65.0	65.6	63.3				0.5	0	158	56.4	
24		1642		80		72		65.3	66.3	66.3				0-5	0	158	54.8	
25		1645		80		73		64.2	65.1	66.3				0-5	1	158	56.6	
26		1647		80		74		63.4	65.4	65.5				0-5	0	158	54.6	
27	2/62	1651		80		75		OVERLOAD						0-5	0	158	55.2	Not Valid
28		1652		90		76		65.8	66.5	65.3				0-5	1	166	55.3	
29		1654		90		77		66.1	67.0	67.2				0-5	0	166	55.0	
30		1656		90		78		66.6	67.0	67.5				0-5	2	~~154~~	56.6	
31		1658		90		79		66.6	67.4	68.3				0-5	1	344	57.9	
PISTON				90		80		✓			POST	113.9						
"				90		81			✓		POST	113.9						
"				90		82				✓	POST	114.1						
—/—																		

*LOG AS RUN NUMBER FOR TEST TURBINE NOISE, OR RECORD TYPE FOR AMBIENT NOISE, PINK NOISE, OR PISTONPHONE CAL

Appendix A.5

Appendix A5: EPC/AWT-26 Variable Speed Field Test Data Processing

The data were saved on a compact disc (CD) in the Excel spreadsheet files listed in Table 1. The particular data files are further defined in Table 2. The primary filtering criteria are listed in Table 3. The processing steps are shown below.

Table 1: File Definitions

Filename	Definitions:
CSGS_57.xls / CSGS_57F.xls	57.14 RPM constant-speed low-slip generator (the baseline configuration). The F denotes filtered and processed data.
VSGS_32.xls / VSGS_32&50F.xls	32 RPM variable-speed generator in fixed-speed operation. The F denotes filtered and processed data.
VSGS_50.xls / VSGS_32&50F.xls	50 RPM variable-speed generator in fixed-speed operation. The F denotes filtered and processed data.
VSGS_SS (1).xls / VSGS_SS(1)F.xls	Variable-speed generator in variable-speed mode, using the (1) "Soft Stall" control strategy. The F denotes filtered and processed data.
VSGS_AC (2).xls / VSGS_AC(2)F.xls	Variable-speed generator run in variable speed mode, using the (2) "Active Control" control strategy. The F denotes filtered and processed data.

Table 2: Data File Configurations

Appendix of performance data for the AWT-26 in fixed-speed and variable-speed operation. The data are power measurements and atmospheric conditions. All results are 1-minute averages from a 1 Hz sample rate.				
Filename	Contents	Power range of the data set as filtered (kW)	Data collection season range	Number of filtered records
CSGS_57.xls	Raw data time series on multiple worksheets			
CSGS_57F.xls	Filtered, tabulated, and plotted results	-7 through 293	March – April	3444
VSGS_32	Raw data time series			
VSGS_32F	Filtered and tabulated	-1 through 38	February - March	1168
VSGS_50	Raw data time series			
VSGS_50F	Filtered and tabulated	-7 through 178	March - April	2941
VSGS_SS (1)	Raw data time series			
VSGS_SS(1)F	Filtered and tabulated	-2 through 243	April - May	1230
VSGS_AC (2)	Raw data time series			
VSGS_AC(2)F	Filtered and tabulated	-2 through 238	January - March	1433
Note: The file table headers are listed in the last four pages of this Appendix.				

Table 3: Data Processing Primary Filtering Criteria

Wind Speed Range Kept (m/s)	Wind Direction Acceptable range
4.25 – Max	166 – 322

Additional Filtering and Processing Beyond That Described in Table 3

CSVS_57

Additional filtering was required for these data. The CSVS_57 data had a problem with the on-line signal, so filtering was used to eliminate the large number of off-line zero-power records. The filtering criteria are shown below.

"Acceptable Average Power Data" 0 kW;
and
"Max Power / Record" >= 0;
or
"Max Power / Record" < -1;
and
"Min Power / Record" >= 0;
or
"Min Power / Record" < -1;

Additional Filtering and Processing Beyond That Described in Table 3

VSGS_32 and VSGS_50

Additional filtering was required for these data. The VSGS_32 and VSGS_50 data were filtered for rpm within ± 5% of the set point. The 32-rpm set-point data were filtered as shown below.

30.4 rpm < 32 rpm (set-point, acceptable data) < 33.6 rpm

The 50-rpm set-point data were filtered as shown below.

47.5 rpm < 50 rpm (set-point, acceptable data) < 52.5 rpm

VSGS_SS (1)

Additional filtering was not required for these data.

VSGS_AC (2)

Additional filtering was required for these data. The first 20 days (Julian day 12-32) of testing was done with preliminary control algorithms. The algorithm was then finalized and remained the same for the rest of the test and no additional filtering was required. The filtering criterion is shown below.

"Acceptable Average Power Data" RPM < 48.9

Power – Normalization to Site Average Density

The measured data were temperature, pressure, and electrical power. Measured data were manipulated as shown below in Figure 1. Figures 2–5 are the normalized power scatter plots for each of the five configurations.

Power = P

Air Density = ρ_{avg}

Pressure = B

Temperature = T

Air Constant = R

Power normalization method

ρ_{avg} = Average site air density $\quad \rho_{avg} = 1.0 \frac{kg}{m^3}$

ρ_1 = Measured density based on T, B $\quad \rho_1 = \frac{B_1}{R \times T_1}$

P_n = Normalized power for a given record

P_1 = Measure power for a given record

$$P_n = P_1 \times \frac{\rho_{avg}}{\rho_1}$$

Figure 1. Method of Normalizing Data for Average Mass Density of Air

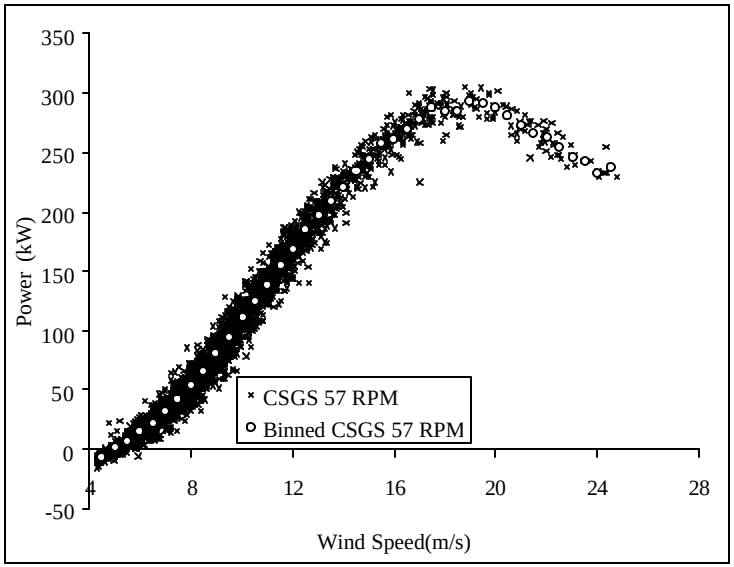

Figure 2. Generator Power CSGS_57

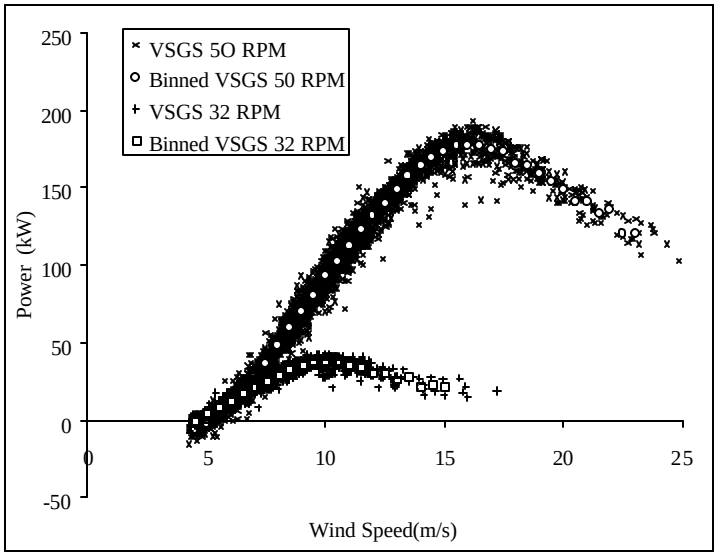

Figure 3. Generator Power VSGS 32 and 50

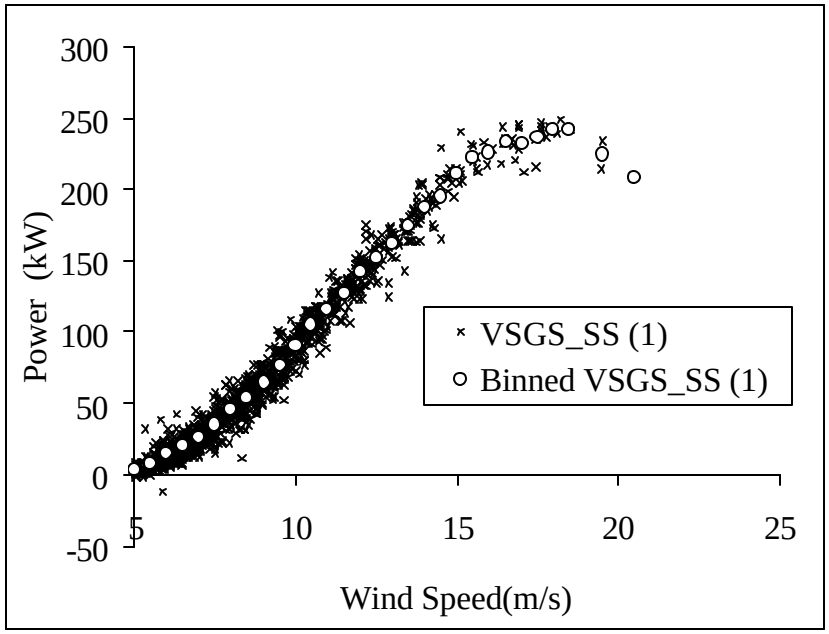

Figure 4. Generator Power Plot VSGC_SS (1)

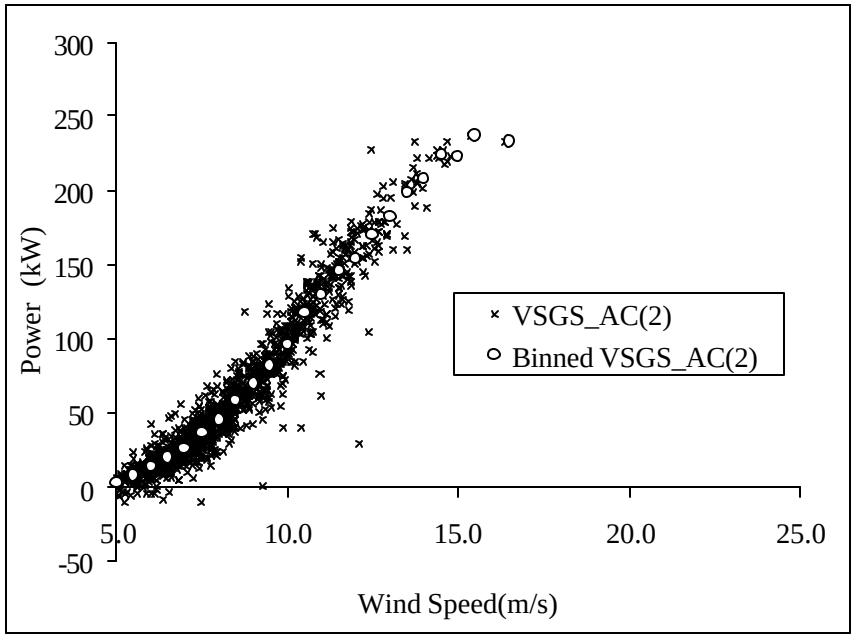

Figure 5. Generator Power Plot VSGC_AC (2)

Power Coefficient

The normalized electrical power is the first step in the calculation process for rotor power and rotor power coefficient. Drive train efficiency data, provided by NREL for the gearbox and generator systems, were incorporated into the calculation for rotor cp. The diagram shown in Figure 6 exemplifies the rotor cp calculation process. The normalized data shown in Figures 2 – 5 were factored by the appropriate efficiency data to produce the cp plots shown in Figure 7 – 10 for each of the generator and control system configurations.

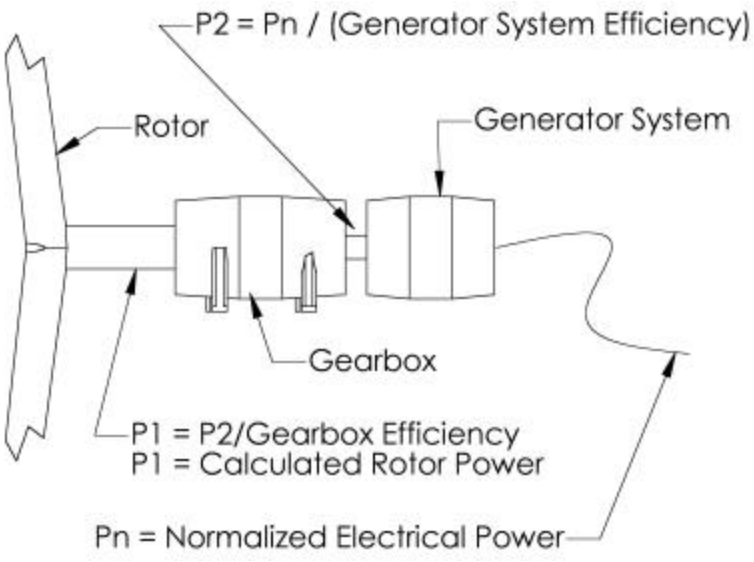

Diameter = D
Air Denstiny = $_{avg}$
Rotor Area = A
Rotor Power = P_1
Bin coefficient of power = cp_i
Bin velocity = V_i

Binned cp calculation

Given

P_n

$A = \frac{}{4} \times D^2$

$cp_i = \frac{P_n}{\frac{1}{2} \times {}_{avg} \times A \times V_i^3}$

Figure 6. Block diagram of the rotor power calculation process and equations for bin (i)

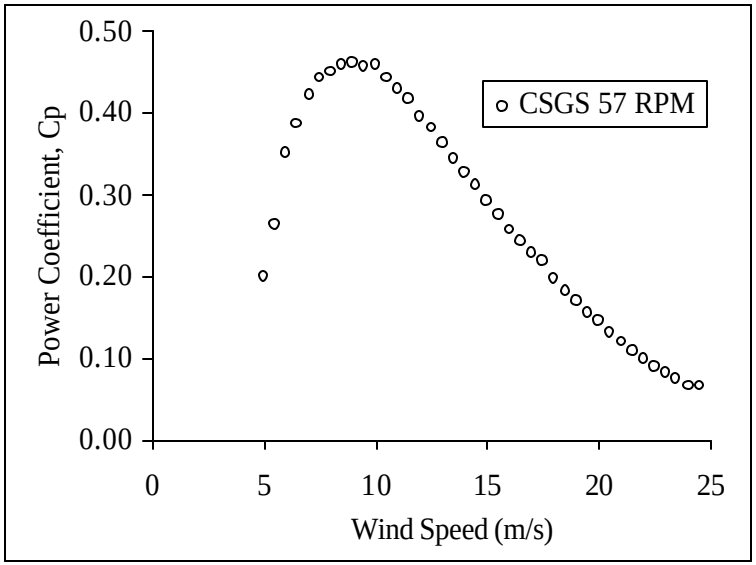

Figure 7. Rotor cp calculated

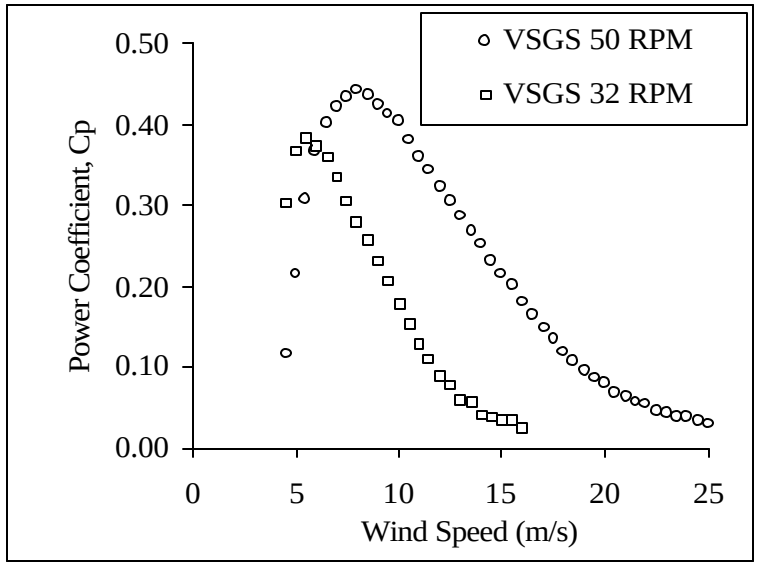

Figure 8. Rotor cp calculated

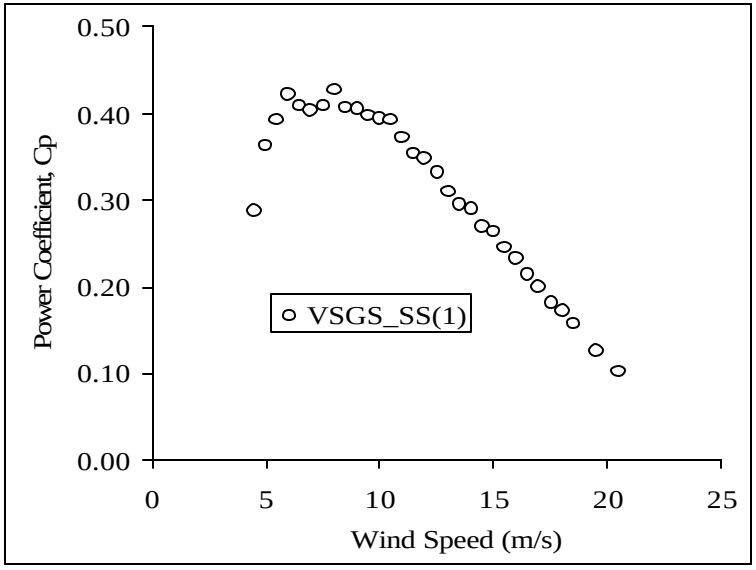

Figure 9. Rotor cp calculated

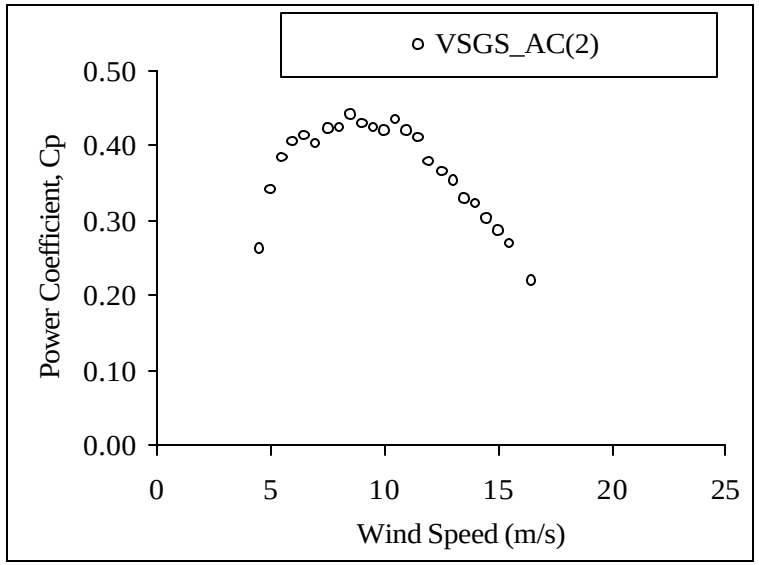

Figure 10. Rotor cp calculated

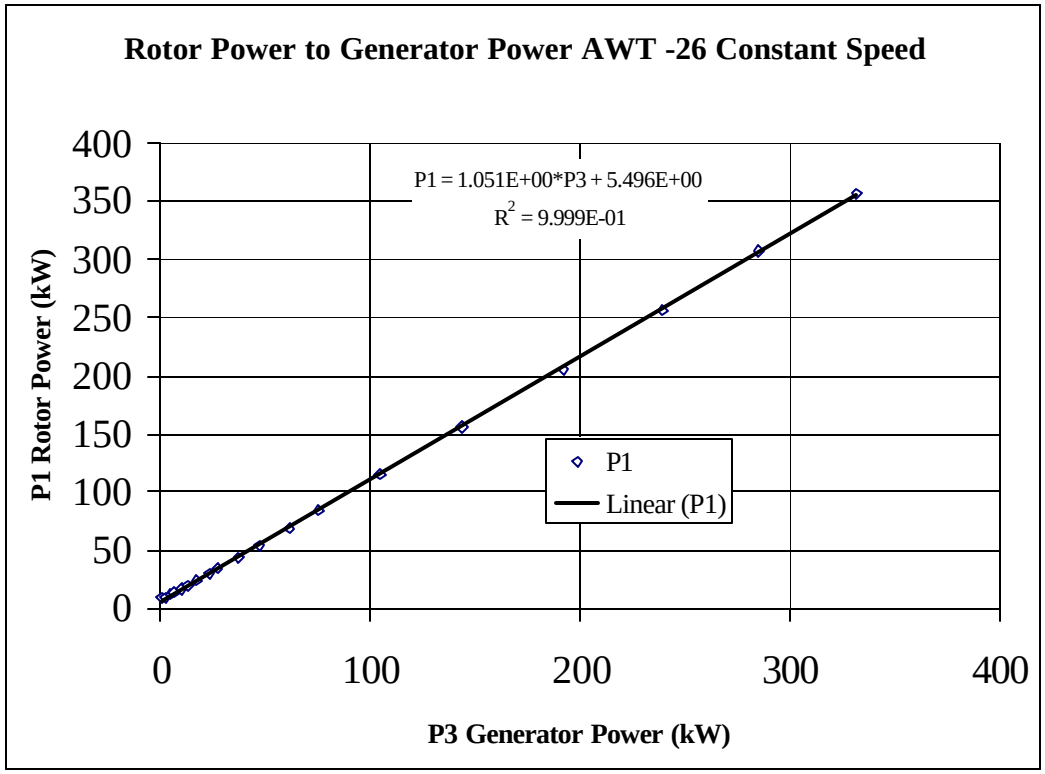

Figure 11. CSVS_57 constant speed generator and gearbox efficiency

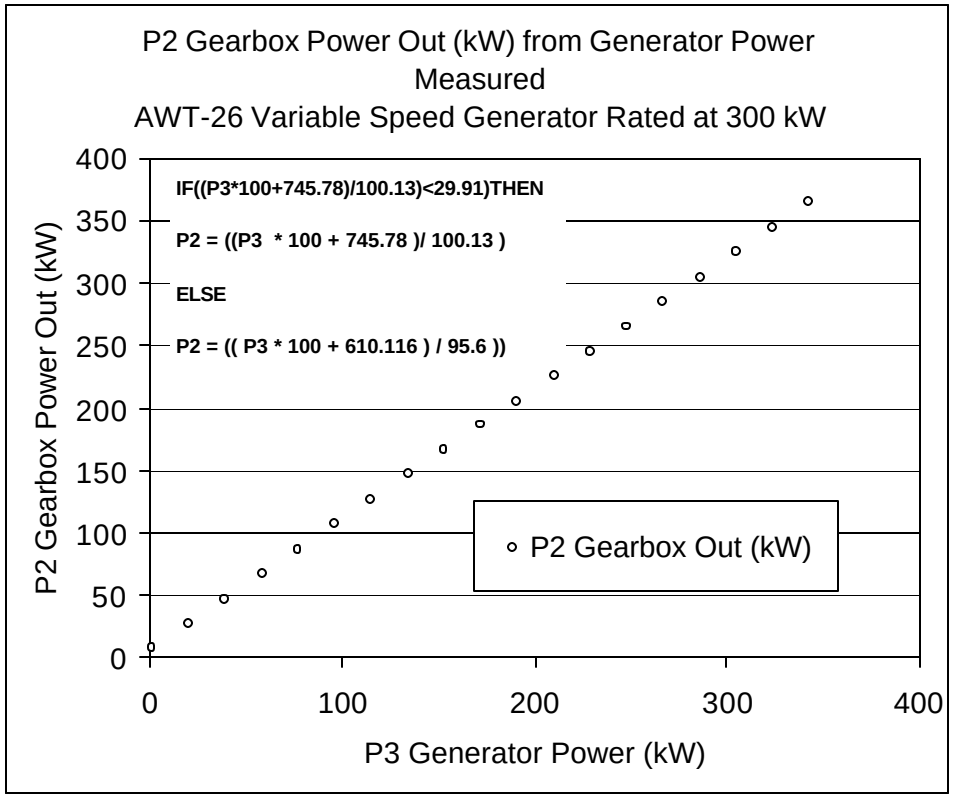

Figure 12. Generator efficiency as function of generator power out (P3) for VS data

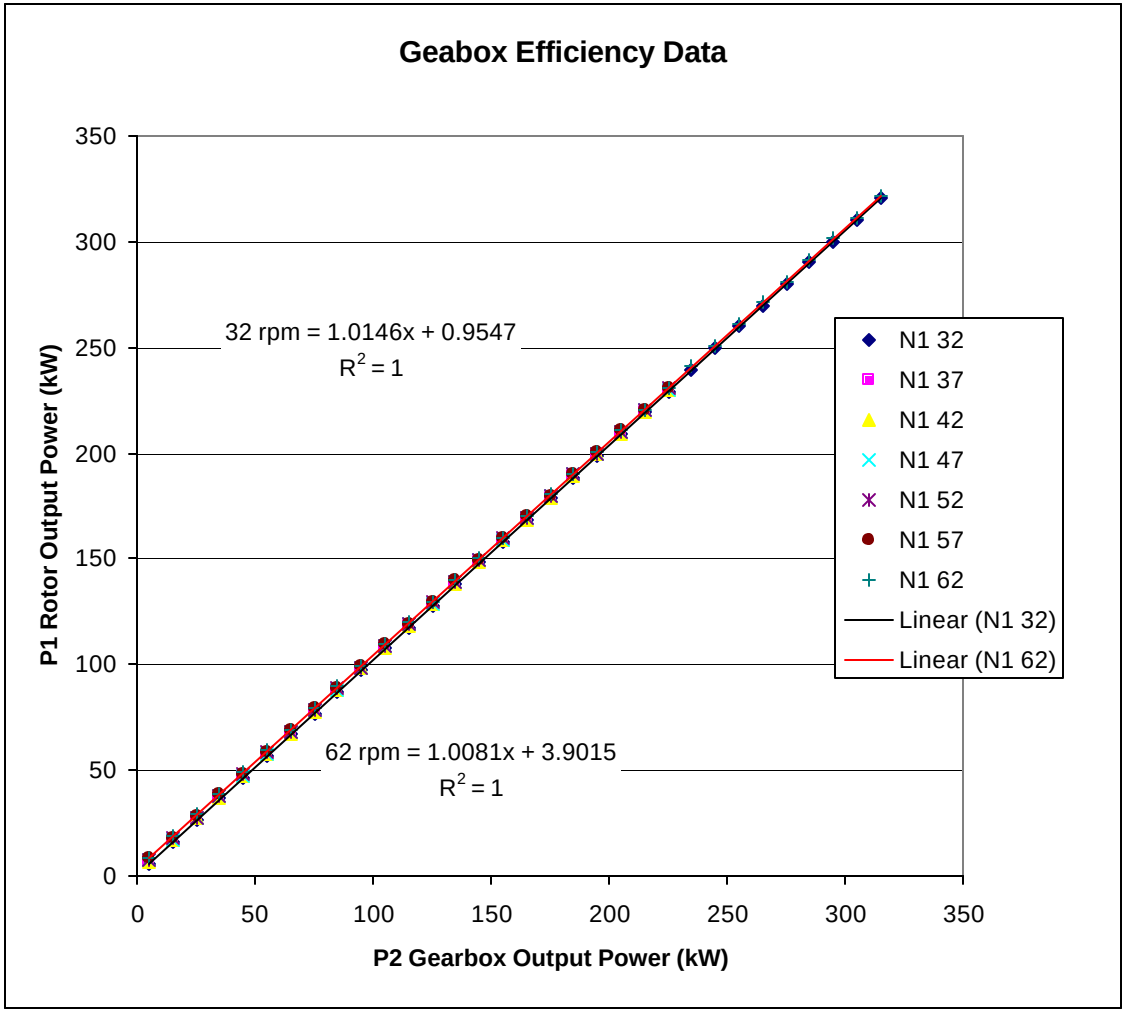

Figure 13. VS gearbox efficiency data used to calculate rotor power 32- and 62-rpm linear fits shown

Station id	Julian date	Time (2400)	Temp (K)	Pressure (Pa)	Vel A Ave (m/s)	Std Dev A	Min A	Max A	VelB Avg (m/s)	Std Dev B	Min B	Max B
23	104	1721	284.63	80649	6.1004	0.53065	4.5479	6.9067	6.1857	0.51583	4.9876	7.1066
23	104	1722	284.64	80654	5.6613	0.75772	4.348	7.9062	5.7919	0.78809	4.4679	7.8262
23	104	1723	284.76	80647	6.0578	1.1299	3.9082	8.0261	6.0544	1.2109	3.6683	8.226

Vel A Avg (m/s)	Direction Avg (Deg)	Std Dev Dir	Min Dir	Max Dir	Power Avg (kw)	Std Dev Power	Min Power	Max Power	Available	Online	Wet	Batt Volts	Campbell Temp	Counts
6.1004	282.02	5.6163	269.26	298.15	14.698	8.5881	-0.76462	31.923	0	0	0	13.601	12.602	60
5.6613	283.66	7.9337	266.87	301.96	16.456	15.012	-7.009	40.588	0	0	0	13.601	12.602	120
6.0578	292.74	6.7651	275.74	308.16	4.4911	11.024	-9.8763	26.316	0	0	0	13.601	12.58	180

Figure 14. CSGS_57 raw data table format for each tab of workbook CSGS_57.

	Average Power (kW)		Power Binned (kW)	
Vel A Ave (m/s)	CSGS 57 RPM	Wind Speed (m/s)	Binned CSGS 57 RPM	# Data Points/bin
7.2085	45.27	4.5	-7.4	40
7.1539	40.36	5	1.2	67

Figure 15. CSGS_57_F filtered electrical power data Tab 1 (RPM 57 CSGS Power).

	BINNED RPM 57
TSR	cp-57
17.4	-0.1037

Figure 16. CSGS_57_F filtered and calculated rotor cp data Tab 2 (TSR-57 CP).

Wind Speed (m/s)	CSGS 57 RPM
4.5	-0.103669634
5	0.199928462

Figure 17. CSGS_57_F filtered and calculated rotor cp data Tab 3 (Wind Speed 57 CP).

ID	Day	Time	Temp	Pressure	Ane A ave	Ane A SD	Ane A min	Ane A max	RPM ave	RPM SD	RPM min	RPM max	Ane A ave	WindDir ave	WindDir SD	WindDir min	WindDir max	Power ave	Power SD	Power min	Power max	GB TEMP ave	Avail	Online	BattV	CR10 Tem	Counts
45	55	1507	286.8	79154	15.408	1.5959	12.424	18.421	1309	3.0951	1302.7	1317	15.408	202.57	6.3965	185.44	217.37	177.89	12.922	138.17	202.16	57.041	1	1	13.444	18.929	60
45	55	1508	286.57	79149	14.663	1.2281	11.624	16.542	1307.1	2.1804	1302.7	1313	14.663	205.62	5.5754	191.92	217.18	171.5	10.829	150	195.73	57.501	1	1	13.444	18.952	60
45	55	1509	286.51	79149	14.863	1.2875	12.144	16.982	1307.9	2.7879	1302.5	1314.7	14.863	202.7	6.0831	191.35	217.18	168.54	15.063	136.39	195.73	57.865	1	1	13.45	18.952	60
45	55	1510	286.47	79155	13.927	1.2497	11.664	18.621	1307.3	3.0327	1300.7	1312	13.927	198.41	5.0036	185.44											

Figure 18. VSGS_30 and 50 RPM raw data table format for raw data workbook (VSGS_32& VSGS_50).

Vel A Ave (m/s) Wind Speed (m/s)	Average Power (kW) VSGS 5O RPM	Vel A Ave (m/s) Wind Speed (m/s)	Average Power (kW) VSGS 32 RPM	Power Binned (kW) Wind Speed (m/s)	Power Binned (kW) Binned VSGS 50 RPM	# Data Poins/bin	Wind Speed (m/s)	Power Binned (kW) Binned VSGS 32 RPM
15.408	185.02	4.5	-0.7	4.5	-6.9	27	4.5	-1.0
14.663	178.24	4.3	-3.5	5	-2.5	50	5	3.8

Figure 19. VSGS_30 and 50 RPM binned and normalized data workbook (VSGS_32&50f) / TAB(RPM 50 & 32 VSGS Power) .

TSR	VSGS 50 RPM	TSR	VSGS 32 RPM
15.1	0.117	9.7	0.3030
13.6	0.215	8.7	0.3667
12.4	0.308	7.9	0.3822

Figure 20. VSGS_30 and 50 RPM binned and normalized data workbook (VSGS_32&50f) / TAB(TSR_5O & 32 CP) .

TSR	Wind Speed (m/s)	VSGS 50 RPM	TSR	Wind Speed (m/s)	VSGS 32 RPM
15.126	4.5	0.117	9.681	4.5	0.303
13.614	5.0	0.215	8.713	5.0	0.367

Figure 21. VSGS_30 and 50 RPM binned and normalized data workbook (VSGS_32&50f) / TAB(Wind Speed_5O & 32 CP) .

ID	Day	Time	Temp	Pressure	Ane A ave	Ane A SD	Ane A min	Ane A max	RPM ave	RPM SD	RPM min
55	114	822	289.19	80107	8.3706	0.4255	7.4664	9.3854	1311	8.2278	1299.7
55	114	823	289.24	80108	8.322	0.51086	7.2665	9.3055	1312.6	7.8727	1294.7
55	114	824	289.26	80112	7.7196	0.52279	6.5469	8.7857	1298.5	6.354	1285.7

RPM max	Ane A ave	WindDir ave	WindDir SD	WindDir min	WindDir max	Power ave	Power SD	Power min	Power max	3B TEMP ave	Avail	Online	BattV	CR10 Temp	Counts
1327.2	8.3706	284.92	3.3391	276.9	294.54	49.843	6.2724	41.858	62.255	19.592	1	1	13.506	16.994	60
1327.2	8.322	284.51	4.3525	275.47	294.92	51.268	5.9613	37.283	62.764	20.759	1	1	13.506	17.039	60
1313	7.7196	283.04	5.4547	270.61	294.92	40.257	4.7287	30.548	51.072	22.045	1	1	13.513	17.085	60

Figure 22. VSGS_SS (1) raw "Soft Stall" data workbook VSGS_SS (1).

Day	Time	Temp	Pressure	Ane A ave	Ane A SD	Ane A min	Ane A max	RPM ave	RPM SD	RPM min	RPM max	Ane A ave
13	939	277.57	80884	5.48	1.46	3.26	8.89	1086.10	172.70	869.5	1452.2	5.48
13	940	277.69	80892	4.80	0.45	3.92	5.76	924.38	34.23	872	999.99	4.80
14	1538	284.76	80798	4.60	0.53	3.75	6.13	1245.50	49.09	1179.7	1351.5	4.60

WindDir ave	WindDir SD	WindDir min	WindDir max	Power ave	Power SD	Power min	Power max	3B TEMP ave	Avail	Online
309.63	17.40	0.32	347.63	10.88	14.90	-9.55	45.37	7.95	1	1
310.11	18.24	260.74	343.82	0.30	2.13	-6.37	4.05	8.60	1	1
255.65	9.06	232.19	273.09	-7.58	3.55	-12.22	0.49	13.28	1	1

Figure 23. VSGS_AC (2) raw"Active Control" data workbook VSGS_AC(2).

REPORT DOCUMENTATION PAGE

Form Approved
OMB NO. 0704-0188

1. AGENCY USE ONLY (Leave blank)	2. REPORT DATE	3. REPORT TYPE AND DATES COVERED
	November 2000	Subcontract Report

4. TITLE AND SUBTITLE
Variable-Speed Generation Subsystem Using the Doubly Fed Generator

5. FUNDING NUMBERS
WER13010

6. AUTHOR(S)
Claus H. Weigand, Hian K. Lauw, Dallas A. Marckx

7. PERFORMING ORGANIZATION NAME(S) AND ADDRESS(ES)
Electronic Power Conditioning Incorporated
4050 Fairview Industrial Drive SE, Suite 100
Salem, OR 97302-1142

8. PERFORMING ORGANIZATION REPORT NUMBER

9. SPONSORING/MONITORING AGENCY NAME(S) AND ADDRESS(ES)
National Renewable Energy Laboratory
1617 Cole Blvd.
Golden, CO 80401-3393

10. SPONSORING/MONITORING AGENCY REPORT NUMBER
NREL/SR-500-27066

11. SUPPLEMENTARY NOTES

NREL Technical Monitor:

12a. DISTRIBUTION/AVAILABILITY STATEMENT
National Technical Information Service
U.S. Department of Commerce
5285 Port Royal Road
Springfield, VA 22161

12b. DISTRIBUTION CODE

13. ABSTRACT *(Maximum 200 words)*

Over the past decade, fixed-speed, utility-scale wind turbines have technically advanced to a point where they can economically complete against nuclear and fossil-fuel-based power plants in geographical areas with a sufficient wind resource. The objective of this subcontract was to compare various electrical topologies allowing variable-speed turbine operation, identify the most suitable for a 275-kW (or larger) utility-scale wind turbine, and then design, build, lab test, and field test this variable-speed generation subsystem based on the previously identified optimum approach. Preliminary tests of the controls for a doubly fed variable-speed generation system rated at 750 kW were performed on a wind turbine. A 275-kW VSGS was thoroughly tested in the laboratory and on a wind turbine. Using field-oriented control, excellent dynamic behavior of the drive train was demonstrated, acoustic tests revealed an 11 dB reduction in turbine noise in low-wind, low-RPM operation compared to fixed-speed operation. The overall efficiency of the electrical system suffered from inadequate efficiency of the power converter at low power. Consequently, a different converter topology has been proposed that will satisfy both efficiency and power quality requirements for future use. This report provides information on all aspects of the project, including events that were unanticipated at the outset. A great deal of information is available in the references, comprised of NREL reports, journal articles, and conference papers on specific project results.

14. SUBJECT TERMS
wind energy; variable-speed wind turbines

15. NUMBER OF PAGES

16. PRICE CODE

17. SECURITY CLASSIFICATION OF REPORT	18. SECURITY CLASSIFICATION OF THIS PAGE	19. SECURITY CLASSIFICATION OF ABSTRACT	20. LIMITATION OF ABSTRACT
Unclassified	Unclassified	Unclassified	UL